NUMERICAL ANALYSIS OF CABLES IN THE OFFSHORE ENVIRONMENT

G. J. DAVIES

B.Sc. (Mech Eng)
University of Cape Town

September 1988

Submitted in partial fulfilment
for the degree of
Master of Science in Engineering
at the University of Cape Town

DECLARATION

I, Graham John Davies, submit this thesis in partial fulfilment of the requirements for the degree of Master of Science in Engineering. I claim that this is my own work and that it has not been submitted in this or in a similar form for a degree at any University.

Signed Signed by candidate

Dated at U.C.T. on 30 September 1988

SYNOPSIS

The extraction of mineral resouces from deep ocean waters has been made possible by the development of large compliant offshore structures. Mooring cables are crucial components in these offshore facilities and form the basis of this study. The aims of this thesis are: to provide a comprehensive review on all aspects of cables, to determine criteria for numerical modelling, and to ascertain the capabilities of the finite element method for cable analyses using the F.E. package ABAQUS.

Difficulties associated with large sag cables arise as a result of their inherent flexibility which causes ill-conditioning of the stiffness matrices. Furthermore, the cable winding configuration causes a nonlinear stress-strain relationship, it's sagged geometry results in nonlinear strain-displacement relations, and the immersion in water leads to nonlinear fluid loadings arising from Morison's Equation as well as uncertainties in the fluid parameters.

Various models, starting with the basic catenary, have been developed. Convergence difficulties at start-up, caused by a lack of stiffness in the transverse direction, are avoided by supporting the cable when applying loads. It is further established that numerical analyses of flexible structures are most stable in dynamic analyses and when under tension. In general both displacement based isoparametric and hybrid beam elements were found to be more reliable and applicable than truss elements.

Cable whip, ocean floor contact and harmonic motions of cables were analysed. Finally a cable/tower interaction was modelled and subjected to a Stokes's wave.

Conclusions ansd guidelines are presented, based on the numerical experiments carried out in this study.

ACKNOWLEDGEMENTS

I hereby acknowledge and express my appreciation to:

Dr. H.T. Pearce of the Department of Mechanical Engineering, University of Cape Town, for supervising this thesis.

The Department of Mechanical Engineering at UCT,
The CSIR (Council for Scientific and Industrial Research),
and SANCOR (South African National Committee for Oceanographic Research), for financial assistance.

AMRU (The Applied Mechanics Research Unit), for providing a forum for the exchange of ideas and the opportunity for advanced learning in the field of finite elements.

NOMENCLATURE

All units are S.I. unless otherwise shown

Arabic letters

A	-	Cross-sectional area
A	-	Wave amplitude
a	-	Acceleration
b	-	Body force
[C]	-	Stiffness Matrix
C_D	-	Drag coefficient (normal)
C_m	-	Inertia coefficient
C_t	-	Tangential drag coefficient
D	-	Cable diameter
ds	-	Differential element along axis
da	-	Differential surface area
E	-	Young's Modulus
F_n	-	Reaction force n
{F}	-	Force vector
f	-	Distributed load
G	-	Potential energy
g	-	Gravitational constant
H	-	Cable span
h	-	element length
h	-	Wave height
I	-	2nd moment of area
[K]	-	Stiffness matrix
k	-	Wave number
L	-	Cable length
M	-	Moment or bending stiffness
[M]	-	Mass matrix
m	-	mass
N	-	Shape function
P	-	Pressure in fluid
{q}	-	Load vector

r	-	Concentrated load
s	-	distance
T	-	Tension
t	-	time
t_{ij}	-	Surface traction
u	-	Cable displacement
V	-	Vertical projection of cable length
$\underline{V}$	-	Fluid velocity field
v	-	Fluid velocity
W	-	Work done
w	-	Weight per unit length
x,y	-	Cartesian global coordinates
X	-	Material point
z	-	Still water elevation

Greek Letters

α	-	Cable helix angle
β	-	Phase angle
π	-	3.141592
σ	-	Stress
μ	-	Wave length
Φ	-	Flow potential
Ω	-	Wave frequency
ϵ	-	Lagrangian strain
η, ϵ	-	Cartesian local coordinates
ρ	-	Density

Glossary of abbreviations

FEM	-	Finite Element Method
FEs	-	Finite Elements
N-R	-	Newton-Raphson Method

Subscripts and Superscripts

$_0$	-	At time zero
$_c$	-	Current configuration
$_e$	-	Elemental value
$_H$	-	Horizontal
$_{i,j}$	-	i and j^{th} component of
$_N$	-	Normal direction
$_{NR}$	-	Normal relative value
$_r$	-	Reference configuration
$_t$	-	Tangential
*	-	Deformed state
^{T}	-	Matrix transpose

CONTENTS

LIST OF FIGURES

INTRODUCTION

The increase in the world's demand for energy requires the extraction of natural resouces from less hospitable environments, besides the researching of alternative energy forms. The continuing search for fossil fuels has led to the increase of offshore exploration to complement inland exploitation. Offshore facilities designed for this purpose were initially rigid structures, built to resist the ocean forces, but the need to drill in deeper waters e.g. 1000m plus, has necessitated a new concept in the design of offshore rigs viz. that of compliant or large displacement structures.

Allowing the structure to comply with an external exciting force instead of directly opposing it, results in a considerable reduction of internal stresses, and therefore lighter, more economical structures can be built.

The manner in which this is achieved is to have either a buoyant rig or a slender articulated tower, both of which are constrained from excessive motion by a network of cables (see figure 1.1).

Necessary physical limitations do however need to be placed on the maximum horizontal displacements of the rig, occurring during large storms. This has been accomplished by introducing clumped weights onto the cable (figure 1.1), which in mild conditions are in contact with the ocean floor, while the occurrence of lift-off (which increases the effective stiffness of the cable) during these large storms, restores the rig to it's neutral position.

The large displacements associated with compliant structures are accompanied by large accelerations and velocities and therefore, the inertia and damping of the fluid/structure interaction should be considered. The inclusion of time

OFFSHORE FACILITIES

Articulated Tower

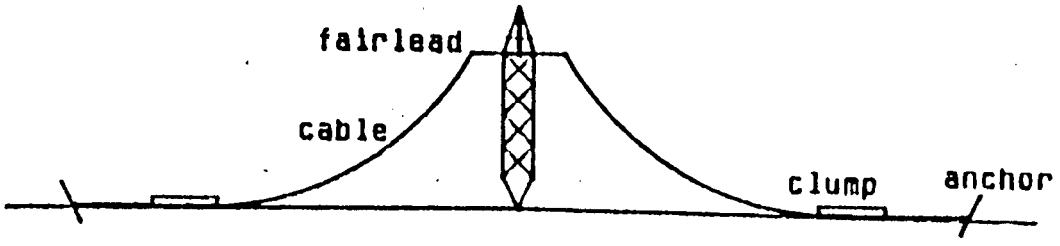

Jacketed Tower

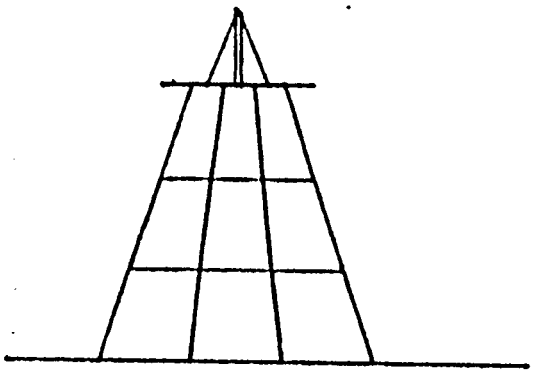

Floating Platform

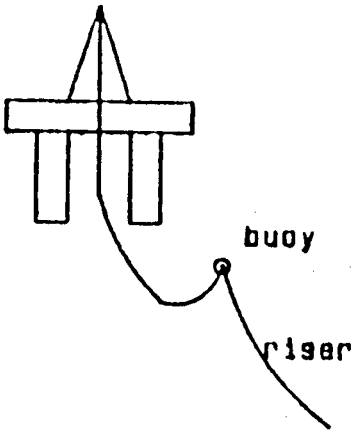

Cables, Risers, Chains — Flexible Structures

Figure 1.1 Offshore Facilities

dependent loads makes the problem by definition a dynamic problem. Dynamic analysis is considered necessary when the fundamental period of the structure is sufficiently larger than that of the ocean waves. Structures which have similar frequencies to those of typical ocean waves must be avoided to prevent a resonance occurring.

To analyse the entire fluid/structure interaction simultaneously is a formidable task, so the system has generally been divided into separate components, which are:

i) modelling the wave, current and wind forces as external loads,
ii) modelling the cables as restraining nonlinear springs, which are interactive with the floating rig itself, and
iii) oil carrying risers or pipelines, which are modelled as flexible structures.

Thus to understand the behaviour of the individual components and to model them accurately, would allow for more effective modelling of the complete system. For this reason the cables are modelled predominantly in isolation.

Although cables are seemingly the simplest of structures, the fluid/structure interaction caused by the combination of enviromental loading conditions and the substantial size of mooring cables, create a number of associated modelling problems, some of which are listed below.

i) large sag and large displacements (introducing geometrical nonlinearities).
ii) cable winding configurations (introducing material nonlinearities).
iii) interaction of the fluid and cable introduces loading nonlinearities.
iv) random fluid loading, caused by the unpredictable nature of waves,currents and wind.
v) the uncertainties in viscous drag, form drag, fluid

inertia.

vi) variation of tension along the cable due to it's own weight (it's weight alone accounts for 20% of it's breaking stress)

vii) the effect of clumped weight lift-off (including contact suction and sliding friction) which changes the stiffness and damping effects of the cable.

viii) vortex shedding (also known as strumming), which not only accounts for most of the drag, but can also cause fatigue in the cable. Because of the costs associated with rigs, they are expected to have a minimum of twenty years life, by which time fatigue could have caused failure.

ix) large motions at the boundary.

x) snap loadings of cables

xi) the sea is a very corrosive environment

xii) marine growths, in an unknown quantity, affect the mass and surface roughness.

A particularly dangerous situation of a cable under random loads could occur if the cable whipped (similar to the tip of a whip cracking) at the fairlead position (the point of contact between cable and rig). This is equivalent to having a negative stiffness (aiding displacement in the wrong direction) or an overturning force acting on the rig. Associated with whipping is the fact that the cable will go slack and may then snap taut, causing an impact load, and possible failure. It may also occur that the cable goes into an unstable compression. This again causes a negative stiffness and may result in buckling and localised strains or kinking of the cable, leading to premature failure.

In many cases, cable analysis is also applicable to riser analysis because they are both long, slender, flexible, structural members, but particular difficulties are encountered as a result of both the cables' winding configuration and their greater flexibility.

As a result of the motivation by the offshore industry, the ultimate aim of this field of research is to obtain working models of applications of large cables in the offshore environment; thus the study was geared to this end.

The aim of this thesis is to:

i) Present a state of the art review on relevant aspects of cable behaviour and analysis, with particular reference to offshore mooring cables.

ii) Investigate the response of cables under various loadings and boundary conditions, using the finite element package ABAQUS, to determine criteria for the future modelling of cables in a design situation.

The finite element method (FEM) is generally accepted as being the most versatile and accurate form of analysis for complex material, geometrical and loading considerations. Experimental validation gives testimony to this statement as discussed in the literature survey.

The general layout of the thesis is as follows:

- Chapter One presents a qualitative and quantitative literature review on the analysis of cables, leading from historical studies up to the current state of the art. The chapter ends with a summary of the numerical aspects of cable analysis, which gives the direction that the modelling section of the thesis takes.

- Chapter Two deals with the formulation of the governing equations of the cable problem. Firstly the well known catenary equations are presented, which is then followed by the derivation of the wave theories used and the statement of the Morison's equation. This is then incorporated in the formulation of the finite element method.

- Chapter Three presents an overview of the use of ABAQUS

and it's limitations with regards to cable type problems. It is necessary to understand and be aware of certain features before an appreciation of aspects in the modelling section can be obtained.

- Chapter Four begins with the modelling of the 'simplest' static equilibrium model, and then progresses to models of increasing complexity until finally a complete tower and cable system is presented. The difficulties encountered and their subsequent solution procedures are presented along the way in order to understatnd the development of the models.

- Chapter Five contains the conclusions and recommendations as well as design considerations of all the previous model analyses.

- Finally a list of papers, articles and books referenced in the thesis follows.

1. LITERATURE REVIEW

1.1 History and Development of Cable Analysis

Most early analysts of cables concerned themselves with only analytical solutions of either the static catenary (defined as the static equilibrium shape of a suspended cable), or the dynamics of a taut string. Dynamic problems were limited to small sag/span ratios and in-plane vibrations. These early papers give a useful insight into cable behaviour, and highlight difficulties that may be encountered when solving for large sag cable problems. For example, although displacements are often large, elastic strains are usually relatively small.

Numerical methods generally require many computations, and as a result until computers had been sufficiently developed to cope with large volumes of information, numerical techniques developed slowly. Thus, early studies were conducted analytically or semi-analytically.

Pugsley [20] analysed chains and cables in the nineteen forties and produced an approximate analytical solution for a uniformly loaded, suspended cable in a geometrically non-linear static analysis. A linear elastic differential element of uniform mass and cross-section was considered. The analysis was limited to small sag, to enable the derivation of a closed form solution.

Kolousek [2] in 1947 appears to be the first to consider a massive guy cable in any detail, and assumed it to have a parabolic shape, but analysed only small vibrations which were approximated by a Fourier series of sinusoidal components.

Dean [1] in 1961 gave a mathematical treatment of sagged cable dynamics about the static catenary. The catenary relations

were used rather than the parabolic approximation. He considered only small displacements, and assumed that the initial tension remained constant throughout the analysis. Out-of-plane and longitudinal vibrations were neglected.

Davenport [2] in 1965 introduced viscous damping and drag into the model, as well as harmonic motion of the cable upper end, and superposition of the transverse on the in-plane vibrations. Observations supported the occurrence of the negative stiffness phenomena. This implies that, instead of the cable applying a restoring force to the tower, the cable attempts to force the tower even further out of an equilibrium position. He also attempted to determine the dynamic guy modulus, which would account for rate dependent effects, from the static modulus (the reaction in a certain direction caused by a unit deflection in the same direction), and recommends future research in this area.

The problem with purely analytical methods is the difficulty of finding closed form solutions, so Buchanan [3] in 1970 applied a regular perturbation technique when solving for the response of nonlinear cables subjected to perpendicular loads. Only two terms in each series approximation were used in order to avoid large algebraic manipulation, which limited the analysis to simple problems, ie. those in which only second order nonlinearity can be analysed.

Soler [4] directed attention to free and forced vibrational response of a single cable using a closed form solution. Results indicated that increased cable sag resulted in significant decreases in the tension, causing the lowest natural frequency to be decreased.

Chang and Pilkey [5] approximated a geometric nonlinear treatment of cables by 'incremental linearization' (a linear analysis but updating at each step) using a perturbation technique in three dimensions. The complete analysis was done in two stages viz. 1) computing an equilibrium position by

slowly applying static loads eg. gravity and buoyancy, and thereafter 2) incrementing forward in time, for the dynamic analysis. The study was only done for small vibrations, but the two stage approach is worth noting as it has subsequently been used to overcome start-up problems mentioned later in the thesis.

Leonard and Recker [6] in 1972 used Hamilton's Principle applicable to the dynamics of a 3-dimensional, lightly stressed cable. A quasi-linear FEM using eight linearly interpolated truss elements was sufficient for an accurate, converging solution. The authors recommend a Newton-Raphson scheme for use with the FEM. Ganapthy in 1974 improved on this by allowing for large displacements, when modelling mooring systems with FEs.

A detailed mathematical treatment of free vibrations of a suspended cable with a sag to span ratio of 1:8, using linear theory,is given by Irvine and Caughey [7]. In-plane symmetric and anti-symmetric vibration patterns are investigated, and the occurrence of a 'cross-over' point was theoretically predicted and also validated by experiment [13]. A cross-over point occurs when instead of the frequency increasing with decreasing length (as is expected), this frequency decreases. This happens as a result of the cable's tendency to vibrate in whole cycle multiples of it's natural modes.

In a later paper [15], Irvine investigated the contributions to the potential energy of a cable with a relatively flat sag. Findings were that a maximum of 2/3 of the potential energy can go into strain energy, the rest being gravitational energy, and the greater the sag, the greater will be the contribution of gravitational potential energy.

Triantaffylou and Bliek [26] gave a linear analytical treatment for in- and out-of-plane large sag cable dynamics. Elastic effects were neglected as they were deemed of negligible importance for determining the first few modes.

Ghambhir and Batchelor [11] in 1977 studied the free vibrations of sagged cables using FEM on the nonlinear package, DYNCBL. Their results are limited to spans of 400m and sag/span ratios of 1:10, and they concluded that:

1) The frequencies and mode shapes of the cables do indeed approach their true values as the number of truss elements (curved or straight) is increased, however the curved element is much superior for large sag.
2) In- and out-of-plane modes can be uncoupled, and out-of-plane modes & frequencies correspond to those of a taut string.
3) At small spans, the frequencies are sensitive to the change in span length and, due to transition in mode shapes, their reordering is necessary. However at large spans the frequencies are reasonably independent of span length.
4) "The natural frequencies depend primarily on the sag, secondarily on the sag/span ratio and are independent of the mass per unit length and axial stiffness of the cable element". However the manner in which they varied the weight was by varying the cross-sectional area; therefore their sentence should read, '..... independent of the size of the cable', ie. the mass and stiffness remain proportional to each other.
5) In general, the frequencies decrease with increasing sag or with reduced tension. However, in the case of even number of in-plane modes of vibration of sagged cables, there occurs a transition (or cross over) in the mode patterns requiring reordering of the modes corresponding to the ordered array of frequencies.
6) Six curved elements (2nd order) gave comparable results to 16 straight elements

Nath [10] in 1976 attempted to collate all existing information for a presentation of the state of the art on analysis of cable dynamics in offshore applications. His conclusions were that :

1) Usually only tensile axial force had been included, neglecting axial compression, bending (which may be important) and shear.

2) Three major conceptual cable models have been proposed to date viz.

   i) The continuum assumption, in which a differential element of the cable is considered, on which all forces act. Partial differential equations are derived, and the most common methods of solution are finite differences, the method of characteristics, or perturbations. Closed form solutions only exist for problems where many simplifying assumptions with regards to the nonlinearity, the bending stiffness and the sagging associated with cables are made.

   ii) The lumped mass approach assumes that a certain length of cable can be approximated by a point mass which is connected to adjacent point masses by springs and dashpots. Hydrodynamic loading and damping can be simulated by added masses (fluid inertia), nonlinear springs (clump lift-off) and dashpots (viscous drag). The discrete system equations can be found by use of a free body diagram, Hamilton's principle or Lagranges' equations, and solved by using for example the Runga-Kutta Method.

   iii) The FEM considers the cable as a number of connected continuum segments which are able to support bending and shear (if desired), and allow for composite nonlinear materials. Nath claims that this method has had the most experimental validation.

3) Boundary conditions had up till then been linearised displacements on the upper end of the cable. Some models have allowed for contact on the ocean floor, and simulated the effect of mud suction by means of springs, and the mud drag and friction by means of dashpots.

4) Forcing functions are usually caused by the action of fluid flow (waves and currents), wind, boundary motions, gravity and buoyancy, however to date no model predicting the cable response to vortex shedding had been proposed. These vortices cause strumming and increase drag and fatigue, and so far have been modelled empirically by a drag coefficient with the drag proportional to the velocity squared.

   An effect of added inertia is caused by entrapped fluid moving with the cable [51], and also more importantly (and correctly) the cable trying to accelerate into the fluid, thus causing an acceleration of the localised fluid [52]. Even if the relative velocity is zero, the added inertia is not necessarily zero, and is in fact most likely non-zero, because the cable needs to impart energy to the fluid to get it moving (or vice versa depending on the vector addition of their accelerations), thereby inducing an in-line reaction on the cable which attempts to retard it's motion. This has been accounted for by an inertial coefficient with the inertia proportional to the relative cable acceleration.

5) Surprisingly, details of the physical properties (eg. nonlinear straining, internal damping, fatigue, abrasion and kinking characteristics) of mooring ropes are not comprehensive or readily available

Nath recommends that areas requiring futher research are hydrodynamic drag, vortex shedding effects on cables, experimental validation of models, and, to what extent marine growths affect structural behaviour.

1.2 Cable Modelling

Although cables appear to be the simplest of structures, there are associated difficulties which bely their appearance. Firstly, the winding configuration gives the cable it's special characteristics. The manner in which the cable is wound is varied, and depends on the required applications, and to date, there are numerous different types of cables designed for specific purposes as shown in the Haggie Rand catalogue [64]. The difficulty in determining the mechanical properties from the material properties and the winding configuration is immense as borne out by Costello [68], who assumed the cable to be comprised of many helical springs in contact with each other. For large cables, there may well be one hundred or more individual strands arranged in geometrically complex patterns, and so analyses of cables are usually conducted from empirically determined physical properties.

Some of the physical properties required for the modelling of cables are: density, area, axial stiffness, bending stiffness, torsional stiffness, shear characteristics, structural damping and elastic-plastic limits. All of the above properties are dependent on the type of material used, and the winding configuration of the cable.

Palo, Meggit and Nordel claim that except for the simplest of cases, a nonlinear model (or models) is necessary [28] for the modelling of large displacement cable analyses. They used commercially available computer packages (details of which appear later) emphasing that the user should fully understand the model before attempting analyses thereof.

Force - displacement relations are nonlinear in both axial and bending directions, and for large displacement analysis it is desirable to use nonlinear (and anisotropic) elastic stress-strain relations.

The structural damping is difficult to determine and is subject to large uncertainties, because of the friction

resulting from the individual strands sliding over each other, as well as the nominal amount caused by the internal material damping of the strands themselves. Usually the effect of structural damping is insignificant compared to that of other loads. Furthermore the structural damping is often lumped with the much larger effect of damping caused by the cable moving through the fluid.

Damping plays an important role in determining the magnification of response, and is critical near resonant responses of the structure [61].

The largest difficulty associated with the modelling of cables is probably that, by their inherent flexural nature, they are sensitive to force and displacement inputs. It is the response of the cable to the various loadings that makes a comprehensive cable analysis a non-trivial pursuit.

1.3 Fluid Drag and Inertia

Hydrodynamic loading has been topical for the past 30 years since Morison developed an equation for calculating the fluid forces acting on an immersed cylinder, caused by drag and fluid inertia; which is now widely used [51,45,43,44,37,23,18,40]. He assumed (based on empirical relations) that the drag was proportional to the relative velocity (between cylinder and fluid) squared, and the added inertia proportional to the relative acceleration of the cyclinder, a now generally accepted relationship for small bodies. For larger bodies, it is necessary to include wave diffraction from the body. Small implies that the cylinder diameter is less than 20% of the wave length of the passing wave [45,54,51].

The coefficients Cd and Cm in the Morison equation are assumed constant in the simple case. The Cd is an empirical

coefficient to be determined from experimental data and would include both the effects of viscous and form (pressure) drag on the cylinder. When a cylinder moves through water, a certain amount of the water clings to the surface, as a result of cohesive and viscous action, and is thus subjected to the same acceleration as the cylinder [16]. Thus the Cm includes both the inertia effect of the empirically determined added mass of fluid, as well as (in this case) the inertia of the cylinder. Care should be taken over whether or not the author is including the cylinder mass in the inertia term, as many authors refer to Cm as simply the added inertia.

Morison's equation has often been linearized [13] in order to avoid the nonlinear effect of the velocity squared term. Borgman's version based on empirical relations [51] provides a good approximation when substituted for the velocity squared term in Morison's equation appears below.

$$|u| \cdot u = (8/\pi)^{0.5} \cdot 0.5 \cdot U \cdot u \qquad 1.1$$

where U is the horizontal root mean square value of u

It was found [48], that the coefficients of variation of the Morison's coefficients (when assumed non-constant), for the nonlinear wave load model, are higher than for the linearized wave load model.

Dawson [51] suggests that the success of the constant-coefficient approximation is attributed to a decreased dependence of the coefficients on dimensionless flow parameters as a result of the circular particle motions and large kinematic gradients of the deep-water waves. He achieved good results using Morison's equation with Stoke's wave theory, and reasonable results by using a linearized Morison equation with linear (Airy) wave theory, when compared to experimentally determined r.m.s. force values.

He states that the theoretical value of Cm for a cylinder in inviscid flow with Re=10000 is 2.0 , 10% higher than their value, and for Cd is 1.2, the same as their value.

In conclusion, the Morison equation with constant coefficients and the Stokes wave theory provides good representation of the total force measurements over the entire wave cycle, including the phase variations between the maximum force and the maximum water surface deflection that result. This is true when either inertia forces or drag forces dominate the maximum force.

Davenport [2], introduced viscous damping and drag into the analysis of his model and showed that damping not only reduces the peaks in the response, but also causes a phase shift. He also noted that immersing a cable tended to reduce it's static weight by 10% (buoyancy effects), but increased the added mass by 10% - 30% . Results of [33] indicate that a damped system has smaller peaks and also lags that of an undamped system, especially in the case of transverse vibrations. Damping was of the Rayleigh type (i.e proportional to the mass and stiffness).

Ramberg and Griffin [13] experimented with marine type cables in air and water in order to determine the natural frequencies, fluid and structure damping and added mass coefficients. They assumed that the damping in air represented the structural damping (for slack cables - always significant and nonlinear), thus the fluid damping could be determined from the total damping in water minus that of air. The difference between the measured frequencies in air and water is interpreted as the added mass effect of water. The fluid damping of slack cables was also estimated from taut cable findings, and it was noticed that the damping increases logarithmically with cable sag.

Nonlinearities in the overall system are introduced in the fluid by the aforementioned dependency of drag on the velocity

squared, and also because Cd is generally dependent on the Reynolds number (which characterizes viscous motion) and in turn therefore, on the displacement of the cable, when submerged in a variable flow field [23].

Dawson [51] adds that Cd and Cm also depend on the Keulegan-Carpenter (K-C) number, which characterizes periodic motion. A dimensionless parameter beta, is introduced, which is the ratio of Re to K-C. As Re is similar for most applications ie. in the supercritical flow regime [45], coefficient data for a specified cylinder diameter and wave period can be regarded as a function only of K-C [51].

The importance of a dynamic analysis compared to that of a static analysis, is largely because of fluid drag and fluid inertia as well as the inertia of the body itself. This was mentioned by Ansari [37] and Morrison [32], as well as by Brinkman [24] who found that hysteretic loops around the linear (static) force-displacement response of mooring cables resulted, when a dynamic analysis was used. He also found that static analysis underestimated tensions by 20% , concluding that nonlinear drag effects are important [13].

Ormberg et al [27] claimed that the most important hydrodynamic force on conventional mooring lines is the drag force due to lateral (vertical) motions of the line, and that "the main contribution to dynamic effects is caused by forced motions in the tangential direction", although these forces are not directly attributed to tangential drag which is of minor importance. These proposals are supported by Leonard, Tuah, Nordell, Meggitt, Dawson and Ansari [40,44,51,37], where tangential drag is often neglected. The former statement is supported by [51,45], but only for large waves; the larger the wave the more the drag force contribution. In an experimental tank using a 50mm vertical cylinder, it was found that for a 250mm wave the drag contribution to the maximum force is about 40%, for a 375 mm wave 75%, and for a 500mm wave 90%, however no prediction as to how this effects larger cylinders is made.

Conclusions which Ormberg et al [27] reached are as follows: drag leads to an apparent increase in stiffness, and the difference between static and dynamic analysis is enhanced with increasing depth.

Decoupling of tangential and normal components of drag is assumed acceptable [39,23], based on experimental evidence, and also by reasoning that the causes of the two components of drag are essentially different. The normal drag, often referred to as form drag, is caused almost entirely as a result of vortex shedding, whereas the tangential drag is caused by viscous action along the cable and is equal to the skin friction of a flat plate having the same surface area as that of the cable [40].

Many authors [51,45], agree that Sarpkaya [55], in his very comprehensive study on coefficients, considerabl y overestimated (i.e. by about 30%) the total measured force on fixed vertical cylinders for large wave heights. Sarpkaya's data were determined from one-dimensional oscillatory flow in a U-tube as part of a fundamental study of the Morison equation, and hence, do not necessarily apply to the case of wave-induced water motions, although they appear applicable for smaller wave heights.

The effect of current on hydrodynamic loading is important only in so far as the current velocity is added vectorially to the wave velocity [45]. This superposition is deemed valid for small waves and currents. A nonlinear interaction has been investigated by Dalrymple, but was found to be of rather minor importance for most practical applications.

In wave action, the velocity and acceleration are generally not collinear, in which case, Fd and Fi (drag and inertia forces) act in different directions in the same plane [45]. In the 3-D form the drag and inertia forces are considered independent. The lift force, always perpendicular to the drag,

should in this case be included.

Most papers which include hydrodynamic drag when dealing with cable dynamics [40,48,37,27,24,23], do so in the time domain. This is because the nonlinear effects caused by drag, resulting in nonlinear damping and phase shift, make the problem time dependent. However, Leonard and Tuah [40] determined the dynamic response by mode superposition in the frequency domain. The nonlinear fluid drag is linearized by a method of statistical linearization, and the cable response is then computer by taking the inverse Fourier transform of the cable frequency response. This modal analysis was performed on random wave loadings.

Mo and Moan [48] reported good correspondence between the spectra of the linearized time and linearized frequency domain, but a significant discrepancy was found between linearized frequency domain solutions and the nonlinear time domain formulation. A discussion on superharmonic resonances and it's effect on Cd and Cm for the tower and the guying system was given.

The notion of a 'smooth cylinder' referred to in the literature for determining coefficients, is largely academic because all members have some roughness, and in particular marine growths. The effect of marine growth is to increase the mass of the structure (cable), increase the roughness - thus increasing drag and, increase the diameter - which then increases the added mass effect and would also give a different K-C number.

Oscillatory motion of cylinders as induced by waves tends to cause the wake of the previous half-cycle to become the oncoming flow for the next half-cycle according to Leonard et al [45]. This kind of wake interaction has not been systematically studied, but it appears that it is primarily characterized by a 'displacement ratio' (amplitude of oscillation/cylinder diameter = K-C/pi). The primary effect

of this wake phenomenon appears to be, that the excess turbulence created by the previous half-cycle results in transition to supercritical flow at reduced values of Re as compared to steady flow. Surprisingly though, the supercritical Cd is seemingly not affected. Increasing the roughness seems to cause an increase in the wake effect [55], but Leonard [45] suggests that the Cd magnitudes were far too large. Available data suggest that the drag in oscillatory flow does converge fairly rapidly to steady flow values as the displacement ratio increases.

Typical values of Cd are: vertical cylinders 0.6-1.0 [32] , 1.2 [51] , guylines 1.0 [24]

Typical values of Cm are: vertical cylinders 1.5-2.0 [32] , 1.8 [51] , guylines 1.0 [24] , clump weights 2.0 [24]

Horton [57] claims that the Morison equation is an oversimplification of drag and inertia, and thus proposes an equation that accounts for 3D, diffraction and temporal effects.

In general, however, there is still a lot to be learnt in the field of drag and inertia, and discrepencies as high as 50% are common, yet the designer has still to use these data. A sound knowledge of qualitative aspects of this field would help in providing an intuitive insight into the problems. Furthermore, he should be be aware of the sensitivity of the solution to changes in the parameters and also know the bounds of his solution according to acceptable bounds on the Morison's coefficient.

1.4 Numerical Techniques of Flexible Structures

1.4.1. Introduction to the Techniques

The various techniques for the analysis of cable behaviour may be categorized as follows:

1) Analytical methods - obtaining closed form solutions limits the technique to simple problems.
2) Semi-analytical methods - start with the governing partial differential equation (PDE) and solve it numerically by integrating directly, eg. by using finite differences, Runge-Kutta, Gill's method, Fletcher's method, perturbation techniques.
3) Discrete elemental methods - The entire model is divided into a number of interconnected simple models with the formulation based on variational principles eg. the Lumped Parameter Method and the Finite Element Method (FEM)

The main thrust of recent developments in techniques, for the calculation of the dynamic response of cable structures, has been to increase the generality of the numerical models, which has necessitated to the discretization of the system into a number of simpler elements. The global governing PDE for a complex system need never be derived, since the form of the spatial variation is implied by the collection of compatible discrete elements. Furthermore simpler forms reduce the entire solution process to a relatively simple set of operations.

A so called 'energy search method' used by Monforton [14] also circumvents the need to solve governing equations, by involving a direct search for the minimum of the total potential-energy of the structure and makes use of unconstrained minimization techniques. This was used in conjuction with FEM [14]. The principle of total potential energy can be stated as follows: Of all displacement fields which satisfy geometric compatibility, those which locally minimize the potential energy also satisfy the equilibrium conditions, and are in stable positions [17].

An alternative to first discretizing the system (as in lumped parameter and FEM), is to initially derive the governing equations before discretizing them in some manner, ie. a semi-analytical method. The finite difference method and the method of weighted residuals fall into this category.

Before any simulation model can be used with confidence, it is essential to compare the results with a broad range of experimental data, in order to establish the credibility of the model.

In 1973 Choo and Casseralla [8], in a survey of solution methods for dynamic simulations of cables, claimed that the FEM was the most versatile and accurate technique, based on experimental validation of lumped parameters, linearization method, method of characteristics and the FEM.

Meggit [17] compared the nonlinear FEM, weighted residuals and lumped mass methods to experimental results of cables subject to stochastic environmental loads (mainly ocean forces). The programs SEADYN and SNAPLD were used, and all the results compared well (i.e. within 2%) with experimental data on an anchor deployment problem. Because of a lack of versatility in the weighted residual and lumped mass methods, only relatively simple problems could be compared.

1.4.2. The Finite Difference Method

Ali [35] in 1985 considered the forced vibrations of a 3D, nonlinear, sagged cable with moveable supports. The problem was defined by three uncoupled PDEs, which were solved using the finite difference method. It was assumed that an homogeneous, isotropic, elastic material with no shear flexure was adequate for modelling small strains, large displacements, initial configurations and changes in cable tension. Results compare well with Leonard (FEM), and it was found that the

cable goes into unstable compression at sag to span ratios of 1:20 . Linear theory was found to give conservative deflections, and also could not accomodate large displacements, when compared to that of the finite difference results.

1.4.3. The Lumped Parameter Method

Early intuition led to the lumped parameter method, which amounts to lumping the effects of mass, internal reactions and external loads at a finite number of points in the system. The equations of equilibrium and continuity are applied to these points to develop a set of discrete equations, of the form shown below.

$$M\ddot{x} + C\dot{x} + Kx = F \qquad 1.2$$

The method of imaginery reactions (a special case of lumped parameters used for static analysis), is the most common method used for obtaining the catenary [44].

Consistent mass formulations in FEM may result in the coupling of translation and rotation, whereas the lumped mass method eliminates rotation unless specifically desired [56], because the masses are considered to be point masses.

Ansari [37] bases his use of lumped parameters (as opposed to FEM) on a paper by Leonard, who concluded that "so long as attention is paid to defining the boundary conditions and the degree of discretization, which may be different for the two methods, both methods can be equally accurate", and also that the lumped mass system is easier to formulate. However the method is limited by it's lack of 'the continuum approach',

implying that the solution is uncertain over the length of the element.

1.4.4. The Finite Element Method

The finite element method is another application of the spatially discrete element model. FEM utilizes interpolation functions to describe the behavior of a given variable internal to the element in terms of a set of generalized coordinates (usually the displacement of the nodes defining the elements). Thus, using the interpolation functions, and substituting them into the kinematic relations (strain/displacement), the constitutive relations (stress/strain) and the equations of dynamic equilibrium, it is possible to obtain the equations of motion for a single element. Assembling the contribution of all the elements, and introducing boundary conditions, leads to a set of matrix equations having the form of equation 1.2 [17,44].

In the FEM it is necessary to compute the mass, stiffness, and damping matrices. When a linearized Morison equation is used, the fluid damping is often lumped with the structural damping matrix. As the structural configuration of the model changes, so do the stiffness characteristics, and therefore a geometrically nonlinear model must include updating of the stiffness matrix to within a specified tolerance at each increment [33].

For nonlinear dynamic problems the best method of solution is to use an iterative procedure, wherein dynamic equilibrium is achieved to a required tolerance before further incrementing forward in time [40]. The Newton-Raphson Method, or versions thereof, is generally the most popular method for solving systems of equations [33,40,49]; the Newmark Method is generally used for incrementing forward in time [27,18,33,40,49].

Bastero et al [22] introduced a functional which, based on the Hamilton Principle, can be applied to cable and chain dynamics with large sag. The functional is derived using variational principles and can be utilised by the FEM. Good agreement for a static sagged cable problem
was obtained when compared to similar analyses of other authors

In 1983 Ormberg et al [27] used the nonlinear FE package, STOCCA (STOChastic Cable analysis) which utilised the Newmark method, to analyse anchor lines numerically and compare with field measurements, in order to give experimental validation to the FEM. The results presented show good correspondence between measured anchor line tension and the computed dynamic response. It was found that for long, heavy lines, a variation of tension along the line occurs. For shallow waters (70m depths) the difference between quasi static-tension and dynamic tension is within 30%, however this difference increases with increasing water depth and with increasing line weight. At depths of more than 300m, it was concluded that "the static stiffness is of little value for estimating dynamic responses.

Henghold and Russel [9], using FEM based on the virtual work principle, investigated the nonlinear equilibrium and the natural frequencies of single span cables. They developed a constant strain, linear truss element which allowed for large geometrical displacements. The catenary was computed by means of a static analysis, and the first four modes of oscillation were obtained from the frequency analysis, however no comparison was made to the work of other authors. They predict that these elements can be applied to cable networks, and also to systems subject to harmonic forcing.

Leonard and Recker [6] introduced a linear element which Peyrot modified by incorporating catenary segments. Ma et al then upgraded the element to an isoparametric third order cable element capable of dealing with large displacements.

This element is so named because it always assumes the shape of a catenary. Lo and Leonard [23] extended Ma's work by including hydrodynamic effects, while still keeping the third order curved element. A coarse grid of only four elements was used in an experiment where twelve linear elements were needed to give comparable results (Migliore and Webster). Newmark's method was used for the solution of the system of equations and gave good results. The reference state was periodically updated to account for nonlinear behaviour, slacking of the cable or localised plasticity.

Fried [19] claimed that high order elements are more efficient in static problems and indispensible in dynamic problems, in his analysis of tethered balloons in air. Gauss integration of the element total potential energy was employed, and the system of equations was solved by N-R. The three noded cable elements performed well eg. they showed the fling occurring at the tip of a cable falling under it's own weight.

Pastoral and Beaulieu [34] used ADINA to model nonlinear cable systems in air. They presented catenary and parabolic cable models and decided that two noded elastic (truss) elements were adequate for a modal analysis. A good comparison between ADINA and experiment was achieved. Analyses of cables in air can be applied to cables immersed in water, but the main differencies are primarily in the fluid damping, and secondly in the added inertia effect and buoyancy (see 2.2 Drag and Inertia), and the fact of high tension.

In 1984 Bergan et al [33] used linear truss (he refers to truss elements as bar or cable elements) and beam elements in FENRIS to model the large displacement, 3D, nonlinear offshore cable response to ocean forces. Ocean floor contact was simulated by means of contact springs. They justified the use of straight elements (as opposed to Fried's [19] curved elements) for the reasons that they are easy to formulate and cheap to compute because they result in the occurrence of a narrow bandwidth in the equation system.

Difficulties in finding a stable starting configuration were reported. It was suggested that an initial prestress be applied to the cable to avoid singularities, and then to ramp on the loads, which in this case was that of self weight.

The system was brought into static equilibrium (the catenary), by slowly applying gravity and buoyancy loads onto a straight cable, and thereafter Newmark's average acceleration method was used for incrementing forward in time. "This solution stategy has been proven to work very well".

A Cholesky factorization which exploits the matrix 'skyline profile' along with a combined Euler forward incrementation and a Newton-Raphson scheme, was used for solving the system equations.

According to the authors, the FEM performs well but there are dangers of getting numerically ill-conditioned matrices for highly flexible systems, because the axial stiffness is much larger than the bending stiffness. Large displacements and small strains accompany this type of problem.

Palo and Meggit [28] compared the FE programs SEADYN and SNAPLD to experimental data. Nonlinear small displacement (strumming) and large displacement (low frequency 'density flows') were included but localised effects eg. kinking and rotation were neglected. They reasoned that a thorough experimental validation of a program was necessary before it could be considered as a reliable solution to new problems. SEADYN can simulate three dimensions, drag, inertia and composite materials, as well as nonlinear material, geometric and load properties.

SEADYN performed well against experiment except that it always tended to underdamp (but it was felt that underdamping was more because of uncertainties in Cd and Cm rather than the model). This reduced the peaks and also caused a forward

phase-shift in results.

The more limited SNAPLD also gave the right trends but was significantly different to SEADYN for the authors to be fully justified in saying that "uncertainties were in Cd and Cm rather than the models".

Leonard and Tuah [40], found the residual feedback method with artificial damping (viscous relaxation) to be an effective method for predicting the static configuration or catenary, and the incremental iterative technique to be effective for dynamic analysis. The dynamic response is generally considered as a disturbance from the catenary. Start-up convergence problems were observed when the initial tension of the cable was low relative to the applied load in the dynamic analyses. This was overcome by introducing artificial damping into the system, the optimum value of which was based on trial and error, and intuition.

Satisfactory results have been obtained by several authors using the single step, implicit, average acceleration Newmark method, and as a result was employed here [40], for both deterministic and stochastic methods. Modal superposition transformed the linear coupled equations into uncoupled equations and solutions were sought in the frequency domain for the nondeterministic analysis. Time domain analysis was also employed and results were similar for heave and surge in the example problem of a single point mooring cable attached to a floating body.

Jayaraman et al [41], presented a small strain elastic catenary element (or curved element), which they used in an explicit stiffness matrix, for reasons that it can be readily incorporated into nonlinear N-R codes.

Peyrot [43] developed a 'true' cable element, which could be considerably longer than standard linear or even curved elements. This cable element included, in it's formulation,

the standard catenary relations as well as additional geometric relations which were derived by integrating the projections and elementary segments along the length of the cable. Hydrodynamic and gravity forces are treated as distributed forces on the cable, while the inertial loads are lumped at the nodes. The authors developed a cable subprogram which required an iterative procedure to solve for the proposed catenary element.

They reasoned that curvature requirements for lifting from the sea floor necessitates a large number of straight elements for accuracy, whereas a few long 'true' elements could be used. Also, as noted by Webster, straight link elements are extremely sensitive to the choice of an initial configuration, resulting in the paradoxical effect that "more effort is often required to perform a static analysis with straight elements than dynamic". Developing the catenary is much easier with the proposed element, as the danger of singularities is much reduced, and the problem of guessing a good initial configuration is eliminated. Furthermore they claimed that there is no danger of instability when the cable goes into compression, unlike using other elements, where the stiffness must be modified. It was also found that snap loads could be predicted. These elements were found to be far more efficient (CPU time) than standard beam elements, when compared in a submerged cable model.

Hibbit [60], implemented hybrid elements on the FEM package ABAQUS. The characteristic of hybrid elements is that the forces and displacements are considered as independent variables, making them more applicable to flexural structure analyses. The coordinates (which relate to the strain and in turn to the forces) and displacements are then interpolated separately, unlike all of the above isoparametric elements.

A paper by Noor and Babuska [46], gives an up to date (1987) account of assessing the reliability of FEM. They claim that assessing the error bounds on a solution is the most difficult

aspect of FE analysis, and bases his review on 195 references.

The reliability of FEM solutions to engineering problems is influenced by the following factors:

a) Reliability of the mathematical model - identifying the range of validity of the mathematical theory used in describing the model, eg. the applicability of linear elasticity, Morison's equation.

b) Errors and uncertainties in the input information - eg. material, geometry, boundary conditions, loading environment, and the characteristics of the probability fields in the stochastic formulation. The stochastic formulation which is used because of uncertainities in the input data, is in effect a deterministic formulation for the mean and correlation functions of the solution. An alternative to stochastic modeling is made by evaluating the response of the system to each of the input parameters, and determining the sensitivity of the model to changes in these parameters eg. the Monte Carlo Method.

c) Discretization errors - the differences between the exact and the approximate (FE) solution, which are caused by the numerical discretization of the continuous mathematical model, as well as by the truncation of infinite processes, eg. iterative procedures. The exact solution is rarely known, but quantitive estimates are obtained by determining the rate of change of the error as the number of degrees of freedom increases, or the order of the elements increases. In general there are two types of discretization errors viz. a priori estimates (qualitive knowledge of the solution characteristics are determined from the asymptotic rate of convergence as the element size tends to zero), and a posteriori estimates (quantitive measurements of errors during the solution process, by determining bounds using

energy norms, interior residuals, or boundary residuals).

d) Roundoff errors - these occur in the implementation of numerical algorithms on computers with finite precision, and may become critical for problems in which ill-conditioning of matrices could occur.

Different strategies used for the adaptive improvement of FE solutions (feedback procedures) are:

i) successive selection of the meshes;
ii) node relocation;
iii) successive selection of the local order of polynomial;
iv) simultaneous selection of the meshes and the local order,

referred to as the h-p method.

The accuracy of displacements,strains and stresses computed from compatible finite element models can be improved by postprocessing, instead of the easier direct computation of secondary data from the FE solution.

Commercially available FE programs are powerful and versatile, as demonstrated by the programs SEADYN and SNAPLD, which have the capabilities for analysing surface waves, non-uniform current, payout/reel-in, ship speed and strumming [17].

A new field of analysis, the Probabilistic Finite Element Method, is perhaps a future alternative for attempting to quantify uncertainties in the response of uncertain systems to stochastic excitation.

1.4.5. Finite Segments

Fried [19] claims that discretization with rod linkages (inextensible pin jointed links) can be expected to perform

well only in equilibrium problems of cables with low curvature, when he was referring to finite segments [8,11,14].

Winget and Huston [8] investigated the three-dimensional, nonlinear, dynamics of finite segments to represent a cable or chain. Lumped masses are placed at the centroids of inextensible truss elements , which are joined by frictional pins.

Huston and Karman in 1981 [18,12] continued the method by including a nonlinear analysis of hydrodynamic loading. They found that the tangential drag was neglible compared to the normal drag, and that varying the buoyancy with depth should be included. Although small motions of the cable corresponded to experimental results, large displacement analysis did not agree particularly well. The reason is probably that their model was a 'chain' rather than a 'cable', the difference being that a chain cannot support a moment, and moreover, the elements used were inextensible.

Monforton and Hakim [14] applied the principle of minimum total potential energy to finite segments joined by frictional pins and allowed for large displacements and strains. The conjugate gradient method was used for solving, as it avoids convergence problems. However this method suited cable networks well, but not long individual cables where extensibility becomes important.

Wilson et al [12] developed detailed expressions for inclined taut cables, and suggested that large sag problems can be represented by a number of taut segments. Applications of this are limited to cables that never become slack.

Finite segment solutions to problems are quick and easy to use and give a reasonable first approximation to the solution, but suffer from a general lack of versatility in their applications.

1.5 External Cable Loading

Cables are not intrinsically complex structures. It is because of the applied loadings that interesting and complex behaviour patterns in cable responses are observed. As a result, much consideration in any cable analysis must be given to these applied loads. The various types of loadings encountered are mentioned in this section, except for drag, inertia and lift discussed above, and vortex induced loads which are described later.

1.5.1. Weight and Buoyancy

As observed by Ramberg and Owen [13], weight alone accounts for 20% of the total breaking stress of large mooring cables, whereas Davenport [2] noted that the effect of buoyancy reduces this static weight by about ten percent.

The weight of the cable is usually considered as a uniformly distributed load along it's length, as is the buoyancy load which is proportional to the mass of the displaced fluid. Buoyancy is usually assumed to be constant with regards to depth, but Huston et al [18] allowed buoyancy loads to vary linearly with depth, due to increased fluid density.

Nordell and Meggit [44] gave a detailed account of bouyancy modules placed along and at the ends of the cable. Their concern was mainly in the application of suspended riser or pipeline systems and their associated drag, and noted that these module systems could easily be applied to lumped mass analyses of cable type problems.

1.5.2. Tension

The weight of large mooring cable or mine winding cables, alone accounts for a substantial amount of the tension under normal conditions. In guyed tower applications, clumped weights are attached to cables to control their stiffness to displacement ratio at the fairlead position, and as a result cable tensions increase noticeably, on clump lift-off [24,30,36].

Ali [35] asserts that the response of a cable and the change in cable tension are a maximum when the frequency of the forcing function is nearly equal to the natural frequency. In this situation the tension may increase by 250% .Hence, it is of considerable importance to take into account the change in cable tension during motion, especially for sagged cables.

Ormberg et al [27], assert that the difference between quasi-static and dynamic tension calculations increases with increasing water depth, and also that the dynamic tension variation along the line becomes more important in deeper water as well as for heavier lines. It has also been found that static analysis underestimates tensions by at least 20% [37].

1.5.3 Current, Wave and Wind

Environmental loadings are essentialy random in time, magnitude and direction, and thus a statistical analysis of some sort is desirable. Due to the complexity of a complete stochastic analysis, deterministic approaches are often adopted. When and where this simplification is justifiable will be discussed below.

Because the density of air is far less than that of water, wind can be considered as a static load on the cable, relative to the larger wave and current forces [40].

Ocean wave forces are caused by the actions of fluid particle motions. The path of the water particle motion under a wave is that of an elliptical orbit, which decays exponentially with depth. These forces are more pronounced on large bodies than on cables [40] because diffraction and inertia become increasingly dominant over viscous and form drag as the size of the body increases.

Currents are caused by density differences in the oceans due to differences in salinity content, tides, and wind. Only wind generated currents are significant in the open ocean [45], especially during storms, where the surface currents are largest but decay with depth. The significance of currents is that the current velocity is added vectorially to the wave velocity. In the case of sheared currents, drag and damping vary along the cable as mentioned by Kim and discussed in section 1.3.

The sea has been divided essentially into two states viz. normal and extreme conditions. Designs are based on, for example, the 100 year storm cycle, which corresponds to the extreme case of the sea state. This is often modelled deterministically based on a previous such storm, and is considered as a 'design wave' [45]. The 'normal' sea state is usually modelled stochastically, and it is in this sea state that a fatigue analysis is considered necessary.

The deterministic method of wave force calculation is commonly used as a primary basis for design, particularly when nonlinear effects associated with drag are important, whereas most stochastic processes require the linearization of Morison's equation for a frequency domain analysis [45].

The low frequency oscillations of mooring cables, due to slowly varying wave and wind forces, have periods which are normally much longer than the natural periods (minutes compared to 10 seconds). The slowly varying motions are

therefore in this case not considered in the dynamic mooring line analysis, but can be regarded as a change of the static position [45].

Meggit et al [17], recommends both nonlinear and stochastic analysis, for analysing a complete cable system, but agrees with others that the random processes of the oceans, are far from understood.

The first consideration concerning wave forces is, how to model them; what realistic simplifying assumptions can be made yet still allow for a reasonable model? Various theories exist, the two most popular being Airy's linear wave model [30,31,47], and Stokes' models [51]. The so called significant wave height (H), and the period (T), are the main parameters used for characterizing waves.

Airy theory assumes an inviscid, incompressible fluid, and the wave amplitude to wave length should be small. The advantage of linear theory is, that it can be used directly in a frequency domain analysis (which requires superposition of responses from a number of discrete waves, or a spectral analysis).

Leonard et al [45] reviewed fluid forces on structures in a paper published in 1981, and arrived at the following conclusions:
Stokes' wave theories provide valid solutions in deep water ie. h/L > 0.5 (where 'h' is the mean water depth and 'L' the wavelength), but the limit of H/T**2 may be as low as 0.012 m/s/s. The theory of Stokes appears to be the most popular as it presents a good compromise between range of applicability and complexity.

The newer cnoidal wave theories of Laitone and Chappelear are mathematically more rigorous, being based on the perturbation expansion developed by Friedrichs. However, these solutions suffer the same difficulty as Stokes' wave theory, viz. As the

wave height (H/T**2) becomes larger, the series diverge. The cnoidal theories tend to overpredict the velocities under the wave crest as the wave height increases. The wave theory of McCowan has shown no tendencies to diverge and predicts velocities under the wave crest of shallow water waves rather well. The Dean Stream Function Wave Theory has been experimentally validated over a wide range of h/T**2 and thus "appears to represent the most appropriate wave theory for engineering applications" [45].

Dawson [51] investigated the effects of regular and random deep-water waves with varying frequencies and heights. Results for regular waves with heights ranging from 50 to 500mm and frequencies from 0.4 to 0.9 Hz, show that Morison's equation, with Stokes' theory and constant Cd and Cm provides good agreement with the measured maximum wave forces, and force variation over the entire cycle. The linearized Morison equation, with linear wave theory and the same coefficients, likewise provides close agreement with the measured rms wave forces for irregular random waves, having approximate Bretschneider spectra and significant heights from 125 to 350mm. A dimensional analysis technique known as similitude can be used to relate these results to ocean waves.

Stokes' 2nd order theory was used because, even for the largest waves, contributions from more than two terms in the Stokes' theory were negligible. The wave frequency in terms of wave number and water depth, for both linear and higher order theory, was expressed as,

$$\Omega^2 = g \cdot k \cdot \tanh(k \cdot h) \qquad 1.3$$

In conclusion Dawson found that the Stokes' theory provides very close agreement with the measured surface deflection, including the nonlinear effect of greater crest than trough deflection from the still water level.

Paliou et al [47], used a wave height spectrum specified by Pierson and Moskowitz for analyzing fully developed sea conditions described by their power spectral densities. The wind induced storm waves are modelled as stationary Gaussian random processes with zero mean and finite duration. This implies that the wave height and water particle velocity are also stationary Gaussian random processes. A Monte Carlo statistical method is used for fatigue analysis, and the occurrence of a storm wave is modeled as an homogeneous Poisson process.

Leonard and Tuah [40], used weakly nonlinear and slightly nonGaussian second order waves on cable and large body systems, utilizing a Fast Fourier Transform (FFT) for simulating the waves. They provide a detailed discussion of nondeterministic (stochastic) spectral amplitudes (NSA) and deterministic spectral amplitudes (DSA). Several peaks in the spectral curve for surge indicated resonance at the natural frequencies. The spectral shape of the large body motion for heave is almost identical with the wave surface spectral shape, and the spectral response for the pitch peaks at a frequency equal to the natural frequency where the modal shape is predominantly pitch.

It is also recommended that the mean of the response spectrum of the guyed tower, varies from that of the wave energy spectrum, by as much as possible to reduce the effect of wave loading near resonant conditions.

Mo and Moan [48] compared the response of guyed towers subject to 3 different wave theories viz. i) Airy's, ii) Airy's with Wheeler's empirical approximation and, iii) Airy's with vertically homogeneous fluid field above mean water level. They describe these theories and also provide a discussion of the discrepencies of the results, and where each theory is best suited. Results of a nonlinear time domain and a stochastically linearized frequency domain were also compared.

It was found that both the mean and the standard deviation of the spectral densities increased with increasing significant wave height for all three models. Wave theories ii) and iii) compared well for all the tests, whereas it was found that the simple Airy theory became erroneous by 50% when the wave height was larger than 20m for a wave height to wave length ratio of 0.1.

Conclusions are that varying the hydrodynamic loading, significantly affects the response of the tower. The probability density function obtained by the nonlinear wave model, was more peaked, with more energy in the tails, than the Gaussian responses obtained with the linearized wave models. The results obtained by stochastic time domain simulation exhibit considerable statistical uncertainties due to the sampling of the stochastic load process. Finally, there is a need for comparison of results from stochastic dynamic response analyses with model and full-scale measurements, to obtain further knowledge about the uncertainties involved.

1.5.4. Boundary Conditions

Nordell and Meggit [44] discuss various types of anchors used to resist the tensile effects of the cable, viz. dead weight anchors, piled or driven-in anchors, and heavy drag anchors. The driven-in anchor can be considered as a fixed end, unable to support a moment ie. allowing only rotation. Drag anchors are more difficult to analyse, because they may move, which would involve both friction and mud-suction effects.

The end attached to the offshore facility could be considered to have a prescribed displacement, if analysis of the whole system is not undertaken, but this entails neglecting the cable/offshore facility interaction, and so is an over simplifying assumption. The extent to which the uncoupling of the cable and offshore facility is true has still to be

investigated.

1.5.5. Tectonic Forces

For offshore rigs in shallow water, the effect of earthquakes should be considered, but generally, guyed towers are located in deeper waters, where earthquake loadings are considered insignificant compared to other environmental loads [47]. According to Leonard [45], because guyed towers have minimal lateral constraint (as a result of their being flexible), earthquake loadings are of secondary importance.

1.6 Vortex Induced Oscillations

Most authors (44,45,23) are concerned with the added drag effect caused by vortex shedding, for cable type problems, rather than the actual mechanism of the oscillations. This is because of the complex nature of these oscillations, and the above assumption is generally regarded as acceptable. Vortex shedding is thus accounted for by simply choosing an acceptable value for the drag coefficient which accommodates both viscous and form drag. Although this simplifies the problem substantially, it may not be sufficient for an accurate response history of cable dynamics. As a result [28], the analysis of vortices will help in :

(i) the prediction of cable response to fluid motion,
(ii) tabulating drag, added mass and lift coefficients and
(iii) the prediction of the propagation of fatigue and the resulting life span of marine risers and mooring cables

A brief explanation of generally accepted knowledge on vortex shedding follows [44,45,16,10] :

Vortex induced oscillations (often termed strumming) are characterised by relatively small-amplitude, high-frequency cable vibration, causing a marked increase in drag, accelerated fatigue and higher stresses [44].

When a fluid flows around a body, lift forces perpendicular to the flow result. In the case of a circular cylinder the lift forces on either side, are theoretically balanced (due to geometric symmetry).

The separation of a streamline from a body occurs when the fluid must take too sharp a bend to keep in contact with the body's boundary. This so called 'point of detachment' causes an instability in the fluid which results in the periodic shedding of vortices, which travel downstream forming a wake known as a Karmen vortex street (see fig 1.2).

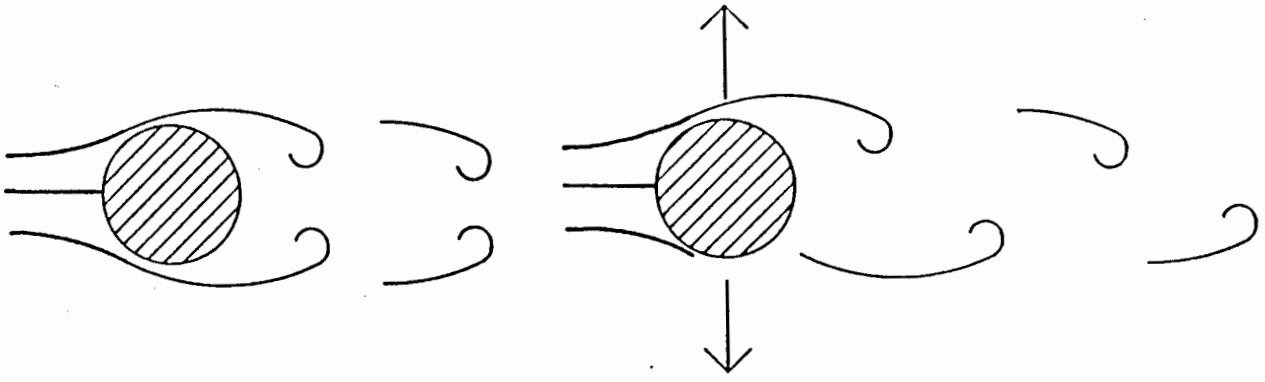

a. Stationary Cable b. Oscillating Cable

Fig 1.2 Vortex Induced Oscillations

The resonant or Strouhal frequency at which this occurs is determined by holding (in our case) the cable stationary and observing the vortex pairs being shed, when subjected to a uniform flow. Once the cable is released the overall situation is unstable in that the slightest lack of symmetry will result in opposing lift forces being out of phase, causing the cable to move perpendicularly to the direction of fluid motion and

towards the side shedding the vortex. This is equivalent to subjecting the cable to a periodic force in the transverse direction at a frequency corresponding to that of the vortex shedding, which usually causes cable oscillation.

Thus steady and unsteady form drag in line with the flow and unsteady lift perpendicular to the flow can result. For lightly damped members, oscillations occur parallel to (as well as perpendicular to) the flow. Transverse oscillations are an order of magnitude larger than in-line oscillations, which would then result in an elliptical motion of the cable.

If the cable and vortex shedding have similar natural frequencies, a phenomenon known as lock-on occurs whereby the cylinder motion takes control over the shedding process [52], and together they enhance oscillation (as in resonance). This happens when the wake's and cable's natural bandwidth or synchronization range overlap and is maintained over a wide range of flow velocities. It is interesting to note that this resonant bandwidth is wider in water than in air.

Strumming has been classified into 4 categories viz.

i) Resonant lock-on, a situation in which stable sinusoidal motion occurs,

ii) Non-resonant lock-on, where because the frequencies are slightly different erratic modulations occur,

iii) Non lock-on, where the natural vortex shedding is outside the synchronization range,

iv) Galloping, where fairly violent non-uniform oscillations occur, often when the member is in the wake of another member upstream.

Researchers generally agree that drag forces on a vibrating cylinder appear to be about 2 to 2.5 times greater than that of a stationary cylinder [16,52,54,44,39,28], and up to 4 times greater in the case of clumped weights [16].

The following dimensionless parameters are commonly used in

analyses: Reynolds number (Re), length to diameter ratio (L/D), angle between the cable and the incident flow (theta), tuning parameter (a function of the cable tension, density and length - which determines the mode of vibration), and the density ratio.

Overvik and Moe [52] from experiments on risers found that non-constant Cd increases more substantially in the lock-in range than in the galloping mode.

In their experiments the inertia coefficient (Cm) and the frequency changed through the lock-in region. Results were: Cm=4.2 for Ur=4.5 (reduced velocity) , Cm=1.0 at Ur=6.8 (maximum response) and Ca=-0.9 at Ur=10.0 . However the frequency of vibration at perfect lock-in is close to the value obtained in still water, deducing that this Cm approximates the still water Cm

Kato et al [53] developed new expressions for in-line and transverse drag coefficients. Using the Keulegan-Carpenter number (K-C) and a velocity ratio (amplitude of cylinder vel/flow vel), values of Cd in various regions were established; the range of Cd being between 0.5 and 1 . They found that Cd depends heavily on the dimensionless frequency (oscillation frequency x diameter/flow velocity) and only slightly on the velocity ratio and K-C.

Few papers concerning cables directly (as opposed to flexible cylinders) exist, but a paper by Kim et al [39] gives comprehensive experimental data on long cables subjected to sheared flows ie. currents in which the flow velocity varies with depth. Experiments were performed in the ocean on small diameter (5mm) Kevlar cables with lengths from 30m to 3000m. As a result the cables were almost neutrally buoyant and therefore the static tension was essentially constant along the length of the cable. The material damping ratio was found to be roughly 0.16% , about a sixth of the fluid damping.

Several important conclusions were drawn, viz:

i) To predict the response of long cables in sheared flows an infinite string formulation may be appropriate rather than the conventional modal analysis which assumes the presence of standing waves along the cable, because the propagation of disturbances along the length of the cable is damped out.

ii) Substantially different frequencies were consistently recorded at three specified locations along the long cable (measured by biaxial accelerometers), implying that single mode lock-in never occurred.The authors conclude that the current shear, structural and hydrodynamic damping are responsible for the variation in response spectra along the length . The response at any location is dominated by local excitation but is a result of superposition of waves that have been excited over the entire length, attenuated by the distance travelled. For linear damping the decay is exponential and for highly damped systems lock-in will not occur.

iii) Values of Cd were much less than those obtained for short cables in uniform flows and lock-in conditions.

iv) Due to length limitations, past research allowed only very low modal density (well separated natural frequencies), which promoted lock-in [16,54]. Furthermore the parameter beta reflects only the properties of the flow and not the structure. As a result a new parameter is defined which is useful for predicting lock-in. A measure of the likelihood of lock-in is given by the excitation bandwidth due to current shear and the separation in frequency between natural modes. This new parameter is described as: the number of natural frequencies contained within the excitation bandwidth. If this number is large, lock-in will not occur. Another parameter cited in the literature L/D [16], is considered of limited importance for long cables compared to the proposed

L/lamda, in establishing the dynamic response.

v) Higher velocities produced larger response. Assuming constant Cl, local r.m.s. displacement response will be proportional to the square root of the local flow velocity.

vi) Though not yet confirmed local Cd appear higher in regions of greater r.m.s. displacement response and since Cd is dependent on response amplitude, relating flow velocity to response amplitude will enable the prediction of a local Cd.

vii) Cd was found to be independent of tangential drag Ct.

iix) Under lock-in, the power injected into the cable by the fluid, is balanced by the power dissipated internally by the material losses, concluding that hydrodynamic damping is irrelevant to lock-in vibration.

ix) Responses along the cable length were not always in the same plane, which would suggest that a 3D analysis should be permormed if possible, depending on the magnitude of the error in a 2D analysis.

Griffin et al [16] in 1980 performed experiments of vortex excited oscillations of marine cables, and found that an increase in flow causes an increase in cable displacement, but negligible change in the frequency. This is in agreement with Kim et al [39] but Overvik and Moe [52] claim otherwise; viz. that in the lock-in range the frequency increases with the flow and in the galloping mode it decreases

In reference [38] a method is outlined for predicting responses of a flexible cylinder in a unidirectional sheared flow. By independently predicting a number of monochromatic, multimode dynamic solutions using rigid cylinder experimental results, their procedure allows for the evaluation of the lift response frequency, amplitude and phase between modes.

It has also been found [59], that as the damping increases, the oscillation amplitude decreases, and the lock-on bandwidth

becomes wider.

Bokaian and Geoola [54] , from experimental investigations on multiple risers, found that galloping only occurred when one cylinder was inside the near wake region of the other one. In this region, the static lift forces had peak values, while the drag forces remained lower than a single cylinder value. However for most purposes cables are isolated from other bodies, but research is being done on spoilers (attachable to cables), to supress vortex shedding and thus change the drag characteristics in a required manner.

The above discussion has been concerned mainly with steady flow. For wave induced oscillatory motion the effect of the previous half-cycle wake should be considered [45]; refer to 2.3 . When K-C is large the vortices shed from the previous half-cycle have time to dissipate before flow reversal, so it is only for the case of low K-C that any interaction of cycles occurs.

Further study is recommended in the field of vortex shedding for steady and oscillatory flow [2,45,44,51].

1.7 Ocean Floor Contact

Mud suction forces on the cable and clump weight as it is being lifted tend to increase the stiffness of the guying system [24]. 'Go, no go' springs were incorporated in the stiffness matrix of the model to account for the suction. These springs monitor the gap between the ocean floor and the cable, and become inoperative at a certain gap; otherwise their stiffness is inversely proportional to the gap size. The effect of the mud simulation was to increase the hysteresis of the response and tension, ie. increase the maximum and minimum values.

Friction has often been neglected when dealing with ocean floor contact, because suction has the greater effect [27,42].

Bergan et al [33], used nonlinear spring elements to simulate ocean floor contact, but friction was neglected.

Peyrot [43], comments that his true cable finite element (see 2.4.4), could easily accommodate ocean floor contact, although he did not include either friction or suction.

1.8 Impact and Snap Loads

Snap loads occur when a cable goes slack and is abruptly retensioned. This happens when the dynamic tensions exceed the static tensions in the line [28]. The magnitude of these snap loads is difficult to predict, but it can, and does, cause line failure or increased fatigue [47]. Snap loads six to ten times greater than the static load have been measured [44].

When the clumped weights lift off the ocean bed in stormy conditions, an impact load is often imparted to the cable [37].

Peyrot [43] claims that his 'true' cable element is capable of predicting the severe shock loads caused, when the cable changes rapidly from a slack to a taut configuration.

Wave slamming (ie. when surface waves impound against a body), on structural members occurs at the free surface of the ocean. This is most critical for members which have a diameter the same order of magnitude as that of the wave length, and is most severe for horizontally placed risers [45]. As a result this loading can be neglected for mooring cables, which are of relatively small diameter, and are placed vertically.

1.9 Guyed Tower/Cable Interaction

Brinkman [24] investigated the effect that guyline dynamics has on an immersed guyed tower. He considered the cable in three sections viz. line, clumped weights and an anchor pile, and obtained good results and illustrations of the clumped weight lift-off and it's associated changes in stiffness, tension and displacement.

The analysis was performed as follows: the tower offset would give a boundary displacement to the cable. This displacement would then change the geometry and tension of the cable which would change the force input on the tower, thus causing a new tower offset for the next step.

A static and dynamic analysis of a guyline system was previously undertaken to observe tension and displacement effects. Hysteretic loops around a static mean resulted from the dynamic analysis, and these loops were at their largest when the velocities were large, and thus in conclusion it was felt that the drag was the dominant dynamic force on the guyline. Interestingly, static analysis overpredicts tower offset, and underpredicts tower tension, again demonstrating the importance of drag. The coefficients used were: Cm = 1.0 , Cd = 1.0 (cable) , Cd = 2.0 (clump).

Morrison [30] considered the cable to be in three portions viz. a catenary from the fairlead position to the clump, the clump weight itself and an anchor line from the clump to the anchor pile. His analysis was essentially based on the fairlead response of a particular 300m tower. Airy wave theory was assumed for the water particle kinematics and Morrison's equation was used for fluid drag and inertia terms. Typically the largest displacements at the fairlead were 15m, which corresponded to tensions of 7000 KN on the weather side, and 500 KN on the leeward side. The dynamic response of the cables (including hysteresis loops) was taken from a FEM analysis, and used as input for SDOF and MDOF models.

For the weather side guyline the force-displacement relationship could be summarized as follows: An initial tightening and increase in stiffness of the cable occurred as the tower moved away, a collapse portion where the tower velocity changed direction, and a plateau portion when the cable force attempted to go below the constant force portion in the cycle. The leeward side used statically derived force-displacement relationships as a starting point each time the tower velocity changed sign.

In a subsequent paper [31] it was found that a SDOF tower model agreed well with a MDOF model for the fundamental mode of vibration, when the frequency of the forcing function is equal to or less than the 1st natural frequency of the structure. Also the simple model gives an insight into the behaviour of the system, and could be used as initial conditions for a more detailed analysis.

In a further paper [32] Morrison states the importance of good modelling of the cable is essential for at least reasonable modelling of a guyed tower. The sensitivity to variations of Cd,Cm, and wave height (between 22m and 30m) were considered.

By increasing the wave height, both the maximum and minimum wave loadings were increased, and the differences between static and dynamic analyses became more pronounced. It was found that the steady state response of the tower had negligible change for Cm changing from 0.37 to 1.0 , although it did increase the total wave force.

A change of Cd from 0.64 to 0.9 substantially increased the wave loading, especially for the dynamic (vs static) model, of the tower.

An increase in wave height from 22m to 30m increased the wave loading, again especially for the dynamic case.

1.10 Subharmonic Responses

Chih-Young [50], investigated the phenomenon of subharmonic oscillations which could occur in flexible offshore structures. Subharmonic oscillation is defined as - the steady state oscillation of a structure, whose vibrating frequency is a fraction (eg. 1/2, 1/3, ... 1/n) of that of the applied force, and is referred to as subharmonic resonance. In this study only frequencies of the order 1/2 were considered.

The combinations of three different linear waves and two values of drag coefficient, were analyzed in the time domain. Numerical results, not only demonstrated the existence of subharmonic components in the responses, but also confirmed the existence conditions for such components. The main source of nonlinearity that causes the subharmonic response in the system is identified to be the large displacement effect in the wave force calculation.

1.11 SUMMARY OF NUMERICAL ASPECTS IN THE LITERATURE SURVEY

The following section summarises the above literature survey with regards to numerical aspects and associated difficulties, as this is the direction of research concerning the thesis.

For a comprehensive analysis of large sag cable dynamics, it seems essential to use numerical methods. The FEM appears to be the most powerful and versatile method available, and as a result is the most popular method.

A taut vibrating string fixed at both ends presents few modelling or solution difficulties. It is the effects of large sag and, small
strain - large displacement which cause numerical difficulties. The larger these phenomena, the more difficult will be the associated problems.

It is still unclear which elements are the 'best' (trade-off between accuracy and cost) to use in the FEM, viz. in this case truss or beam elements. Furthermore there is a discrepency whether to use many straight (first order) elements, which are easy to formulate and produce a narrow bandwidth in the matrices, or fewer curved (higher order) elements.

Uncertainties in the solution are determined a priori and/or a posteriori. By applying the a priori approach - which entails comparing runs of different numbers and orders of elements and observing the asymptotic rate of convergence - an idea of the efficiency of the various elements can at the same time be obtained.

Before any dynamic behaviour of cables can be analysed a static catenary must first be obtained from an initial

straight line configuration. This has been achieved statically by allowing for small forward increments; or dynamically by having a large artificial damping coefficient, a large numerical damping coefficient or simply moving the cable very slowly, to avoid oscillations or spurious modes. Prestressing of the cable has often been applied in order to prevent a singular, initial stiffness for the elements.

Allowing for inertia further alleviates the problem of initial singular matrices, and this is why a dynamic analysis has often been preferred as a start-up procedure. Gravity forces were applied incrementally at the same time that auxiliary forces were removed. These initial increments were small to avoid non-convergence.

Because of the very nature of cables viz. slender flexible structures, ill-conditioning of the matrices in the FEM is likely to occur. This is as a result of the low bending stiffness compared to the relatively large axial stiffness. The likelihood of ill-conditioning, in both the stiffness and mass matrices, is further increased if modelling of the effect of clumped weights attached to the cable, is considered.

The literature appears conspicuous by the absence of a complete cable/tower interaction under the influence of waves. This is probably because of the computational costs involved, and due to the interest being mainly on cable response, as well as of the still further increased effect of ill-conditioning, which arises out of having a very stiff tower (bending and axial) compared to the compliant cable. Methods which attempt to alleviate ill-conditioning are the so called regularization and P-adic methods, which entail programming algorithms particular to the problem.

The two most popular wave theories used are Airy's and Stokes'. The former is less expensive, while the latter, which comprises a non-linear theory, is more applicable in deep water, especially if Stokes' 5th order wave theory is used.

There is still controversy over what values of drag and inertia coefficient to use in the generally accepted Morison Equation. It is also unclear how sensitive the system is to varying choices in these coefficients. This difficulty is further enhanced when one considers vortex shedding, and it's effect not only on increasing cable fatigue, but also by increasing the drag on the cable by as much as 2.5 times. To date, no numerical model of cables has accounted for vortex shedding directly, and it is usually considered acceptable to combine the effect of both viscous and form drag into one coefficient.

Further difficulties are encountered as the complexity of the model is increased, and therefore nearly all the analyses are performed in two dimensions because the added costs incurred in three dimensions are not always justifiable.

Ocean floor contact has been considered by a number of authors, and has demonstrated that more localised stressing occurs as a result of the cable impacting on the sea floor. Furthermore, only crude models of mud suction and sliding friction have been considered. In this case friction was modelled as a dashpot and mud suction as a nonlinear spring.

2. FORMULATION OF THE SUBMERGED CABLE PROBLEM

This section deals with the mathematical formulation of cable problems as described in the literature survey in chapter one. The catenary relations are derived, followed by the wave theories used in the thesis. The statement of Morison's equation is included, and the above is then combined to formulate the finite element method.

2.1 Development of the Governing Equations

The mathematical formulation of the equations modelling a flexible structure forms part of the class of general boundary value problems. The cable catenary and an elemental section thereof are shown in figure 2.1 . All loadings (weight + fluid forces), internal forces (axial and bending) and dynamic responses (accelerations, velocities and displacements) are shown on the element for the case of oscillating cable motion.

The well known catenary differential equation [2, 43, 65] of a perfectly flexible, inextensible cable hanging under it's own weight, assuming a linear tension along the cable, is of the form

$$F_t \frac{d^2y}{dx^2} dx = w\, ds \qquad 2.1$$

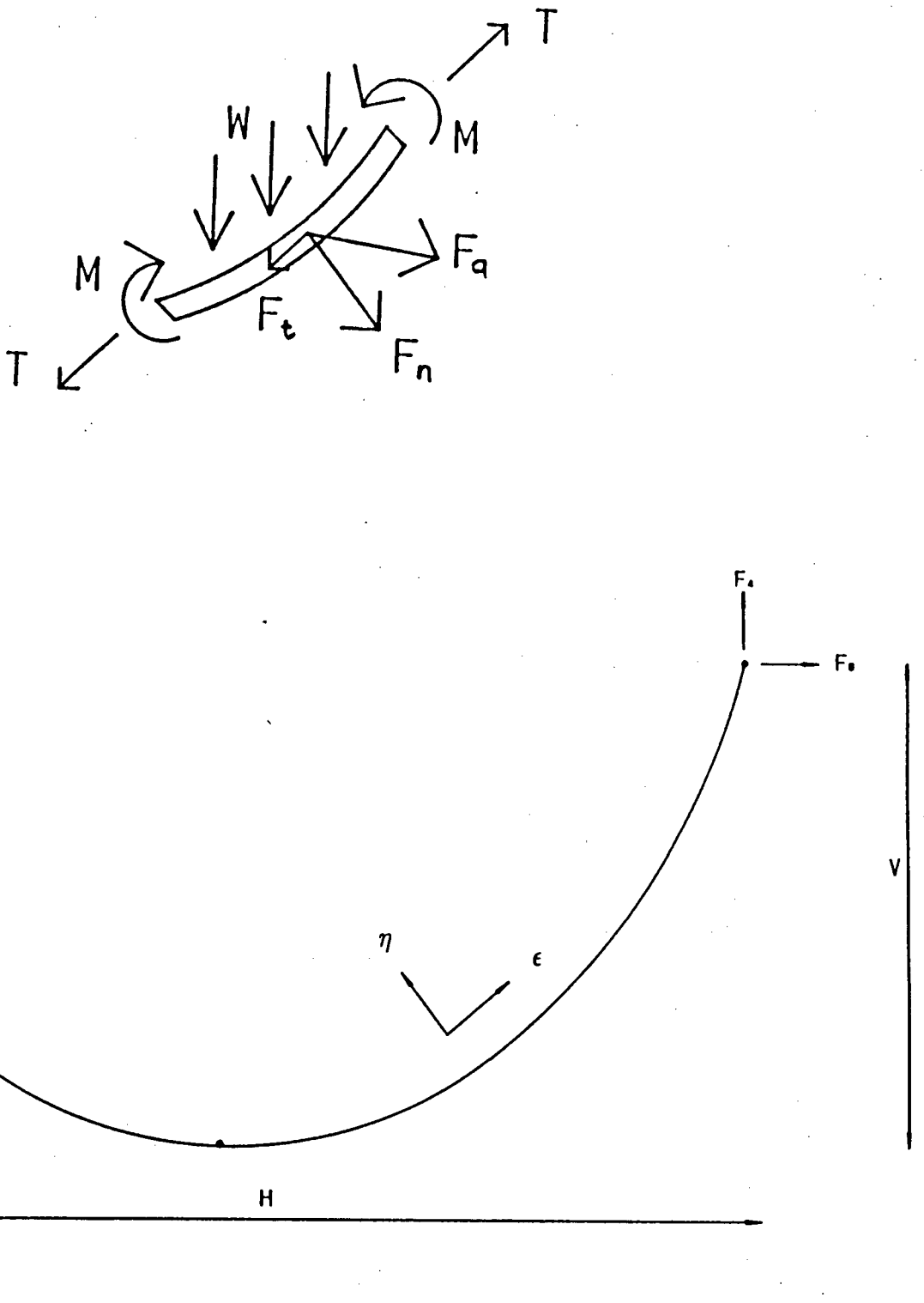

Fig 2.1 Cable Catenary and Cable Element

Integrating equation (2.1) twice and solving for the constants with boundary conditions x=0 at y=0, x=L at y=H, shown in reference [1], yields the following catenary relationships;

$$L^2 = V^2 + (H/\lambda)^2 \sinh^2 \lambda \qquad 2.2$$

$$F_2 = \frac{1}{2} w (- V \coth \lambda + L) \qquad 2.3$$

where (for F_H being the horizontal component of F_t),

$$\lambda = \frac{w |H|}{2 F_H} \qquad 2.4$$

For perfectly flexible elastic cables, Peyrot [61] derived three additional geometrical relationships by integrating the projections and lengths of elements along the length of the cable, and obtained;

$$H = -F_1 \{ \frac{L_u}{EA} + \frac{1}{w} \log \frac{F_4 + T_j}{T_i - T_2} \} \qquad 2.5$$

$$V = \frac{1}{2EAw} (T_j^2 - T_i^2) + \frac{T_j - T_i}{w} \qquad 2.6$$

$$L = L_u + \frac{1}{2EAw} \{ F_4 T_j + F_2 T_i + F_1^2 \log \frac{F_4 + T_j}{T_i - F_2} \} \qquad 2.7$$

The next development (not chronologically) was to include bending, which most authors have considered to have negligible effect compared to other parameters.

Costello [65], an authority on material and mechanical properties of cables, considered the cable to be a composite of many helical springs in frictionless contact with each other, and arrived at the expressions for bending as;

$$M = \left\{ \frac{6\ (\ 2\sin\alpha\ )}{2 + v\cdot\cos^2\alpha} + 1 \right\} \frac{EI_s}{R_c} \qquad 2.8$$

for a 7 stranded cable, where

I_s = 2nd moment of area for a single strand

α = Helix angle - usually about 70 degrees

v = Poissons ratio

R_c = Radius of curvature

Interesting to note is that typically a cable of equal diameter to that of a steel rod has 8% of the bending stiffness, or 12% of the bending stiffness for equal metallic cross sectional area. This can be used for a first approximation to the cable bending stiffness.

However because of the difficulty involved in calculating the bending characteristics from the wire strand properties and winding configuration, it is usually acceptable and often better to use empirically tested values of bending for given curvatures. Including bending as a function of curvature affects the cable in approximate proportion to that of EI affecting a beam. Typically, bending is described by

$$M_{cable} \approx \frac{1}{12} M_{beam} = \frac{1}{12} \cdot \frac{ED^4\pi}{64} \cdot \frac{1}{R_c} \qquad 2.9$$

and when combined with equations (2.5), (2.6) and (2.7)

results in lengthy algebraic expressions, which for a fixed span (H) and height (V) result in a smaller cable length (L), ie.bending stiffness decreases the extension of the cable, but causes higher stresses in the outer fibres of the cable.

Incorporating dynamic behaviour into the model further complicates matters especially if non-conservative effects eg. damping are considered. Summing forces on the cable element in a direction normal to the cable yields the equation

$$-T\frac{\partial\eta}{\partial\epsilon} + \left(T + \frac{\partial T}{\partial\epsilon}d\epsilon\right)\left(\frac{\partial\eta}{\partial\epsilon} + \frac{\partial^2\eta}{\partial\epsilon^2}d\epsilon\right) = \rho d\epsilon\frac{\partial^2\eta}{\partial t^2} \qquad 2.10$$

For small vibrations equation (2.10) reduces to

$$\frac{\partial}{\partial\epsilon}\left(T\frac{\partial\eta}{\partial\epsilon}\right) = \rho\frac{\partial^2\eta}{\partial t^2} \qquad 2.11$$

because 2nd order terms become negligible. However for large displacements, the main concern of this thesis, equation 2.10 should not be simplified. Converting equation (2.10) into X and Y coordinate directions, yields

$$\frac{\partial T_H}{\partial x}dx = dm\frac{\partial^2 x}{\partial t^2} = \rho A dx\frac{\partial^2 x}{\partial t^2} \qquad 2.12$$

and (where T_H is the horizontal component of tension),

$$\frac{\partial^2 y}{\partial x^2}T_H + \frac{\partial T_H}{\partial y}\frac{dy}{dx}\cdot dy = \rho\frac{\partial^2 y}{\partial t^2} \qquad 2.13$$

If equation (1.1) is reordered we get

$$\frac{d^2y}{dx^2} = \frac{w}{T_H}\cdot\left(1 + \left(\frac{dy}{dx}\right)^2\right)^{\frac{1}{2}} \qquad 2.14$$

Differential equations (2.12), (2.13) and (2.14) describe the motion of an inelastic cable vibrating in air. Obtaining a closed form solution of these equations is difficult and cumbersome, but would result in an equation for the cable shape of the form,

$$y = F(w, T_H, x, t, \rho) \qquad 2.15$$

Incorporating axial elasticity and bending stiffness into the dynamic model complicates the solution to a degree which necessitates the need for numerical methods, where the elemental governing equations are then derived for the simple continuum element which are linked together by the compatibility equations as shown in section 2.4.

2.2 Wave Theories

The expression for the equilibrium of an accelerating fluid element is expressed as

$$\rho\left(\frac{\partial \underline{V}}{\partial t} + \underline{V} \cdot \frac{\partial \underline{V}}{\partial t}\right) = -\rho \frac{\partial G}{\partial \underline{x}} - \frac{\partial P}{\partial \underline{x}} \qquad 2.16$$

where $\underline{V}$ is the vector velocity field.

The first term in brackets describes the local rate of change of V at a fixed point, while the 2nd term (which introduces the nonlinearity), describes how the elements velocity changes due to it's changing position. In linear theory, the disturbances are considered so weak as to be negligible, and

so the 2nd term is dropped. This is acceptable for the assumption that the wave height is small compared to the wave length.

Lighthill [67] describes the reason for nonlinear wave analysis as "By a nonlinear wave is implied, any feature of real wave motion that can't be reproduced in a linear analysis". This is to say, that as soon as waves become large (ie. when the amplitude to wave length ratio exceeds a given criteria eg. 0.2, or the water depth increases above a certain amount relative to the wave height), a nonlinear theory becomes necessary for reasonable accuracy. As the thesis deals largely with storm 'design' waves, a nonlinear theory is desirable.

Since irrotational flow is assumed, the flow potential obeys Laplace's equation,

$$\nabla^2 \phi = 0 \qquad 2.17$$

with the fluid velocity described as,

$$\underline{V} = -\frac{\partial \phi}{\partial \underline{x}} \qquad 2.18$$

Combining (1.16) and (1.18) and integrating with respect to position yields,

$$\rho\left(-\frac{\partial \phi}{\partial t} + \frac{1}{2}\underline{V} \cdot \underline{V}\right) = -\rho G - P + F(t) \qquad 2.19$$

where F(t) is an arbitrary function.

The derivation for obtaining wave particle motion as a

function of t and x in linear or Airy theory is standard and can be found in references [65,66,67]. The term $\underline{V}\cdot\underline{V}$ is considered negligible for small $\underline{V}$, and is set equal to zero, so the particle motion then becomes,

$$\Phi = 2\, A^{-kh} \{\cosh k (Z + h)\} \cdot \{\sin (ks + \Omega t + \beta)\} \qquad 2.20$$

where

$$\Omega^2 = \frac{gk \sinh (kh)}{\cosh (kh)} \qquad 2.21$$

$$\mu = 2\pi / k \quad \gg \quad A \qquad 2.22$$

To get fluid particle velocities, apply equation (2.18) to equation (2.20).

For nonlinear theory, Kortweg and de Vries approximate Ω as

$$\Omega = g\, h_0\, k^2 \qquad 2.23$$

with higher terms neglected, when they developed the cnoidal wave theories. This was later updated to

$$\Omega = k \sqrt{gh_0} \cdot [\, 1 + k^2 h_0^{\,2}/6 + 9\beta^2/16 k^2 h_0^{\,2} + \ldots . \,] \qquad 2.24$$

The 2nd term shows the crucial dependence of the dispersion relation (or wave frequency) on the wave amplitude.

Stokes' original result for deep water waves was

$$\Omega^2 = gk (1 + k^2 a^2 + \ldots .) \qquad 2.25$$

which is used in the Stokes' wave theories. His 5th order

theory corresponds to five terms in the above wave frequency approximation. In shallow water, the difference between Stokes' and Airy's waves is fairly negligble, but in deep water, the Airy theory starts becoming inaccurate in the wave particles' motion, and the Stokes' theories are preferred.

2.3 Morison's Equation

In 1950 a semi-empirical equation was introduced by Morison, which essentially relates the motion of fluid particles to the load that they impart onto the cable. Morison's equation is applicable to structures with diameters substantially less than the length of the applied wave, which is typical for all real cable problems. For larger diameter to wavelength ratios, wave diffraction effects should be included.

Referring to figure 2.1, the total fluid loading is comprised of

$$F = F_n + F_a + F_t + F_l \qquad 2.26$$

where

F_n = normal drag force (includes form and viscous drag)

F_a = fluid inertia force

F_t = tangetial drag force (skin friction)

F_l = lift force

Lift forces occur perpendicular to the plane of the cable and are usually neglected because of their nominal importance. For a two dimensional analysis, these lift forces are non-existent, although in reality periodic lift forces create

vortex shedding, which increases the total drag in line with the fluid velocity by about 200% . This added drag is incorporated in the empirical drag coefficient.

With this simplification Morison's equation is expressed as,

$$F = \frac{1}{2}\rho C_d D V_{NR}|V_{NR}| + \frac{1}{4}\rho \pi D^2\left[C_m A_N + (1-C_m)\ddot{u}_N\right] + \frac{1}{2}\rho G \pi D V_{NR}|V_{NR}| \qquad 2.27$$

where

$$V_{NR} = V_N - U_N \qquad 2.27b$$

where Cd, Cm and Ct are often considered constant for the sake of simplicity, as is the case in ABAQUS. Tangential drag (skin friction along the length of the cable) is usually orders of magnitude smaller than the other forces and is often neglected, but in this case is, for the sake of completeness, is included.

The double nonlinearity that arises out of equation (2.27a) for non-constant coefficients is because, firstly the drag force is a function of the velocity squared, and secondly, the drag and inertia coefficients are dependent on Reynold's number, which in turn is a function of velocity.

Given the motion of the structure, and the motion of the fluid (from the wave theories and specified current velocities) Morison's equation can then evaluate the induced load. However the way in which Morison's equation is applied in a dynamic analysis is that the Morison equation and the equation of motion are in fact implicitly coupled together, and an

iterative procedure is thus necessary to compute the cable response.

2.4 The Finite Element Method

Since cable dynamics are often considered as perturbations from the catenary, the analysis is conceptually divided into two sections viz. static analysis to obtain the catenary, and thereafter dynamic analysis which satifies the equation of motion, and occurs about the static equilibrium position.

Only the equations of dynamic motion will be presented, bearing in mind that for a static analysis, velocities and accelerations are set equal to zero.

Finite element formulations of cable problems are obtained by applying variational principles or using virtual work and can be found in references [9,33,40,23].

Hookes' law is used in relating Lagrangian strain (satisfying the kinematic constraints) to stress, in order to obtain the constitutive equations for linearly elastic materials.

Standard polynomial shape functions are used for interpolating the displacements. All this is accepted FEM technique and can be found in references [9,33,40].
From Henghold and Russel [9], the statement of the principle of virtual work for large elastic deflections applied to an element is,

$$\delta W = \int_0^L \delta X_N^{*T} f^* \, ds + \delta X_N^{*T} r - \int_0^L A \sigma \, \delta\epsilon \, ds = 0 \qquad 2.28$$

where Lagrangian strain is,

$$\epsilon = \frac{1}{2}\left\{ \left(\frac{\delta s^*}{\delta s}\right)^2 - 1 \right\} \qquad 2.29$$

Applying Hookes' Law and using polynomial interpolating functions, N, leads to the elemental equation of motion viz.

$$M\ddot{x} + K_e x = F \qquad 2.30$$

where

$$M = \int_0^L m \, N^T N \, ds \qquad 2.31$$

$$K_e = \frac{1}{2}\int_0^L AE \left\{ X^{*T} N'^T N' X^* - 1 \right\} N'^T N' \, ds \qquad 2.32$$

$$F = \int_0^L mg \, N^T h \, ds + \int_0^L N^T f \, ds \qquad 2.33$$

From Leonard and Tuah, the equilibrium of a differential element is expressed as,

$$\text{div}\, \underline{\sigma} + \underline{b} = \rho \underline{a} \qquad 2.34$$

Multiplying by δu_j and integrating over the volume gives the virtual work expression,

$$\frac{1}{2}\int_{vol} \sigma_{ij} \left\{ \frac{\partial(\delta u_j)}{\partial x_i} + \frac{\partial(\delta u_i)}{\partial x_j} \right\} dV = \int_s t_j \, \delta u_j \, da + \int_{vol} (b_j - \rho \ddot{u}_j) \, \delta u_j \, dV \qquad 2.35$$

All variables are evaluated at and referenced to time t. For nonlinear material behaviour, a pseudo-Hookian law can be applied [40]. This is based on the definition of engineering

stress and strain,

$$\sigma_c = \sigma_r + E_r \left(\frac{ds_c - ds_r}{ds_0} \right) \qquad 2.36$$

where the stress in the current configuration is related to a reference stress of a previous configuration. If the reference and initial stresses are equal, then equation (2.36) becomes that of the linear Hooke's law. Applying the pseudo-Hookian material relationship, and using isoparametric interpolating functions, leads to

$$[A\sigma K_L + A(\sigma + E\lambda) K_{NL}] \{\Delta u\} = \frac{A\rho}{\lambda} [M] \{\ddot{u}\} + \{F\} - A\sigma [K_L] \{X\} \qquad 2.37$$

where $\lambda = A/A_c$, K_l is linear and K_{nl} is nonlinear.

The loading F, from Morison's equation can be lumped at the nodes which causes values from fluid effects to be placed along the diagonals, thus avoid non-symmetric matrices [40,23]. The combination of all of the above results in the equation of motion in matrix form,

$$[M] \{\ddot{u}\} + [C] \{\dot{u}\} + [K] \{u\} = \{q\} \qquad 2.38$$

The time incrementing procedure used is the standard Newmark method with constant acceleration over the step, as shown in reference [23], and gives the solution at required time intervals.

A simplified description of the algorithm required for solving for the immersed cable problem subjected to wave motions is shown in figure 2.2 and described below.

The wave theory, combined with any ocean currents present, describes the motion of the fluid particles w.r.t. time as if the structure were not there.

Morison's equation evaluates the forces imparted to the structure caused by the motion of the fluid relative to the structure.

This loading, together with weight and buoyancy which remain constant, is applied to the structure.

These last two steps are in fact implicitly related, ie. they are interdependent, and so Newton's method is used for solving the equilibrium equations by an iterative process, until both the stresses and the displacements satisfy the specified tolerance. Newmark's method increments forward in time, to produce new cable motions.

At the next time increment, the wave theory updates the particle motion, and by using the evaluated accelerations from the previous step, one can then find the new structure displacements and velocities. By repeating the above procedure in this manner, the solution progresses forward in time.

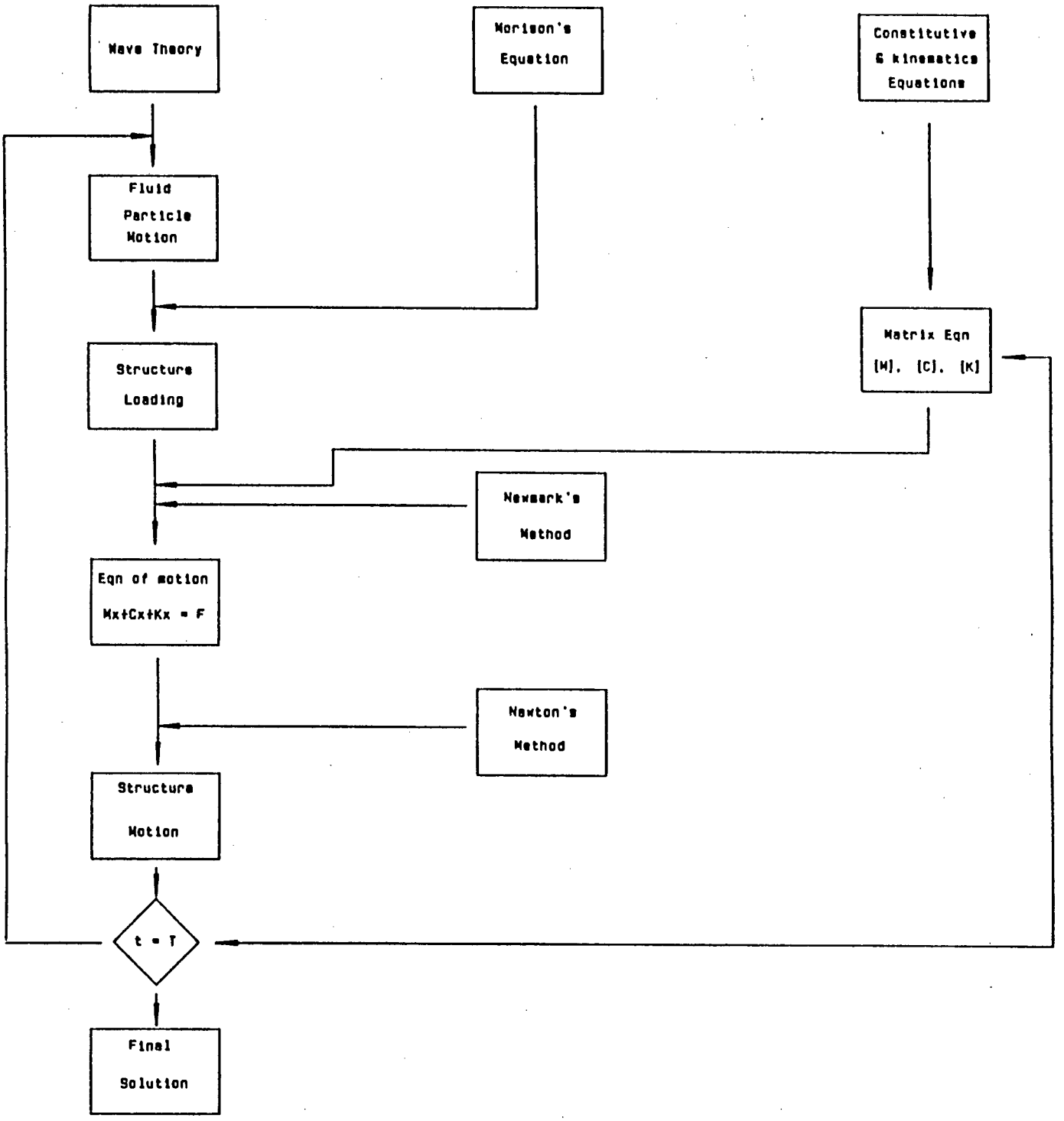

Fig 2.2 Solution Algorithm

3. USING ABAQUS FOR THE ANALYSIS OF FLEXIBLE STRUCTURES

An overview of the use of ABAQUS, it's capabilities and limitations, with regards to cable type problems is presented. ABAQUS is a commercially available finite element package produced by Hibbit, Karlsson and Sorensen Inc. with regular updates. The version used in this thesis is 4.5.169 which is implemented on the Sperry mainframe at UCT.

The reason for this chapter is, i) for the user to obtain a familiarity with certain ABAQUS features, which should be understood in order to appreciate modelling features in the next chapter, ii) to avoid lengthy technical details relating to the using of ABAQUS in chapter four.

The Newmark method is used for incrementing forward in time, and a frontal solver together with the Newton, quasi-Newton and Newton-Raphson techniques are used for solving the system of equations

3.1 Data Input

The input is divided into two sections viz. the model definition and properties, and the history of the problem. Data of a more complex nature eg. non-linear properties or harmonic boundary motions, can be input by means of subroutines.

3.1.1 The Model Definition

These include details of it's length, diameter, nodal coordinates, element type, number of elements, density and elasticity and any other material properties, coefficients in Morison's equation and

wave characteristics. This information cannot be changed during a run (except for the case of element removal). This means that in order to perform a parametric study, a complete rerun is necessary for every change of parameter.

3.1.2 The Loading and Displacement History

Loading conditions, boundary conditions and nodal displacements are entered in the form of steps. There is no constraint on the order nor the number of steps required to describe the history.

Once the model is fully defined in the properties section, the load and displacement history can be carried out.

It should be noted that gravitational attraction is not assumed by ABAQUS, and therefore a uniformly distributed load along the length of the cable is needed to simulate gravity.

Both dynamic and static analyses are entered in an identical manner to each other, ie. both are incremented forward in time - the difference is that inertia and damping are neglected in static analyses.

3.2 Steps and Increments

The end of a step signifies the end of a prescribed loading (or displacement) history, which can be removed at a later step if desired. Any number of steps can be specified in a single run, but there must be a specified maximum to the number of increments in a step, to avoid run-away situations.

Dynamic equilibrium is achieved at the end of each increment to a specified tolerance, and thus the loading-time (or displacement-time) path is traced out over the duration of the step.

For nonlinear processes the solution would be iterated a number of times to achieve convergence to within a specified tolerence at the end of each increment, if convergence can be achieved.

3.3 Time Stepping

Both fixed and automatic time stepping options are available for incrementing forward in time. A minimum time increment must be specified in order to reduce the amount of wasted computer time when using the automatic option. This avoids situations where the computer may attempt to use ridiculously small time steps, in a problem where convergence cannot occur to the required tolerance.

An axial force tolerance (PTOL) must be specified for each step, and there is a further option of using a bending moment tolerance (MTOL). Both tolerances must then be satisfied for convergence to be achieved. The choice of tolerance is usually 1% of typical force values occurring at the nodes in the problem, and can be varied for each step. No allowance for choosing a displacement tolerance is made to the user in ABAQUS, which could be a useful option in displacement dominated problems. This is justified from the point of view that an additional iteration is necessary every time in order to monitor displacements as well.

PTOL does not ensure equilibrium throughout the increment, only at the end of the increment. For the purpose of ensuring the accuracy of this solution, the tolerance during the increment needs to be monitored. Thus a half-increment tolerance, referred to as a half-step tolerance (HAFTOL), was

introduced by ABAQUS, and is typically 10000 times bigger than the end of increment force tolerance (PTOL).

HAFTOL can also be used for obtaining an error estimate of the solution, by monitoring the half-step residuals and comparing to the equilibrium rsiduals.

3.4 The Restart Option

At the end of any step, the then current information can be saved onto a file (*RESTART option) to be assigned at a later date in order to continue a particular run. This is useful in a situation where one would like to vary certain parameters only from, for example, the 5th step onwards without the necessity of repeating the identical first steps. It should be mentioned that only the history and not the properties can be varied in this manner. This makes for a costly parametric study, because of the required repetition of previously acceptable steps.

3.5 Element Types

The available elements provided by ABAQUS which appear suitable for flexible structural problems are truss and beam elements. First, second and third order interpolating functions as well as two and three dimensional elements are avaialable for both categories of elements. The option of using a hybrid beam element designed specifically for large displacement - small strain problems, typical of slender structures, has also been introduced.

The basic characteristics of the elements follows:

Truss - Axial elasticity, zero bending stiffness at the pin jointed nodes.

Beam - Axial elasticity, bending stiffness along the element

Hybrid - Axial elasticity, bending stiffness along the element. Mixed formulation. The displacements and forces have separate independent interpolating functions.

Formulation of the B21, B22, B31, B32 elements is by the simplified Cosserat beam theory of Dupuis, by which is implied that transverse shear is allowed. The B23 and B33 elements use Euler-Benoulli theory.

For more details of the procedures and options available, refer to the ABAQUS User's Manual [60].

3.6 Capabilities and Limitations

Computer limitations in ABAQUS version 4.5.169 on the Sperry mainframe which have been discovered during the course of this thesis are:

- Non-linear material behaviour for elasticity does not work for beam elements, so bounds on the minimum and maximum Young's Modulus occurring in cables must be used to gauge the importance of non-linearity, for future updated versions.

- Quadratically interpolated truss elements can't be used in the negative X-plane. This was discovered while trying to place the cable symmetrically

about the Y-axis. Models were thus kept totally in the positive-X plane

- Truss elements have no facility for fluid loadings

- Springs for simulating bending stiffness are not available; this feature would have been used in conjuction with truss elements.

- Modal analyses are only applicable for symmetric matrices, non-symmetric matrices arise when nonlinear fluid loading is applied.

- Morrison's equation does not have the facility for being linearized. This implies that modal analysis for submerged cable problems can't be done.

ABAQUS was designed as a general F.E. package and can be used for a wide range of applications, unlike programs which have been specifically for cable aanalysis eg. CABANA, STOCCA, SNAPLD. Existing fluid capabilities include the use of Stokes' or Airy's wave theories, as well as the facility for superposition of ocean currents, to describe fluid flows, and the implementing of Morison's equation to evaluate the fluid loading from the interaction with the structure.

4. NUMERICAL ANALYSIS OF CABLE MODELS

ABAQUS is used for the analysis in this thesis because of it's versatility, sophisticated modelling capabilities and the availability. Most of the following analysis is applicable to the numerics of the cable problem itself, and not necessarily the particular solution algorithm or computer program used. Nevertheless, there are aspects which pertain directly to ABAQUS, which may not necessarily occur in other F.E. codes. The reader will be informed of this at the particular aspect in question.

The chapter begins with the 'simplest' static equilibrium position and then presents models of increasing complexity which are all directed towards the situation of a guying system. However, a variety of models have been attempted along the way in order to clarify certain issues relating to the numerical analysis of cables in general.

4.1 The Catenary

The first question arising is; from what configuration does one start a cable analysis? The shape that a stationary hanging cable takes up is known as the catenary of that cable, see figure 4.1 , but this cannot be the starting position because the specific catenary is unknown.

The catenary differs for each different cable, and even if it were known, starting from this position would erroneously imply that this was the manufactured and thus unstressed shape. The first requirement in an analysis is therefore to obtain the catenary shape, and the associated stresses from an initial, straight line configuration.

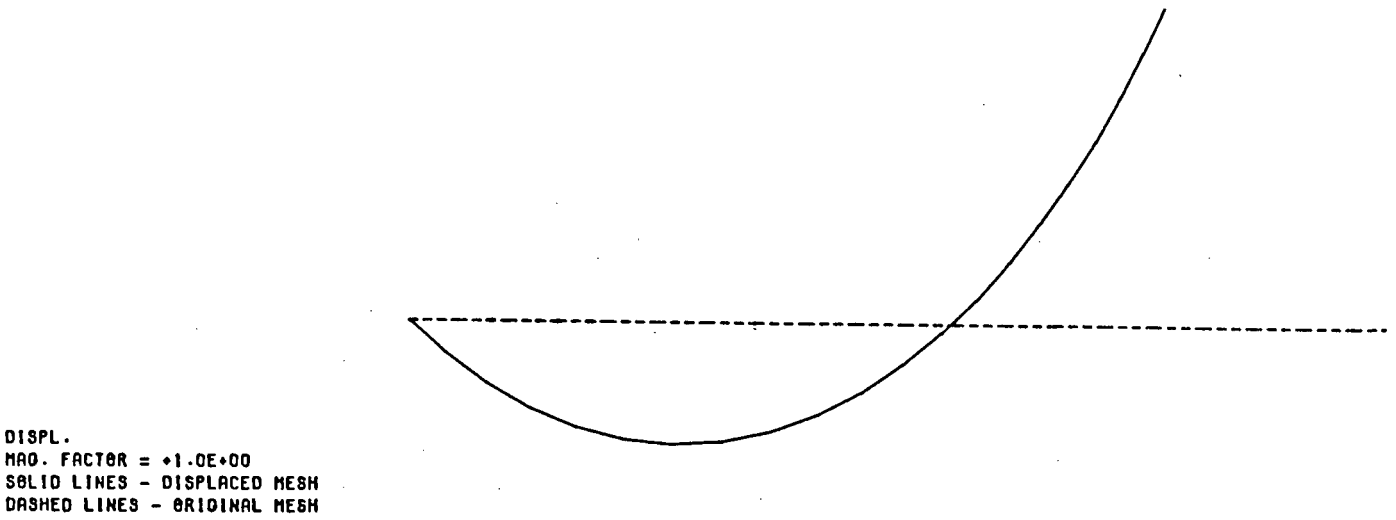

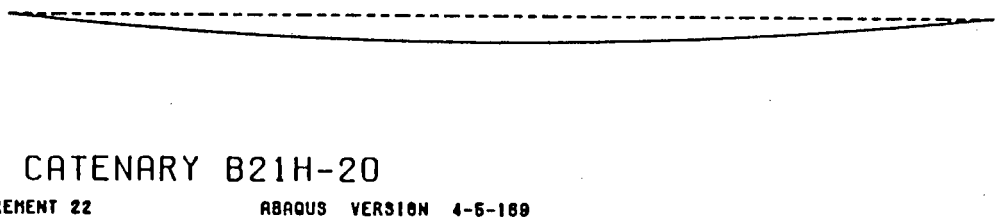

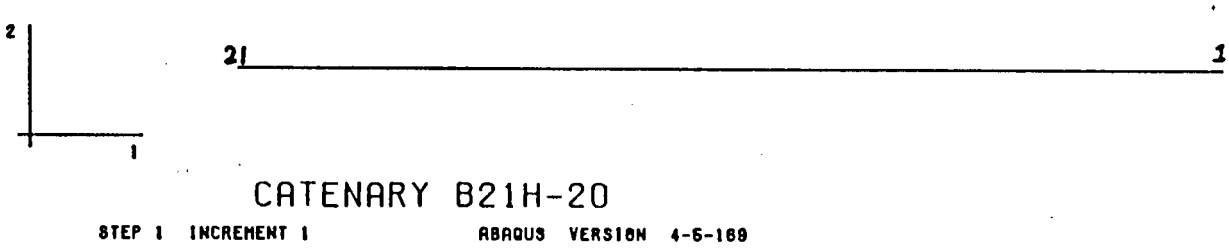

Fig. 4.1 The Catenary Model

Based on the work done by Phaal [63] and Bergan et al [33], it was decided to obtain the desired results using linearly interpolated elements, as these elements are easier to use and from these authors' findings are no less reliable, nor significantly less efficient than higher order elements, for cable type problems. Further confirmation of this was obtained when fewer higher order elements were used in later sections and took 20% longer CPU time than the two noded elements.

The elements applicable to cable analysis which are available in the ABAQUS library are: truss, isoparametric beam , and hybrid beam elements; all of which were used in the thesis. The motivation for using truss elements is because of their simplicity, ease of formulating the problem, and anticipated (reported) reduction in computer time because no bending calculations are performed.

4.1.1 Truss elements

As the catenary is by definition, the stationary hanging configuration of a cable, it seems logical to use a static analysis to obtain this position, thus the initial analyses were performed statically, using the data shown in Figure 4.1.

The first step in obtaining the catenary was to apply self weight which was modelled as a uniformly distributed downward load. This had to be done while the cable was supported at each node, otherwise singularities in the computation would arise (with the message " **Solver Problem - Zero pivot when processing node n, D.O.F. m ") as a result of zero stiffness (resisting force) in the transverse direction, ie. in line with the defined force of gravity.

This can be explained numerically by the fact that a zero (or approximately) arose in the stiffness matrix as a result of no bending or lateral stiffness, as demonstrated in equation (4.2). At the instantaneous application of the load, the lack

of stiffness in that direction lead to a situation where there was no unique solution. This would be equivalent to trying to analyse free fall motion statically, which is what's happening at the first infinitesimal increment at the start of the step.

Thus, Step 1 involved statically ramping on the loads while the cable was supported. At the end of this step the weight of the cable was then supported by reaction forces at the nodes. As this step took only one increment to completion, there is no necessity to ramp (as opposed to step) on the load. However the reason for ramping on the load is that if convergence difficulties are encountered, automatic reduction of the time increment reduces the applied load increment, making convergence more likely.

Step 2 involved an attempt to ramp off the reactions at the same time that the cable end was lifted, to form the catenary. This also resulted in singularities being produced at the nodes due to the aforementioned lack of lateral stiffness. Consider the model shown in figure 4.2, and the associated stiffness matrix.

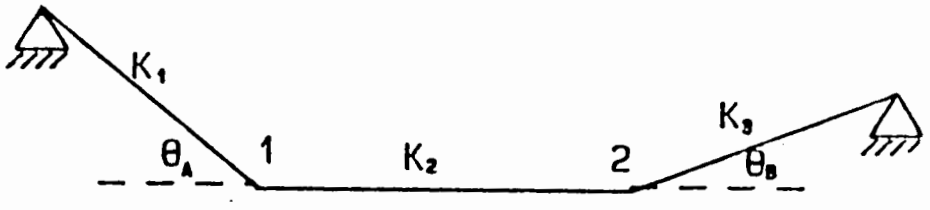

Fig. 4.2 Lateral Stiffness Criteria

The stiffness matrix for this model is:

$$\begin{pmatrix} k(\cos\phi_A+\cos\phi_B) & 0 & -k\cos\phi_B & 0 \\ 0 & k(\sin\phi_A+\sin\phi_B) & 0 & -k\sin\phi_B \\ -k\cos\phi_B & 0 & k(\cos\phi_B+\cos\phi_C) & 0 \\ 0 & -k(\sin\phi_B) & 0 & k(\sin\phi_B+\sin\phi_C) \end{pmatrix} \quad 4.1$$

if and when theta equals zero, the stiffness matrix becomes

$$\begin{pmatrix} 2k & 0 & -k & 0 \\ 0 & 0 & 0 & 0 \\ -k & 0 & 2k & 0 \\ 0 & 0 & 0 & 0 \end{pmatrix} \quad 4.2$$

with the resulting zeros in the diagonal

By applying tension in step 1 by moving node 1 a distance of 0.1% of it's length to the left, the singularity problem was overcome. The applied tension provided the necessary transverse stiffness to avoid the singularities at the nodes when the reactions were gradually removed (ramped off).

Having solved the initial start-up problem, an attempt was made to obtain the catenary by lifting the end node to a position such that the cable would be freely hanging. It was found that instead of the cable sagging under it's own weight it seemed to lock into position, as shown in figure 4.3, and subsequently came under unrealistically high compression, as node 1 was moved to it's catenary position. This phenomenon will henceforth be referred to as jamming. The cable would then suddenly spring out of this position and oscillate violently, in a manner similar to that of buckling, and as a result was unable to continue the rest of the step.

This increased compression that resulted, as the step

progressed caused an instability in the cable model and so lead to the sudden springing out of the 'jammed' position.

Numerous techniques were applied to the problem to avoid this phenomenon, eg. using two then twenty elements, higher order elements and increasing the force tolerance (PTOL), none of which helped.

A model was attempted such that it's final position (end of step) would occur just before buckling. The analysis was completed satisfactorily, as far as the computer was concerned, but in the fully jammed position.

Eventually it was discovered that by increasing the axial flexibility (by reducing Young's Modulus from 110.0 Gpa to 1.0 Gpa) the model started sagging as the end node started to move, and continued sagging through the rest of the step. Obviously in this case the sag was large as a result of the axial flexibility.

It was concluded that the problems involving high axial stiffness relative to their weight are prone to this jamming phenomenon, but what is surprising is this; that truss elements, which are connected by frictionless pins (simulating chain links), and therefore have no bending stiffness, should be subjected to jamming. The cause of this phenomenon appears to be as a result of the very high axial to vertical (gravitational) force ratio.

Jamming in the original model (ie. 110 Gpa) was avoided by displacing the central node downwards, in order to get the cable out of the straight line mode as well as applying a tension, and only then lifting node 1. This enabled the attainment of the fully developed static catenary. The displacment of the central node down by a distance of about 1% of the length of the cable, is a general solution to jamming, and is thus the best procedure to adopt when starting this type of analysis.

Truss Lifting

Length	500m
Diameter	75mm
EA	2.21E9 N
Bending Stiffness	Zero
Elements	10 x C1D2

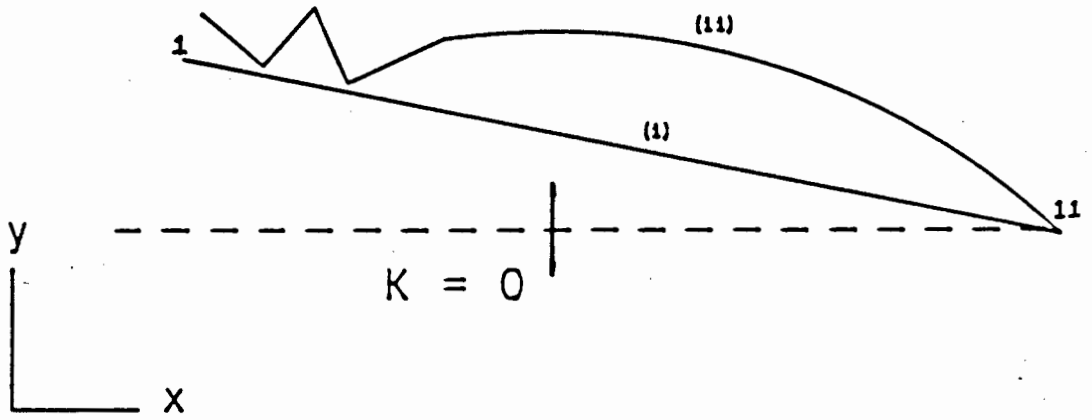

Fig 4.3 Truss Locking

The procedure finally adopted for obtaining the catenary using truss elements in a static analysis was:

STEP 1 - Apply loads while supporting all nodes.
STEP 2 - Displace central node vertically downwards.
STEP 3 - Move end node to desired position and simultaneously ramp off reaction forces.

It made very little difference (in both the outcome of the results and the computer efficiency) whether the reactions were removed and then the end node (node 1) moved to the desired point, or if they were done in the same step.

In a subsequent start-up model, the cable catenary was obtained dynamically ie. by including inertia and damping, to observe their influence on start-up characteristics.

By applying dynamic analysis to the same model the likelihood of singularities or non-convergence occurring is reduced. The inertia of the cable acts as a resistance to motion, and so provides a stabilising influence. Numerically, the combination of the stiffness and the mass matrix results in a non-singular, well conditioning system.

The only damping included in the model was numerical damping for which an initial value of alpha=-0.05 (as recommended by ABAQUS) was chosen for the Hilber-Hughes-Taylor operator.

In the dynamic analysis, the cable was supported when weight was applied, keeping step 1 the same as in the static analysis.

Hereafter a number of different procedures were attempted viz.

i) Step 2 - displace central node, Step 3 - lift and ramp off reactions
ii) Step 2 - ramp off reactions, Step 3 - lift
iii) Step 2 - step off reactions, Step 3 - lift

Option (ii) was the 'best' in that the cable oscillated the least and therefore reached static equilibrium soonest; (i) simulated the plucking and releasing of a guitar string; and in (iii) the initial free fall of the cable set up oscillations.

Numerical damping was necessary to avoid oscillations, and by artificially overdamping the cable, it was possible to obtain the static catenary more efficiently with regards to CPU time. This is because of the reduction of oscillations at the end of the step, and also because of the reduced time taken for those oscillations existing at the end of the step to die away.

One would expect that the disadvantage of a dynamic analysis is the extra computer time involved, as a result of the increased storage and computations necessary for the additional mass and damping matrices. However, this is not the case. The time taken to compute the extra matrices is compensated for by the fact that the danger of start-up singularities is significantly reduced, making large time increments permissible compared to the miniscule "time" increments needed in the static analysis. This characteristic is also exhibited in the section on beam elements, and is shown in figure 4.4.

The cable problem is sensitive to parameter changes in a static analysis, especially at start-up, (as shown in the aforementioned example when Young's Modulus was varied), and is likely to run into solver problems for each different model. What this entails is that a different stepping procedure may well be necessary for each different model, resulting in a loss of generality.

Thus, to model cable behaviour using truss elements, it is recommended that a dynamic analysis be performed throughout, because of the greater reliability of obtaining solutions and at no extra cost in terms of human or computer time. The

capabilities and limitations of truss models are discussed with more detail and finality in a later section, where after the harmonic input model, it was decided to use beam elements exclusively.

4.1.2 Beam Elements

The major characteristic of cables is their bending flexibility, and therefore the value of the bending stiffness has to be of a relatively small value to be realistic. The value of Young's Modulus was kept at 110 GPa for the beam element problems, while the bending stiffness was calculated to be 700 Nm, from data supplied by Haggie Rand [64], for a typical cable of the type modelled in this thesis.

Because of the allowance for bending stiffness in a beam, the likelihood of non-convergence or singularities is reduced; the higher the bending stiffness, the decrease in the likelihood of non-convergence.

To obtain a means of comparison between truss element analysis and beam element analysis, the same stepping procedure (viz. Step 1 - load, Step 2 - ramp off reactions, Step 3 - lift), for both the static and dynamic cases was employed.

For the static analysis, the same initial start-up problems as in the truss elements were experienced, although to a lesser degree. It was still necessary to ramp on the weight while the cable was supported, and in the second step ramp off the reactions, or alternatively displace the centre node downwards.

If the step function was used in Step 2, zero pivots resulted in the solver routine, for the same reasons that they occurred in the truss element analysis. This singularity problem is also a result of the ill-posing inherent in cable problems, because of the large axial versus small bending stiffnesses.

Unluckily this is a characteristic of cables with which we must live, as such ill-posing does not occur in for example 'I-Beam' analysis where both the bending and axial stiffnesses are large.

No incidence of jamming was found in beam element analysis, even though one would expect that having a bending stiffness should increase the likelihood of jamming. Jamming in truss elements may well be attributed to the particular algorithm employed in ABAQUS, as this phenomenon has not been reported in the literature.

Although it is possible to leave out Step 2 and still get the same displacement and stress results, it is more efficient (and safer) for it to be included in a static analysis. The minimum time increment required when Step 2 was left out was 1.E-8 of the total step, which occurred at the start of the step. Once the program overcame this initial start-up problem, the time increments then increased dramatically to reasonable sizes of 20% of the step. Even when Step 2 was included the minimum time increment was very small viz. 1.E-6 of a step.

For the case of a dynamic analysis, the minimum time increment was considerably larger than in the static case at 4E-2 of a step, but thereafter the increment size increased to only 10% of the step. This is shown graphically in figure 4.4, where it can been seen that dynamic analysis took 1 increment to get 10% of the way, whereas static analysis took 34 increments.

55. Sarpkaya T. , VORTEX-INDUCED OSCILLATIONS; A SELECTIVE REVIEW, J. Appl. Mech. , vol 46, June 1979

56. Patel M. H. and Sarohia K. F. , FINITE ELEMENT ANALYSIS OF THE MARINE RISER, Engrg. Struct. , vol 6, July 1984

57. Horton T. E. and Feifarek M. J. , THE INERTIAL PRESSURE CONCEPT FOR DETERMINING THE WAVE FORCES ON SUBMERGED BODIES, J Eng Res Tech. vol 104, March 1982

58. Wolfram W. R. and Gunderson R. H. , STRUCTURAL DESIGN OF PRODUCTION RISERS AND OFFSHORE PRODUCTION TERMINALS, Offshore Technolgy Conference 1979, pp 1569-1576

59. Griffin O. M. and Ramberg S. E. , SOME RECENT STUDIES OF VORTEX SHEDDING WITH APPLICATION TO MARINE TUBULARS AND RISERS, J Eng Res Tech. vol 104, March 1982

60. Hibbit, Karlsson and Sorensen Inc. , ABAQUS USER'S MANUAL, Version 4-5 , revised Nov 1985

61. Peyrot A. H. and Goulois A. M. , ANALYSIS OF CABLE STRUCTURES, Computers and Structures vol 10, pp 805-803, 1979

62. Hibbit, Karlsson and Sorensen Inc. , ABAQUS THEORY MANUAL, Version 4-5 , revised Nov 1985

63. Phaal R. , COMPUTATIONAL AND MODELLING ASPECTS OF MARINE RISER ANALYSIS,. M.Sc Thesis, University of Cape Town, 1987

64. Haggie Rand Ltd. , STEEL WIRE ROPES, Catalogue of available cables for 1987

65. Irvine H. M. , CABLE STRUCTURES, 1st edition 1981, Mass. MIT Press

66. Lighthill M. J. , WAVES IN FLUIDS, 1st ed 1978, Cambridge, University Press

67. Witham G. B. , LINEAR AND NONLINEAR WAVES, 1st ed 1974, Canada, John Wiley and Sons.

68. Costello G. A. and Butson G. J. , SIMPLIFIED BENDING THEORY FOR WIRE ROPE, J. Eng. Mech. ASCE, pp 219-227, April 1982

69. Costello G. A. and Phillips J. W., EFFECTIVE MODULUS OF TWISTED WIRE CABLES, J. Eng. Mech. ASCE, pp 171-181, July 1976

70. Ronson K. T., ROPES FOR DEEP WATER MOORING, Twelth Offshore Technology Conference, May 1980

71. Scalzi J. B. and McGrath W. K., MECHANICAL PROPERTIES OF STRUCTURAL CABLES, J. Struct. Div. ASCE, pp 2837-2844, May 1972

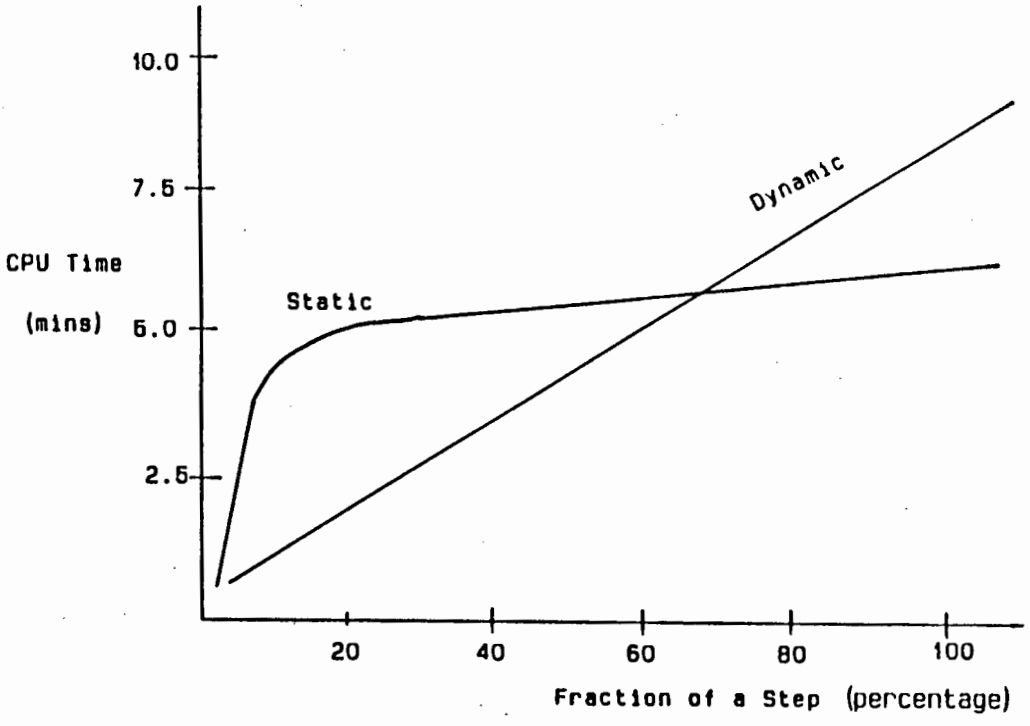

Fig 4.4 Computer Time

The reason for the discrepancy between statics and dynamics is that the inertia of the cable at start-up provides a stabilising influence by virtue of its resistance to motion. This is envisaged numerically by the fact that the stiffness matrix consists of very small numbers (which represent the lateral stiffness) alongside large numbers (which represent the axial stiffness), ie. the matrix is ill-conditioned, whereas the mass matrix is comprised of large numbers of very similar values. The combination of these matrices overides the ill effect of the stiffness matrix in isolation, and allows for faster convergence.

As time progresses however, the inertia causes higher loads (than in the static case), and resulting oscillations need monitoring in dynamics, which in turn limits the size of the time increments. This is especially true if the reactions are stepped off instead of ramped off.

Obtaining the catenary dynamically took 8 mins 58 seconds CPU time compared to 6 mins 32 seconds in the static case.

The number of linear isoparametric beam elements was also found to be 10 to give reasonable results. Typical force discrepancies which occurred with different numbers of elements is shown in figure 4.5, where it was found that there was a discrepancy of less than 0.1% at nearly all nodes except for the centre nodes where a 5% error occurred in the x-direction force. This is deemed acceptable, seeing as trends rather than design loads are being investigated.

The error estimate in figure 4.5 is based on observing the asymptotic rate of decrease to zero of the differences as the number of elements is increased. The largest difference occurring between the 30 element model and the 60 element model was about 0.1%, well within our set tolerances. The error estimate is then based on the value of the discrepency relative to the 60 element model.

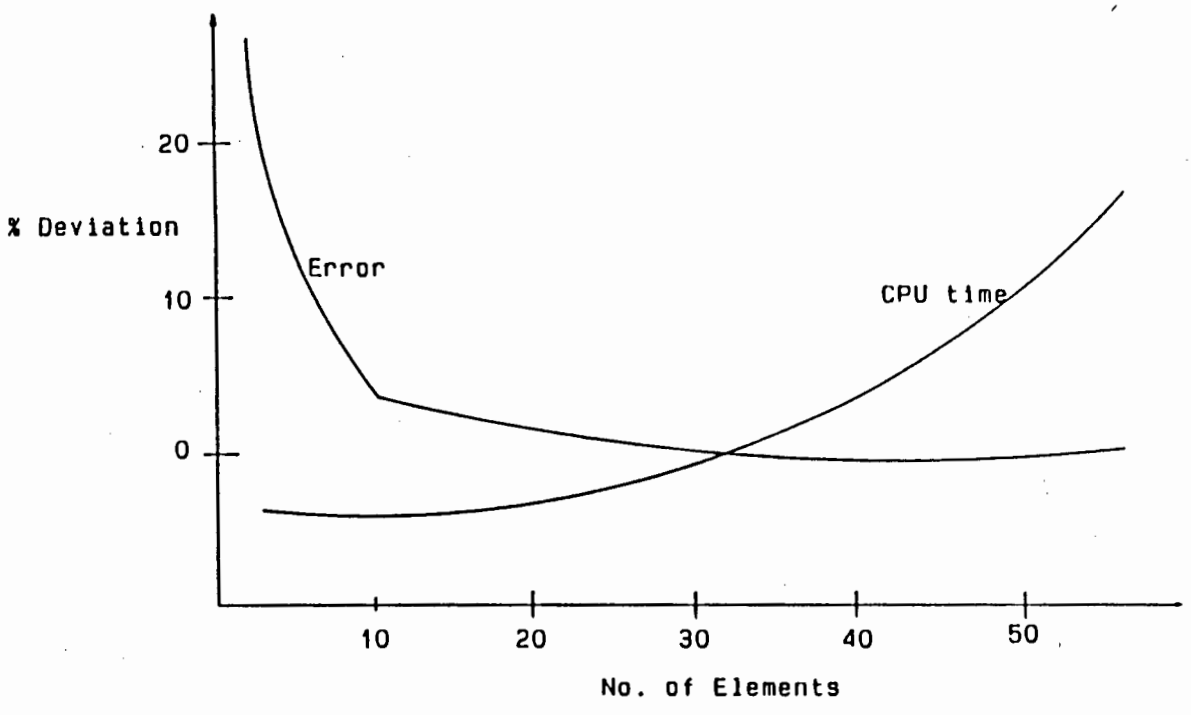

Fig 4.5 A Priori Error Estimate

An observed result produced when different bending stiffnesses were used was that, a higher bending stiffness resulted in higher stresses, while the displaced shape of the cable remained very much the same. This is typical of cable behaviour where (unlike beams) large variations in the bending forces are still insignificant relative to the large axial forces present.

When the bending stiffness was very small eg. 1.0 Nm, the solution didn't converge as a result of ill-conditioning. Typically (for values of bending stiffness between 10000 and 500000 Nm), the smaller bending stiffnesses would convergence faster, because of the resulting reduced stresses and thus a decreased number of iterations needed for satisfying the force tolerance.

As the bending stiffness goes below about 1000 Nm, convergence becomes slower again because of ill-conditioning, which starts occurring to an increasingly noticeable degree, until ultimately the analysis is aborted because of the resulting singularities.

Non-conservative forces, for example damping, are insignificant in the cable itself, and fluid drag plays a minor role in the outcome of results for analyses performed in air. Therefore in the first four sections of this chapter physical drag and damping are neglected, although numerical damping is included. For the case when numerical damping is set equal to zero, the computer algorithm is reduced to the Newmark scheme.

When the maximum value of the Hilber-Hughes-Taylor damping operator of Alpha=-0.33 was used, the fastest convergence was obtained. This was the case when the cable was moved moderately slowly to the catenary position ie. a real time of 100 seconds. However, when the cable was moved very slowly, using a large value of alpha slowed the process down.

Various clumped weights of 1000 Kg to 10000 Kg were attached to the cable at node 6 in a 20 element analysis, to investigate possible ill-conditioning in the mass matrix and the effect of these weights on the dynamics of the cable.

No ill-conditioning was observed in these catenary examples, although the analyses did take longer when larger masses were selected. This extra computer time taken is most likely solely due to the higher forces involved than to any added effects of ill-conditioning in the mass matrices. Cable forces went up by typically 600% in the vicinity of the clump when the 10000 Kg mass was attached to the already 11300 Kg cable.

In Step 2 of this model the reactions were abruptly removed while the ends were pinned, to allow for the instantaneous free fall of the centre portion of the cable, and subsequent deceleration caused by the increasing tension in the cable. The oscillations were plotted until the cable position asymptotically approached that of the catenary. This is shown in figure 4.6.

The natural frequency of the cable in this position was about 0.2 Hz (period 5 seconds) as shown in figure 4.6. It is interesting to note that there is absolutely no variation of tension along the length of the cable during the free oscillation in the second step of the analysis. Only once the cable end is lifted in Step 3 do we see a variation of tensions at the nodes. This supports the view that tension variations along the cable are negligible for flat cables, but become large for slack catenaries.

At this stage large high-frequency oscillations arose, which ultimately died away at the end of the step. The fact that these oscillations show large negative forces implies that the cable undergoes compression. The manner in which this occurred is as follows: the cable 'bounced' up to it's original position after 10 seconds (the end of Step 2), at which point node 1 is moved in the positive Y and negative X direction.

This caused a sudden compression of the cable and set up the high frequency oscillations. It is possible that a certain component of this variation in tension is also caused by spurious oscillations.

In the last 30% of Step 3, it can be seen that the minimum tension at all three nodes is about the same, whereas the maximum is biggest at node 1 as is expected. From this example it can be seen that the cable reached a quarter of it's breaking force - a situation which relates to large cable dynamics problems, where "a large proportion, perhaps 20%, of the breaking force is caused by the cable weight alone" [13].

A comparison of linearly interpolated isoparametric beam elements (B21) with linearly interpolated hybrid beam elements (B21H) revealed that for the various models attempted, the hybrid elements were 10% less efficient with regards to CPU time, although their convergence characteristics were noticeably better (the minimum time increment was far greater, and the force residuals were generally less).

The results differed by as much as 8% in the forces and reactions and 3% in the displacements. As an earlier 'a priori' observation of the residuals estimated that 20 B21 elements was sufficient for the required accuracy, it was unexpected that there was such a deviation for so simple a problem. As a result both elements were used in subsequent analyses as a further means of comparison.

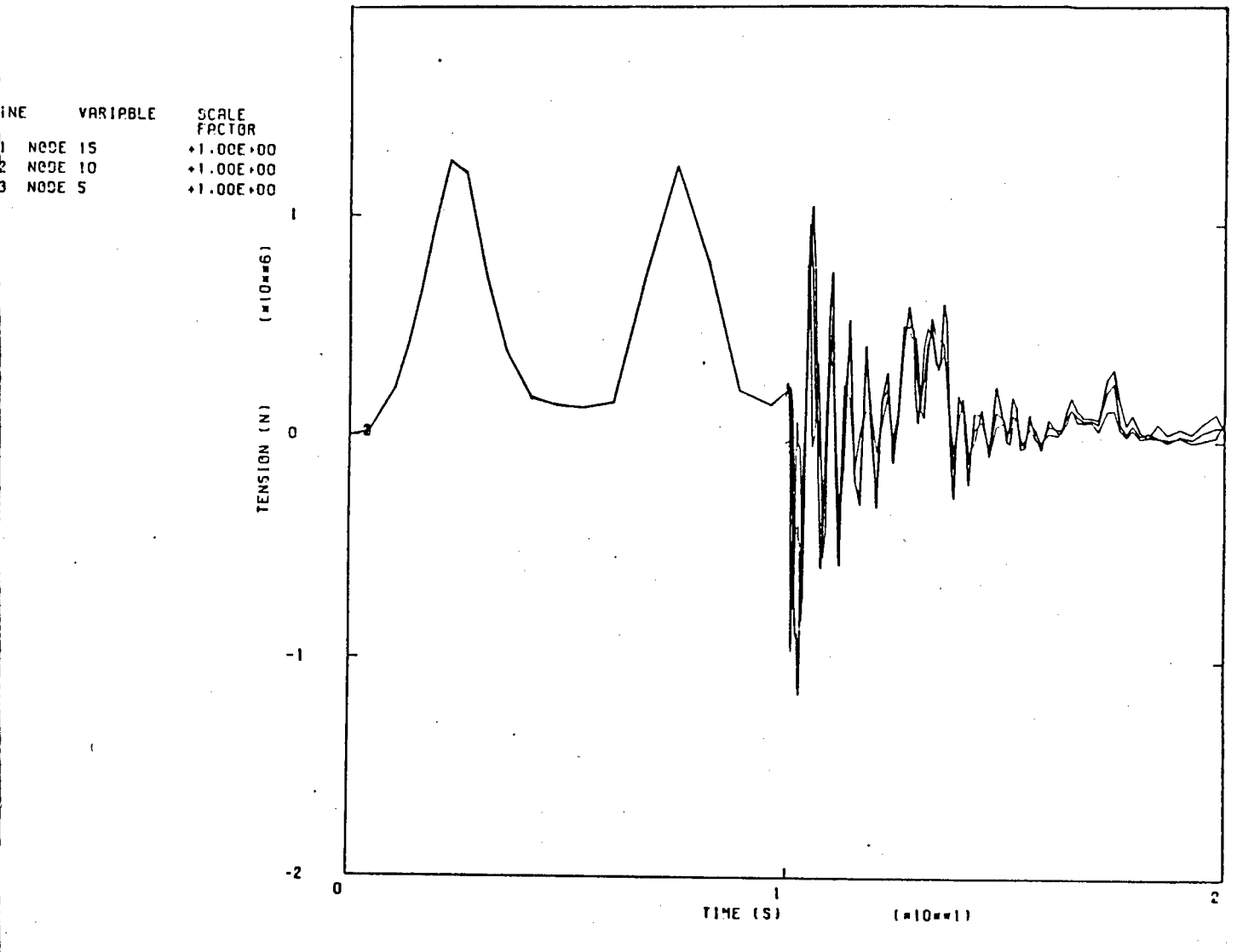

Fig 4.6 Dynamic Catenary

4.2 Taut Vibrating String

During the process of obtaining the cable catenary, two sideline models were attempted in order to help establish the reasons for the initial difficulties experienced with truss elements.

Firstly, it was decided to try a basic free fall problem to uncover the root cause of the start-up/non-convergence singularity problems. In this case the model was loaded in the usual way, and this time all the reactions were instantaneously removed in a dynamic analysis.

As no problems occurred, and the cable followed the laws of free fall motion, it was concluded that the difficulties experienced with the catenary could be attributed to the cable being fixed at both ends. The next phase was to consider a taut string pinned at both ends.

This example essentially models that of a very large guitar string. Tension was applied to the cable, the centre node was moved down a certain amount and then released. The results of this time domain solution were compared to that of a modal analysis performed on the same model using the *FREQUENCY option, in the frequency domain. Both analyses produced the same results and in nominal CPU time ie. everything behaved as desired.

By reducing the tension in subsequent models, it could be observed how the minimum time increment decreased (which resulted in more increments per step), and the CPU time increased. Eventually the model was reduced to that of the catenary model, at which point start-up singularities resulted.

The above indicated that a cable when under tension was easier to model numerically, than when slack. Thus another undesirable characteristic of the numerical solutions of large

sag cable problems, (besides their inherent flexibility), is that a lack of tension could result in fatal numerical difficulties. Although cables are usually always under substantial tension, cable whip can and does occur and results in low cable tensions, leading to solver problems.

4.3 Shaking the Cable

Two models with prescribed boundary displacements, referred to as 'shake' models, were attempted; one starting from the catenary position, and the other starting from a straight line and neglecting gravity. Both were subjected to a prescribed harmonic motion at the free end of the cable in a dynamic analysis using truss and beam elements, and for this they required a user defined subroutine.

The first model simulates the shaking of a cable in a horizontal plane on a frictionless surface, and was performed to test dynamic characteristics.

4.3.1 Harmonic input on a frictionless surface

A nominal tension was applied to the cable to avoid start-up singularities, but was removed once the cable had reached a stable oscillating stage.

10 and 30 linear and 15 quadratically interpolated truss elements were used in 3 models. Although the same features or trends of the three element types were similar, their positions with respect to time were markedly different ie. there appeared to be a phase shift. The same analysis was then performed with 20 beam elements, and it was found that these results compared most favourably with the 30 element truss model. CPU times for these models were: 10 linear truss

elements - 15 mins, 30 linear truss elements - 45 mins, 15 quadratic truss elements - 55 mins, 20 beam elements - 30 mins. From this it can be noticed that even though beam element analysis requires further calculations for the rotational degrees of freedom and the monitoring of the bending tolerance, the bending stiffness in the beams stabilizes the problem, and avoids convergence difficulties to an extent where less CPU time is taken.

From these analyses, it was finally concluded that truss elements (as they presently stand in ABAQUS) are not suited to slack cable dynamic problems as they were subject to the aforementioned jamming phenomenon, zero pivot and also they became erratic if not under tension.

This erratic behaviour is attributed to the lack of bending, which causes numerical difficulties if two adjacent elements end up in an approximate straight line, which in turn causes the aforementioned (chapter 4.1) singular problem due to the lack of lateral stiffness. The resulting very large pivot ratio could cause misleading or unrealistic displacement or tension results, because of the sensitivity of the problem to displacement inputs in this configuration. At the very least, much computer time is used up in allowing for stabilization of the problem, and as mentioned earlier, trusses become less efficient than beams.

Furthermore, in ABAQUS there is no facility for truss elements having drag loadings, or interface elements for boundary contacts (ground contact and fluid drag are common features of cable problems), and thus it would seem that they were never really intended for submerged cable type analyses. As a result only beam elements will be used henceforth.

Although truss elements can be used for models under high tension or for simple large sag cable models, their (sometimes) increased effiency over beam elements is of minor significance.

4.3.2 Harmonic Input on the Catenary

In this model, the static catenary was obtained as before, followed by an harmonic displacement input of the upper end. Steps 1,2 and 3 were the same as in the earlier catenary models, and in step 4 a horizontal harmonic motion in the vertical plane was applied to node 1 about it's static catenary position.

The static analysis, shown in figures 4.8a and 4.8b, gives a clear picture of the tension and displacement histories of what should happen if the above model had the prescribed displacement moving incredibly slowly, as was the case for a further model shown in figures 4.9a and 4.9b. The dynamic model can be seen to approach that of the static model for the case where the cycle time was 500 seconds (the time taken to move node one 75m to the left and back, then 75m to the right and back again is 500 seconds).

In figures 4.10a and 4.10b, we see both a tension and displacement history of various elements and nodes under a 'fast' prescribed boundary motion. Between the times 0 and 200 seconds the catenary is obtained, and thereafter the results caused by the harmonic motion of period 50 seconds, are seen.

The reason for the observed large initial tension in figures 4.8, 4.9, and 4.10, is because of the way in which the catenary is obtained: removing the midspan supports causes the cable to take up a position of small sag, leading to the high peaked tension.

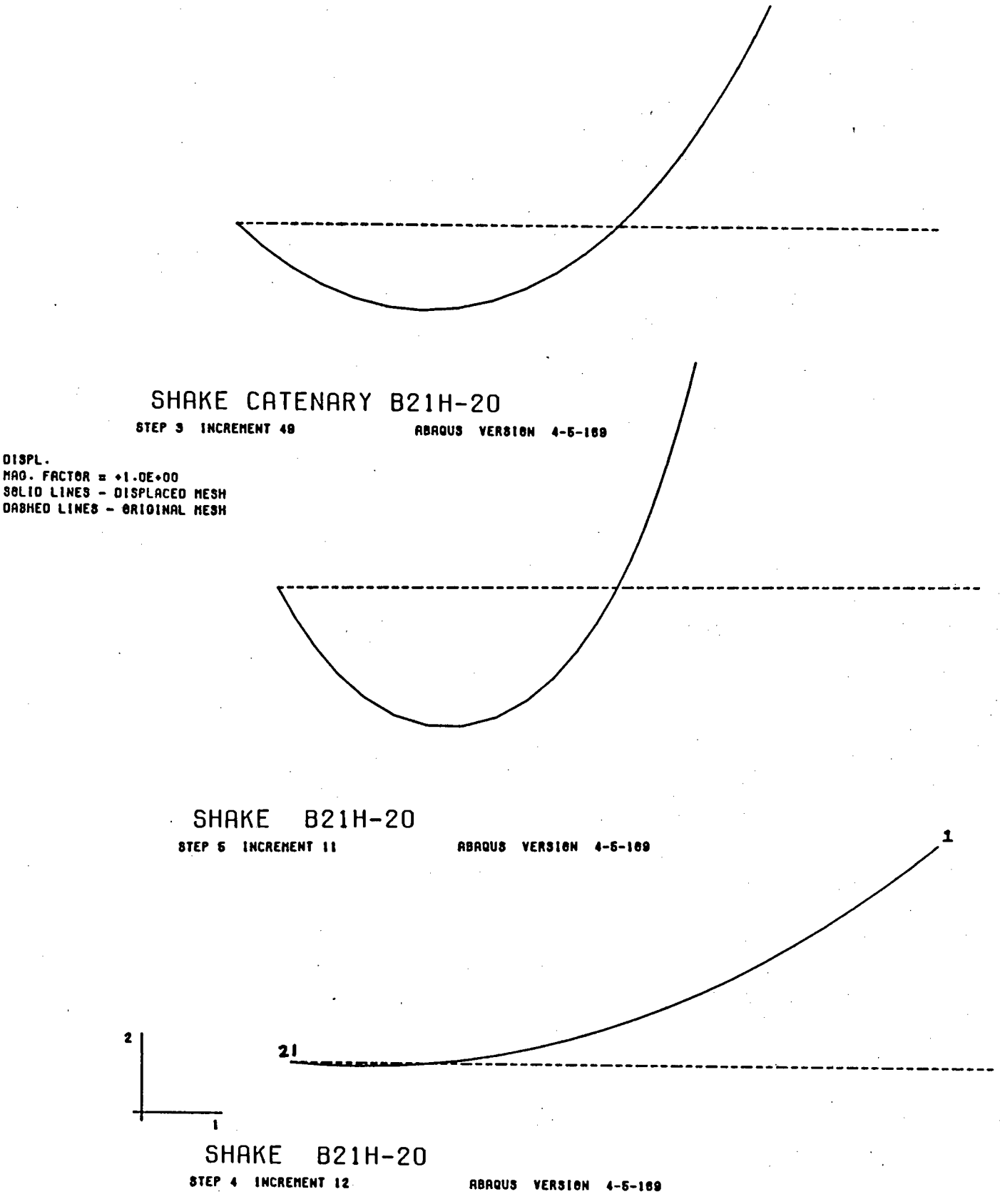

Fig 4.7 Catenary Shake Model

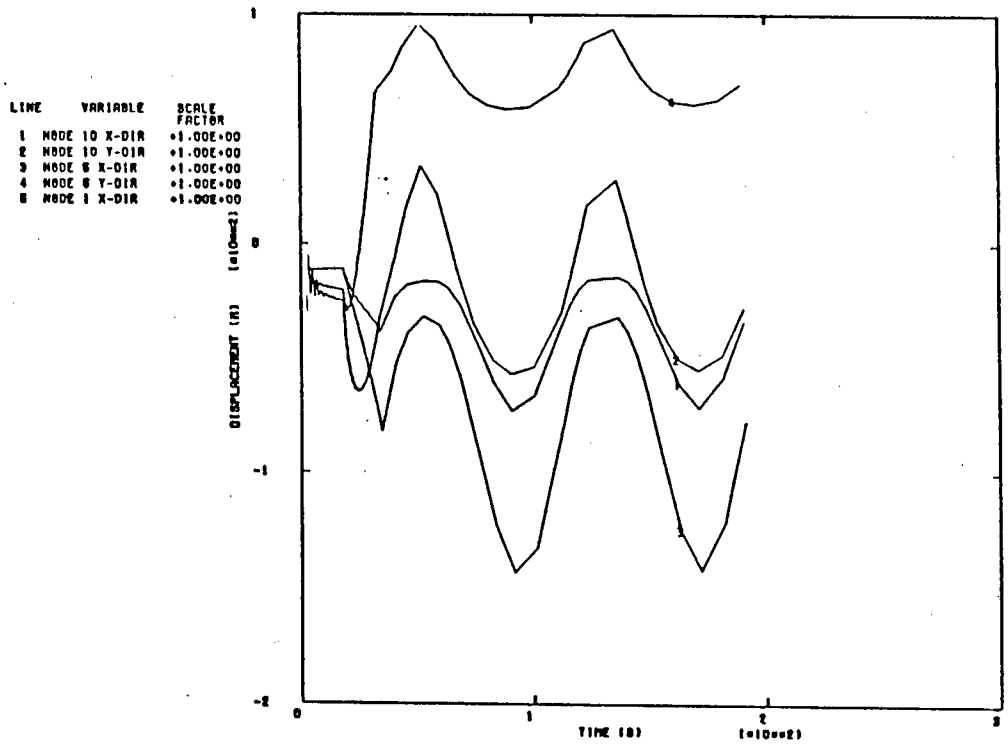

b. SHAKE PRESCRIBED HARMONIC MOTION ABOUT THE CATENARY

ABAQUS VERSION 4-5-188

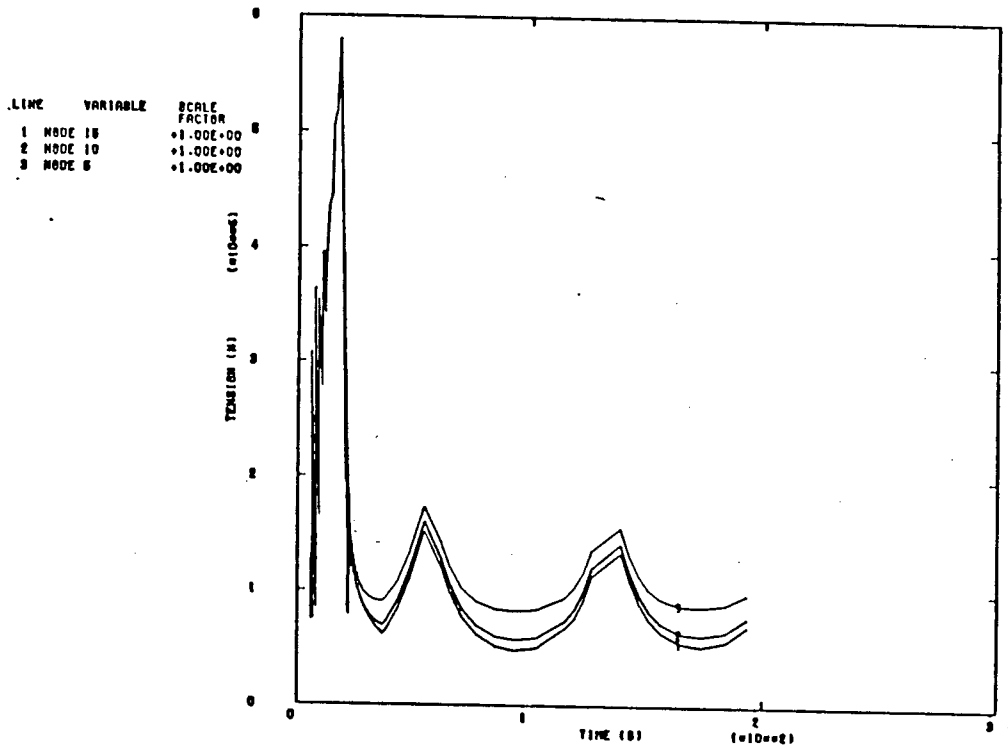

c. SHAKE PRESCRIBED HARMONIC MOTION ABOUT THE CATENARY

ABAQUS VERSION 4-5-188

Fig 4.9 Slow Harmonic Motion

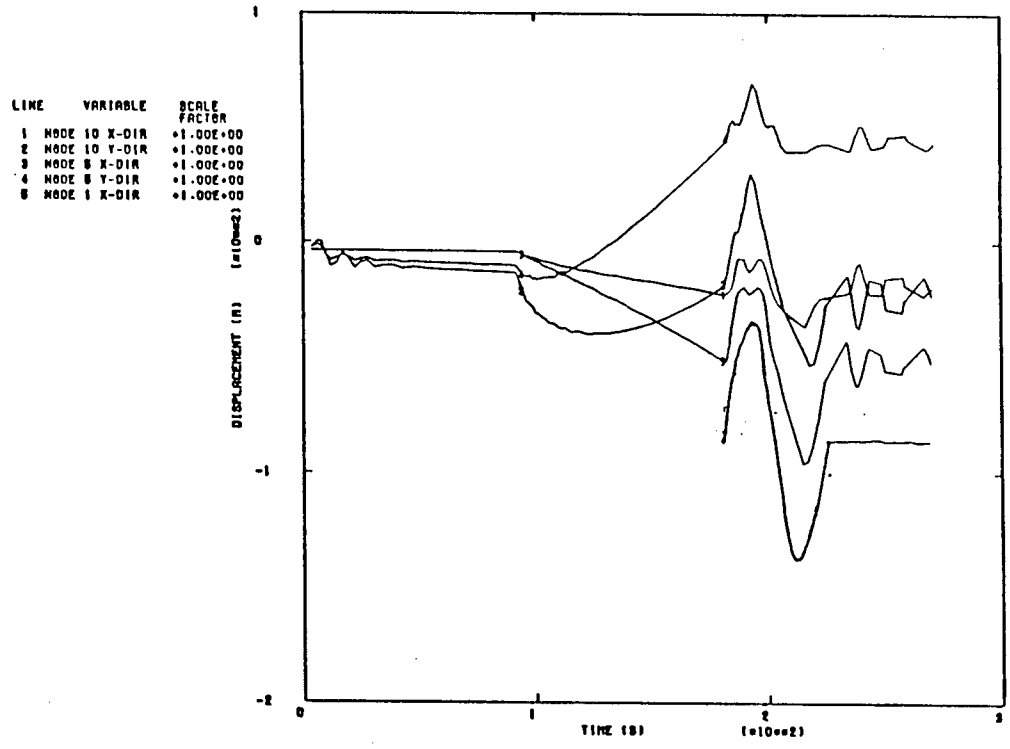

b. SHAKE PRESCRIBED HARMONIC MOTION ABOUT THE CATENARY

ABAQUS VERSION 4-6-168

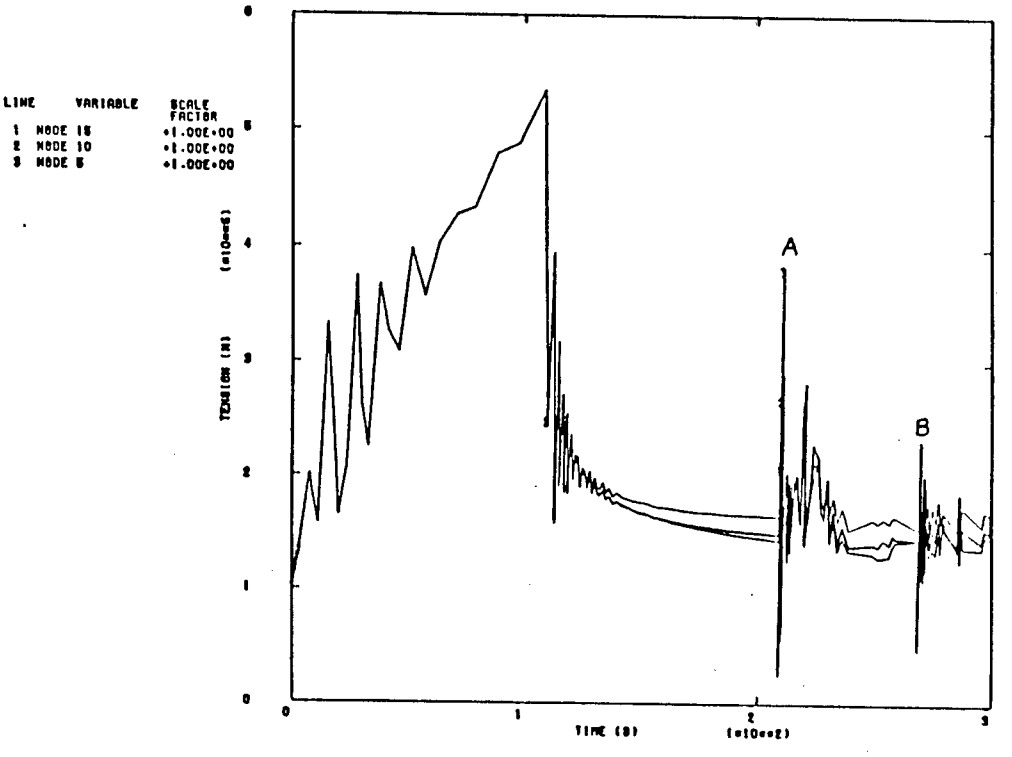

a. SHAKE PRESCRIBED HARMONIC MOTION ABOUT THE CATENARY

ABAQUS VERSION 4-6-168

Fig 4.10 Fast Harmonic Motion

Interesting to note is the spurious oscillations or noise generated at the start of steps one (0 to 100 secs) and two (100 to 200 secs) in the dynamic analysis, which weren't prevalent in the previous catenary analyses. The noise in the results was with the Hilber-Hughes-Taylor operator (HHT) equal to -.05, supporting the earlier recommendations to use larger values of the HHT. Noise generated on the displacement graphs is just noticeable, but this corresponds to large peaks in the tension plot.

The reason that these oscillations (at 0 to 10 seconds) are attributed to noise and not simply dynamic oscillation is that, firstly the reactions were ramped off slowly over a period of 100 seconds real time, and secondly, the vertical displacement should at least go negative before it can bounce up back to it's original position. In fact vertical displacements should be negative throughout step 2 if the simulation is to be correct.

The same stepping and model data were used for the three models, and the only difference (besides the implied neglecting of damping and inertia in the static analysis), is that in the 'fast' model, node 1 has a prescribed harmonic motion for one cycle only, whereas in the previous analyses the harmonic motion was throughout the step.

A tension-displacement plot at the fairlead position is shown in figure 4.11 for all three situations, where hysteresis of the fast dynamic model about the static model can be seen. These hysteresis loops would be similar to those obtained by Morrison [32] if the cable had been moved more slowly. The slow dynamic model and the static model coincide almost exactly and demonstrate the nonlinearity caused by the cable geometry.

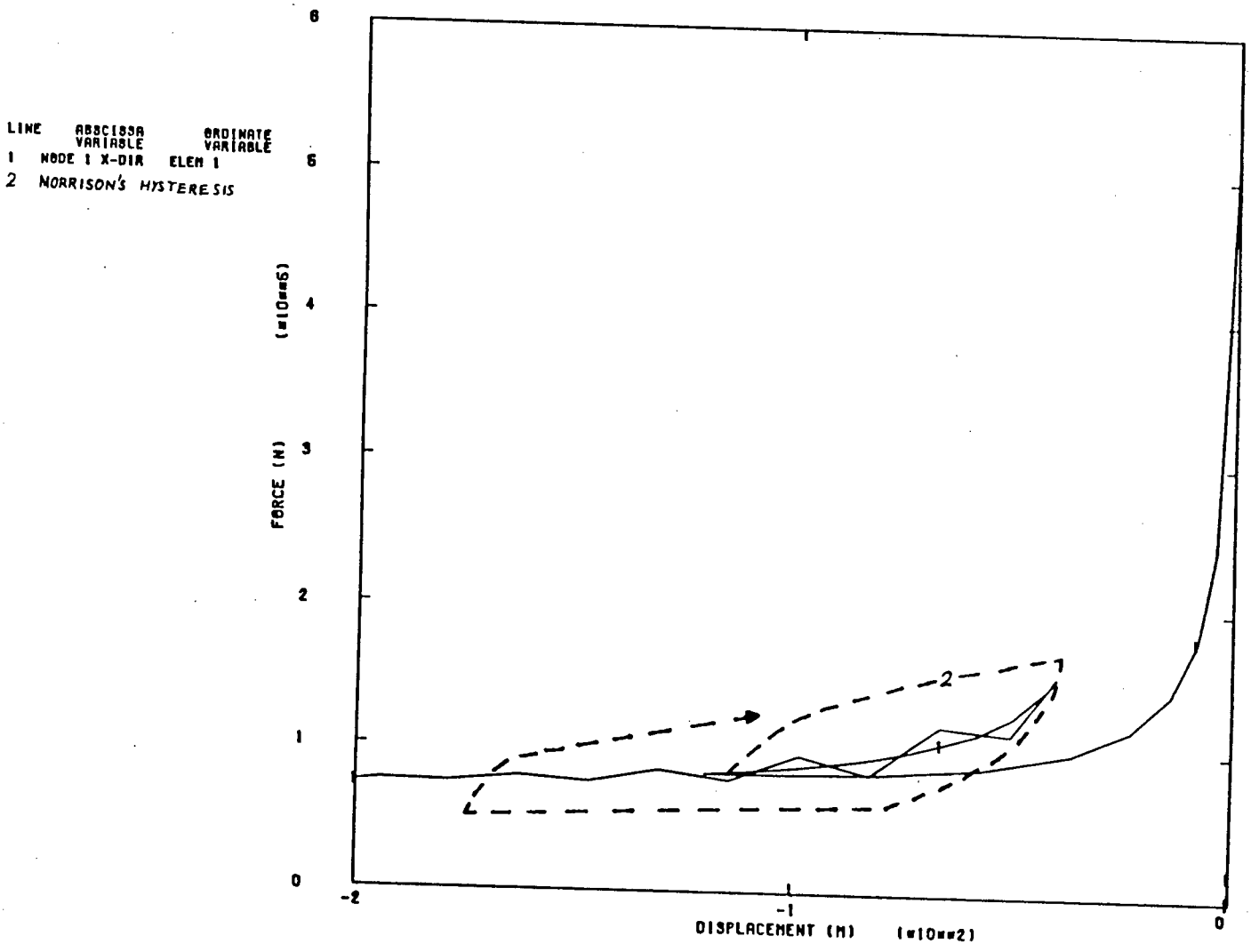

Fig 4.11 Fairlead Reaction

This nonlinear behaviour in the tension-displacement characteristics at the fairlead position is often assumed to be the input for a tower and guyline study [32, 24, 30 65]. The results in the rapidly moved dynamic analysis have been smoothed to eliminate the peaks, in order to clarify the dynamic effects. The cable inertia 'holds the cable back' at the initial motion of node 1, resulting in a higher tension, than that which occurred in the static analysis. This higher tension then causes the cable to 'twang' forwards, (overshooting the static position) to a position of lower (than the static analysis) tension. This repeated motion causes the oscillations about the static equilibrium postion.

When the cable was moved too fast, high tensions resulted at the points of high accelerations, ie. where there are abrupt velocity changes as indicated by points A and B on figure 10b. These points respectively correspond to the instances that the velocity of the sine wave is brought from zero to it's maximum in one increment, and from it's maximum to zero in the last increment before the cable end is held in position. This is actually a feature of the way in which the sine wave is applied, and it is this abruptness that causes unwanted compression in the cable.

In general, the displacements of all the cable nodes follows that of the prescribed displacement at node 1. Dynamic oscillations (and noise) are more easily observed when there is no forcing function, this is why node 1 is held in position after one cycle. Here it can be seen that soon after the cable end is held, the X-displacement results of the respective nodes follow each other exactly; similarly with the Y-displacements, although differences are quite marked during the time that node 1 is moved. This shows how the cable will try and oscillate stably in the first mode position, with a natural period of 17.2 seconds, and slowly die out, at a rate dependent on the amount of damping.

Limiting the maximum time increment in a step or reducing the half step tolerance, would smooth the jaggedness in the curves.

4.4 Cable Whip

A further test model developed was that of a free falling cable pinned at one end, in order to establish whether problems of an ill-conditioning nature in a whip or snap load situation could arise. The free end of the cable was of particular concern in this regard, and so the nodes were numbered to the fixed end (fixity or region of high rigidity) from the region of flexibility which in this case is the free end, as recommended by Phaal [63].

The falling of the cable and it's subsequent pendulum like motion and cable whip is presented graphically in fig 4.12 (i),(ii) & (iii).

A similar analysis using FEM was performed by Fried [19] where they too noted the 'cracking of a whip' phenomenon at the free end of the cable. Because of the dangers associated with snap loads and cable whipping, it is desirable that a finite element analysis can model this phenomenon, if and when it should occur in later models to be analysed.

Because only numerical damping and not internal viscous damping or fluid drag was incorporated in the model ie. there was a conservation of energy, the cable reached a height equal to it's original position after the first half period, albeit in a curved configuration as a result of the flexibility of the cable.

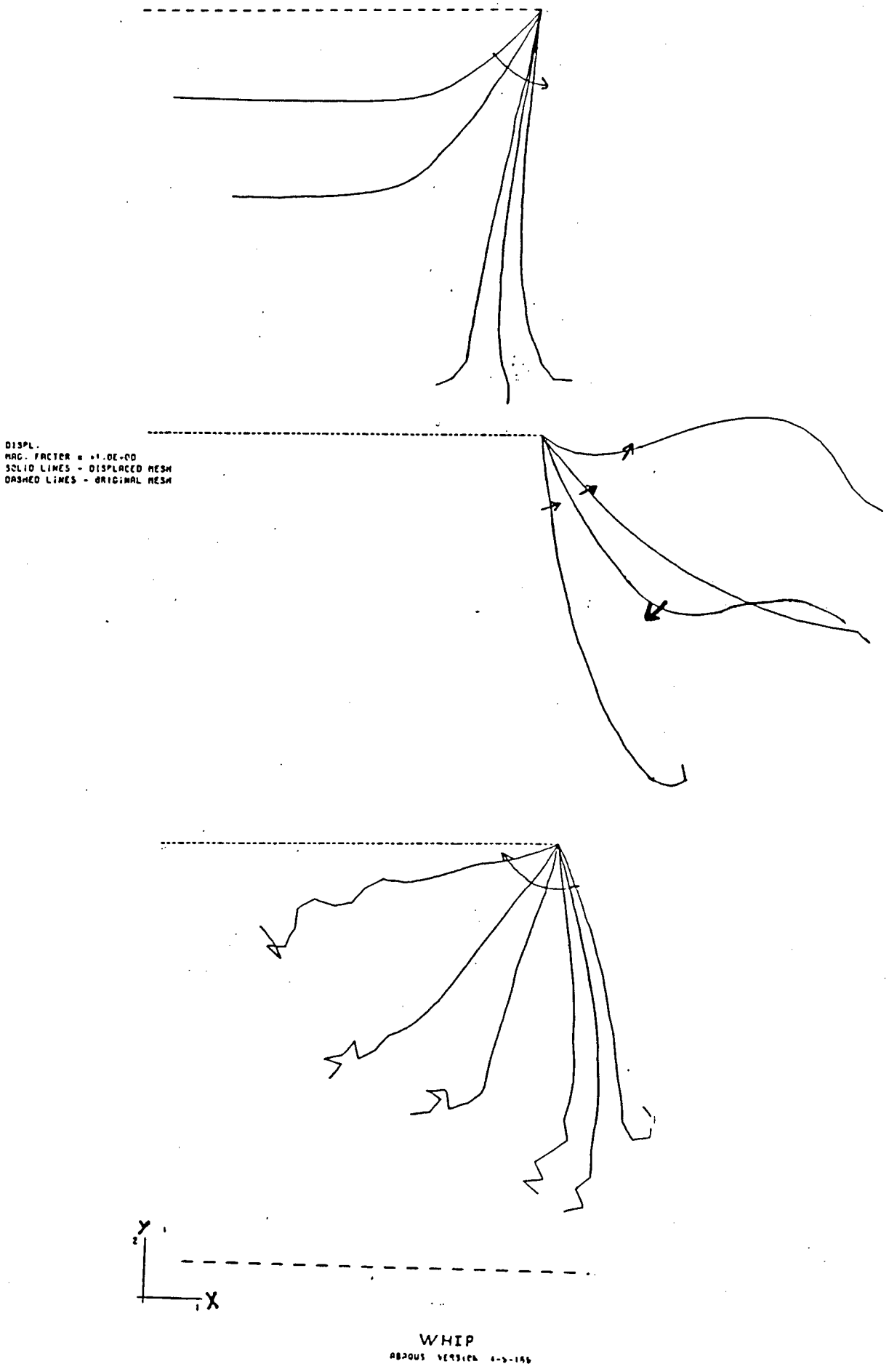

Fig 4.12 Cable Whip

As a further test of ill-conditioning, the nodes were numbered in reverse order viz, from the fixity to the free end, and even in this case no convergence difficulties were experienced, although the CPU time went up by about 50%, with an accompanying 10% difference in the displacement results. This is in support of the importance of node numbering as mentioned by Phaal [63].

This example negated the fear that a free end of a cable could cause numerical difficulties, and further demonstrated the possible applications and versatility of the FEM in this regard.

4.5 Submerged Cable

Although the suspended hanging configuration of the cable in air has been successfully achieved, what is really required is that of a submerged mooring cable, anchored to the ocean floor and constraining the offshore facility, subjected to dynamic loads.

Firstly, because of the large sag associated with large mooring cables in the offshore environment, it is typically found that half the cable rests on the sea-bed in normal conditions, as shown in figure 1.1 . It is this normal state catenary position that is required before the dynamics can be attempted.

The ocean floor is considered undeformable and thus the rigid surface option (*RIGID SURFACE) was used in ABAQUS. It is necessary when using this option to introduce interface elements between the cable and ocean floor, as portrayed in figure 4.14. These elements monitor the contact pressure or the gap that exists (as the case may be) between the cable nodes and the respective closest point to the rigid surface.

Length	500m
Diameter	75mm
EA	2.21E9 N
Bending Stiffness	700m
Elements	20 x B21H
Water depth	383m

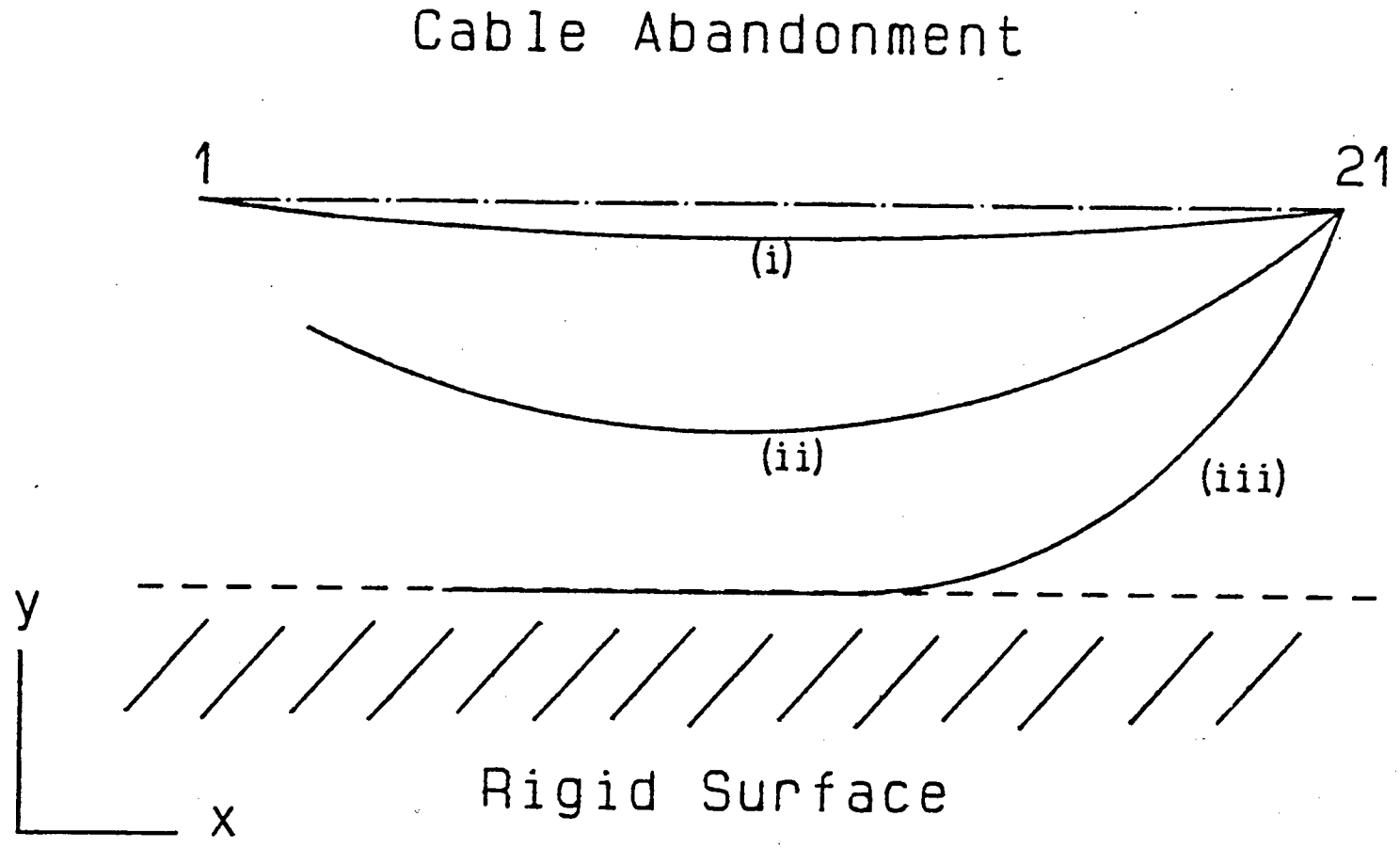

Fig 4.13 Submerged Cable Problem

Although on a macroscopic scale the seabed is rigid, closer up it can be assumed to be covered by a layer of mud. This mud introduces sliding friction and a suction effect. Sliding friction in a two dimensional analysis has a negligible effect on the cable tension and response because the only sliding that occurs is as a result of elasticity in the cable, but for completeness and at no extra difficulty, it was included. In fact it is recommended, because this friction gives some resistance to motion in the horizontal direction, thus avoiding possible singularities.

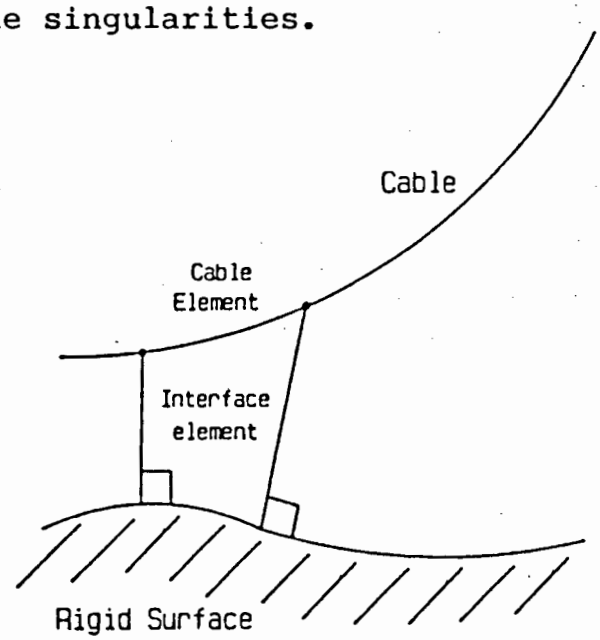

Figure 4.14 Interface Element

In the situation where the cable is lowered to the seabed by the end to be anchored (the process referred to herein as 'abandonment'), one has to be aware that the cable will slide (and needs to slide about 20m) so that care should be taken not to have too high a coefficient of friction and 'stiffness in stick' otherwise buckling can occur. Different values of friction had no effect on either the results of an analysis or the CPU time involved.

Mud suction on the other hand may not be negligible, as typically the viscous action of the mud on the cable, can be larger than the cable weight itself, especially if the cable

has been resting for a long period of time, and has buried itself in the mud.

The suction effect of the mud was modelled as a downward pressure acting on the cable, which decreases exponentially to zero as the gap between the cable element and the rigid surface approaches a user specified height.

The coefficients for Morison's equation were chosen as Cd=1.0, Cm=1.0 and Ct=0.001, which are typical values used in the literature, and were kept constant throughout the analysis; ABAQUS does not have the facility for variable coefficients. Buoyancy is considered to be constant with depth and to act vertically upwards. It is therefore acceptable to simply reduce the distributed load of the weight acting downwards by 15% (the mass of water relative to steel).

Having defined all the properties of the model, we now determine the history of the model. Firstly the catenary must be obtained, for which there are seemingly two options, 'abandonment', or' recovery'. Recovery entails lying the cable on the seafloor, anchoring one end, and then lifting the other end to the fairlead position on the offshore facility. Abandonment entails supporting the cable on the surface of the sea, fixing one end at the fairlead, and then moving the end to be anchored to the desired position on the seafloor.

Both methods were tried, and needed to obey the 'catenary start-up criteria' established earlier viz. ramping on weight while supporting the nodes, then ramping off the reactions. The abandonment method took less than half the CPU time of the recovery method to converge to a nearly identical (0.1% discrepency) solution, and was as a result used thereafter. This result is attributed to the fact that there is less ocean floor contact in the case of abandonment. However, when contact occurs it does so in the form of an impact load, necessitating a vast reduction in the time stepping to achieve convergence. In a static analysis, there is again a large

reduction in the time stepping, due to the highly nonlinear effect of the ground support on the cable.

It was concluded that the continual monitoring of the gap conditions and the kinetic energy imparted to the rigid surface, combined with the higher stresses occurring, albeit locally, resulting in further iterations to keep within the tolerance, absorbs a significant proportion of CPU time. This view is supported by also noting the increase in CPU time from 6 to 14 minutes of the freely hanging catenary of chapter 4.1 compared to that of the catenary in contact with the seabed.

Convergence difficulties were experienced at lift-off, which were directly attributed to the modelling of the mud suction in ABAQUS, as convergence was easily achieved for analyses where mud-suction effects were ommitted. Various values of suction pressure were tried, and it was found that even when the pressure was set to zero, CPU time increased by 40%. The problem seemed particularly sensitive to increased pressure values, and for simplicity mud suction effects were ommitted in subsequent runs.

Although the cable was submerged in these models, Morison's equation is discounted in a static analysis, as the relative motion between the ocean and structure is not considered. Moving the cable dynamically to the catenary position caused substantial increases in CPU time because of the fluid loading nonlinearity, and resulted in marginally different results. The difference between the two becomes less as the cable is moved slower.

In a further development, an identical cable was attached to the first cable at their respective fairlead positions. The model was then symmetrical about a vertical axis going through the fairlead position, allowing horizontal constraints at this point to be removed. A 15m Stokes' wave was then passed over the cable to check that everything was working correctly, prior to modelling a cable/platform interaction. This wave

caused a maximum displacement of two metres at the apex, which showed the nominal effect of the fairlead response to cable drag alone ie. nearly all the motion caused at the fairlead in an offshore facility is caused by the the fluid drag on the facility and not on the cable.

The motivation behind this submerged cable model was to act as a forerunner to the articulated tower and floating platform, which are discussed in the following sections.

4.6 Floating Platform

The motivation behind modelling a complete mooring system, when we are primarily interested in only flexible structures, is that cables are rarely used in isolation and are generally used for joining two inflexible structures. As we are concerned with i) the effect cable motion has on itself (in terms of stresses) as well as ii) the effect that cable motion has on attached bodies and in particular the cable/structure interaction, the following models were deemed useful in the analysis of large cables.

In figure 1.1 we see the two types of offshore drilling stations that are of concern to us; the articulated tower and floating platform. The modelling of a floating platform with it's attached guying system was attempted first, because these are the more common type of offshore mining facility presently found off the South African coast.

The initial simulation of the platform was that of a short rigid (large bending stiffness relative to the cable) isoparametric beam element, with a mass and buoyancy corresponding roughly to that of the 'Omega' at Mossel Bay. As only a two dimensional analysis was performed no allowance could be made for roll, yaw and sway. This simplification is made in order to save on computer time, and is deemed

acceptable for initial, 'order of magnitude' analyses of this kind. Twenty hybrid elements were attached at either end of this element to model the mooring cables attached at the fairleaders.

The modelling procedure was as follows:

Step 1 - Support the cable and platform on the ocean surface and apply weight.

Step 2 - Move the cable into position by abandoment while still maintaining the platform reactions.

Step 3 - Ramp off the reactions and simultaneously ramp on the buoyancy load.

Step 4 - Subject the model to a wave loading.

The first problem was that the very large platform element coupled with the adjacently small cable elements caused singular matrices as a result of the large ill-conditioning.

The platform was then given an axial and bending stiffness equal to those of the cable, while keeping it's weight and inertia the same. This simplification is however of little concern as the interaction of the platform on the cable is essentially unaffected. The change produced better conditioning of the stiffness matrix and allowed for the achieving of the cable catenary.

Choice of the tolerance was critical - for too tight a tolerance, regardless of how small the time increment was, the solution couldn't converge. For too large a tolerance the solution could converge to an inaccurate solution and jeopardise convergence in the next increment.

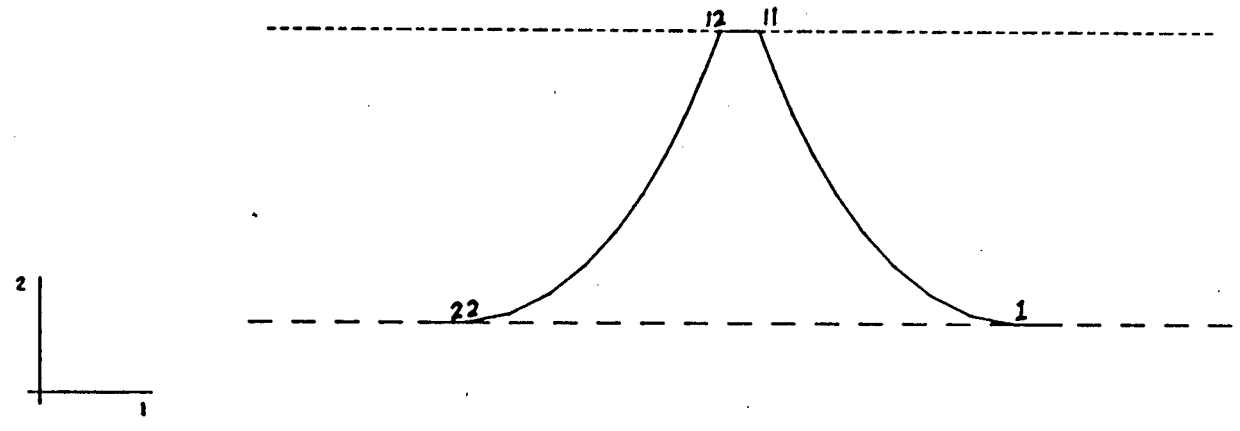

BUOYANT RIG

STEP 2 INCREMENT 50 ABAQUS VERSION 4-6-169

DISPL.
MAG. FACTOR = +1.0E+00
SOLID LINES - DISPLACED MESH
DASHED LINES - ORIGINAL MESH

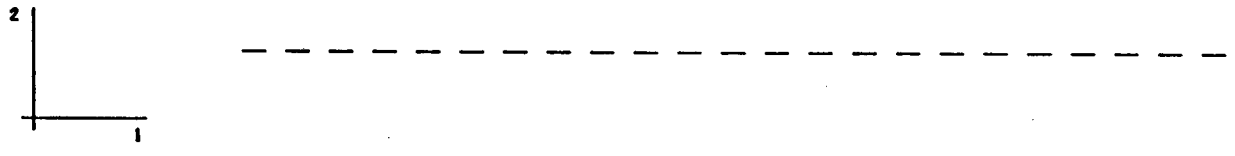

BUOYANT RIG

STEP 1 INCREMENT 1 ABAQUS VERSION 4-6-169

Fig 4.15 Floating Platform Model

Convergence could not be attained for step 3 ie. the step in which buoyancy was added. When dynamic analysis was applied, non-convergence resulted because of ill-conditioning in the mass matrix, as the stiffness of the tower had already been reduced to that of the cable, and the same bending and axial stiffnesses as in the submerged cable section were used. By reducing the time step, convergence to the first couple of increments was achieved, but the results obtained were totally unrealistic (eg. reactions of 1.0E20). Attempting the analysis statically also produced convergence difficulties, and it was later suspected that the buoyancy loading was the cause. The buoyancy load, being large in order to support the weight of the system, coupled with the already ill-posed problem, further increased the likelihood of non-convergence.

The buoyancy and weight were reduced by 75% (physically, an arbitrary amount) while still keeping the buoyancy load larger than the combined weight of the cable and platform, but to no avail in the static analysis. However in the dynamic analysis it was found that convergence was obtained throughout the step, but now a different problem arose; the platform sank!

Even though the step was completed, the results of the ground reactions were ludicrous (1.0e32) which is why the platform was pulled under. These results had all the symptoms of ill-conditioning, and demonstrate a particular danger of ill-posed problems viz. that even though convergence was achieved, the accuracy of the solution was nowhere near the specified tolerance.

Furthermore, zero pivots were occurring at nodes 44 and 45 internal to the program. These nodes correspond to points on the rigid surface and are the nodes on the interface elements where the large ground reactions were occurring, but insufficient information is given by the computer to deduce the cause. This phenomenon did not occur in any of the other previous models where a rigid surface was used, but without access to the ABAQUS code, conclusions as to the cause cannot

be drawn.

Much work was (is still) needed on this model to overcome mass and axial to bending stiffness ill-conditioning before a useable model can be presented. At this stage useful results were being obtained in the articulated tower model, and so it was decided to rather channel efforts here instead of the floating platform, where at the moment, the situatition is still unclear.

4.7 Articulated Tower

This model was set up in a way similar to that of the floating platform in that the cable catenary was also obtained by abandonment, and the same stepping procedure was applied. In this case a relatively light articulated tower was pinned at the ocean floor.

For the sake of simplicity, the constraining cables and the tower apex meet at the same point, whereas usually the cables are separated by the length of the drilling platform.

Figure 4.16 shows i) a schematic diagram of the articulated tower and guying system on the rigid surface, ii) static equilibrium showing the cable catenary and iii) the resulting displaced shape in a shear current of 5 m/s at the ocean surface and zero at the ocean bed. The relevant model and history data are shown alongside the diagram.

There were no numerical problems in obtaining the catenary or static equilibrium of the model, with the node numbering from a low to a high stiffness region. The cable should be numbered first then the tower according to the previously established numbering from a flexibility to a fixity [63]. Numbering the tower first and then the cable leads to ill-conditioning at the start of second step.

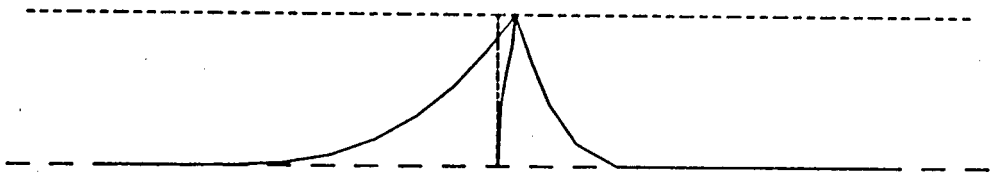

ART-TOWER
STEP 3 INCREMENT 153 ABAQUS VERSION 4-6-169

DISPL.
MAG. FACTOR = +1.0E+00
SOLID LINES - DISPLACED MESH
DASHED LINES - ORIGINAL MESH

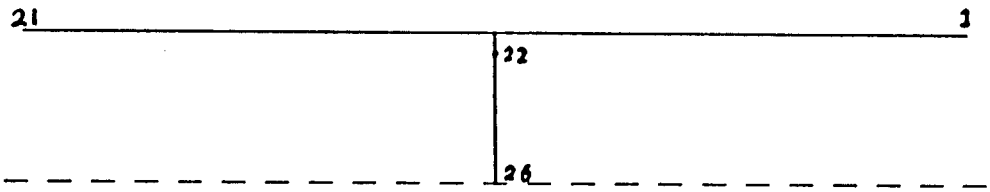

ART-TOWER
STEP 1 INCREMENT 1 ABAQUS VERSION 4-6-169

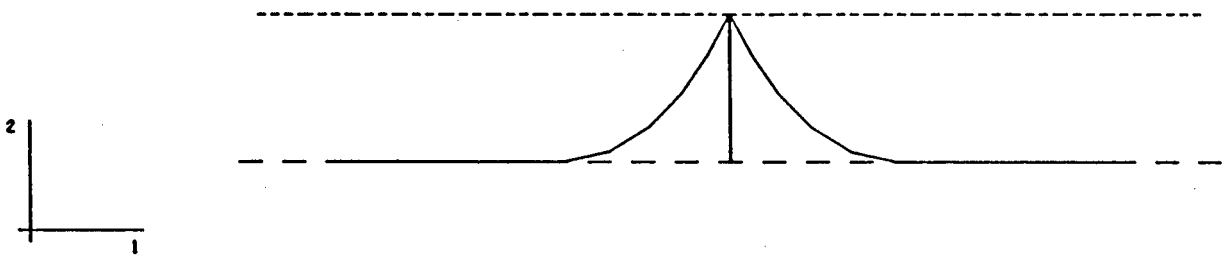

ART-TOWER
STEP 2 INCREMENT 66 ABAQUS VERSION 4-6-169

Fig 4.16 Articulated Tower Model

Two things to note about the results are firstly, that the cable tension in the model increased by about 15% from the sea bed to the fairlead position, and secondly the cable tension at a particular node increased approximately exponentially, as the distance between the tower and the point of contact of the cable and ocean floor increased. This was observed when the anchor position was moved out in order to increase the tension in the line, but can also be seen if the fairlead position is displaced statically to the far side. A typical increase was from 1.1E5 N to 1.5E5 N when the cable was moved out 25m, about 5% of the horizontal projection of the catenary length. The reason for trying these different catenary positions was to establish tensions at various positions, enabling a comparison with later dynamic analyses.

The nonlinear tension-displacement relationship can be seen in figure 4.17 for the fairlead reaction on the high tension side, and for midspan elements on either side of the fairlead, in the displacement of the statically moved fairlead position.

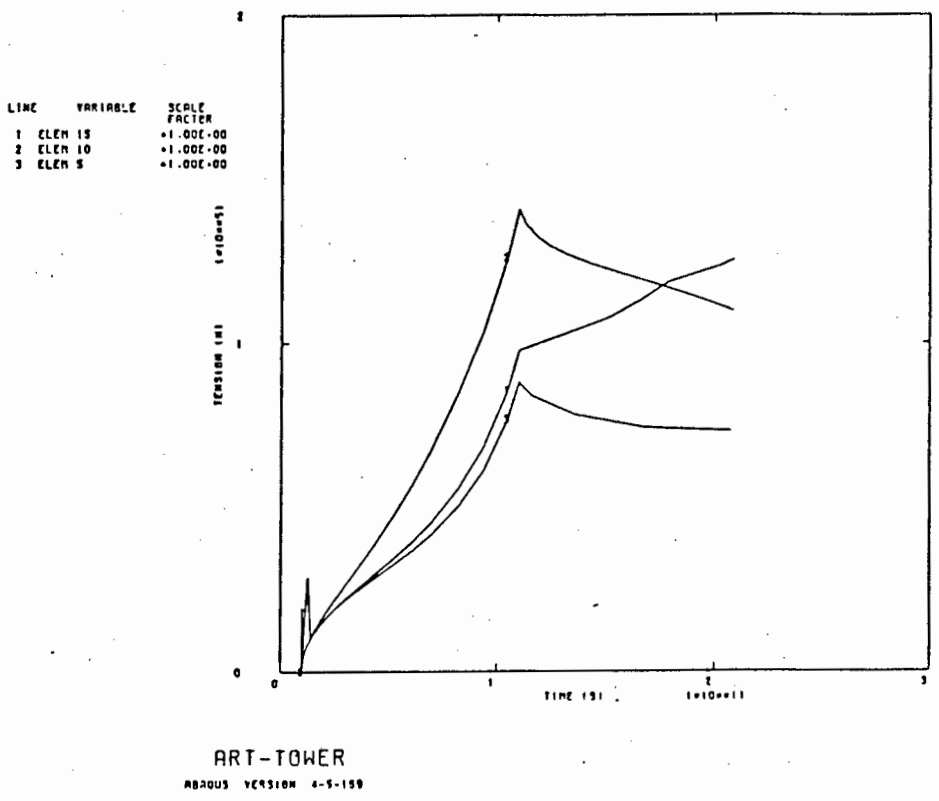

Fig 4.17 Static Displacement Input

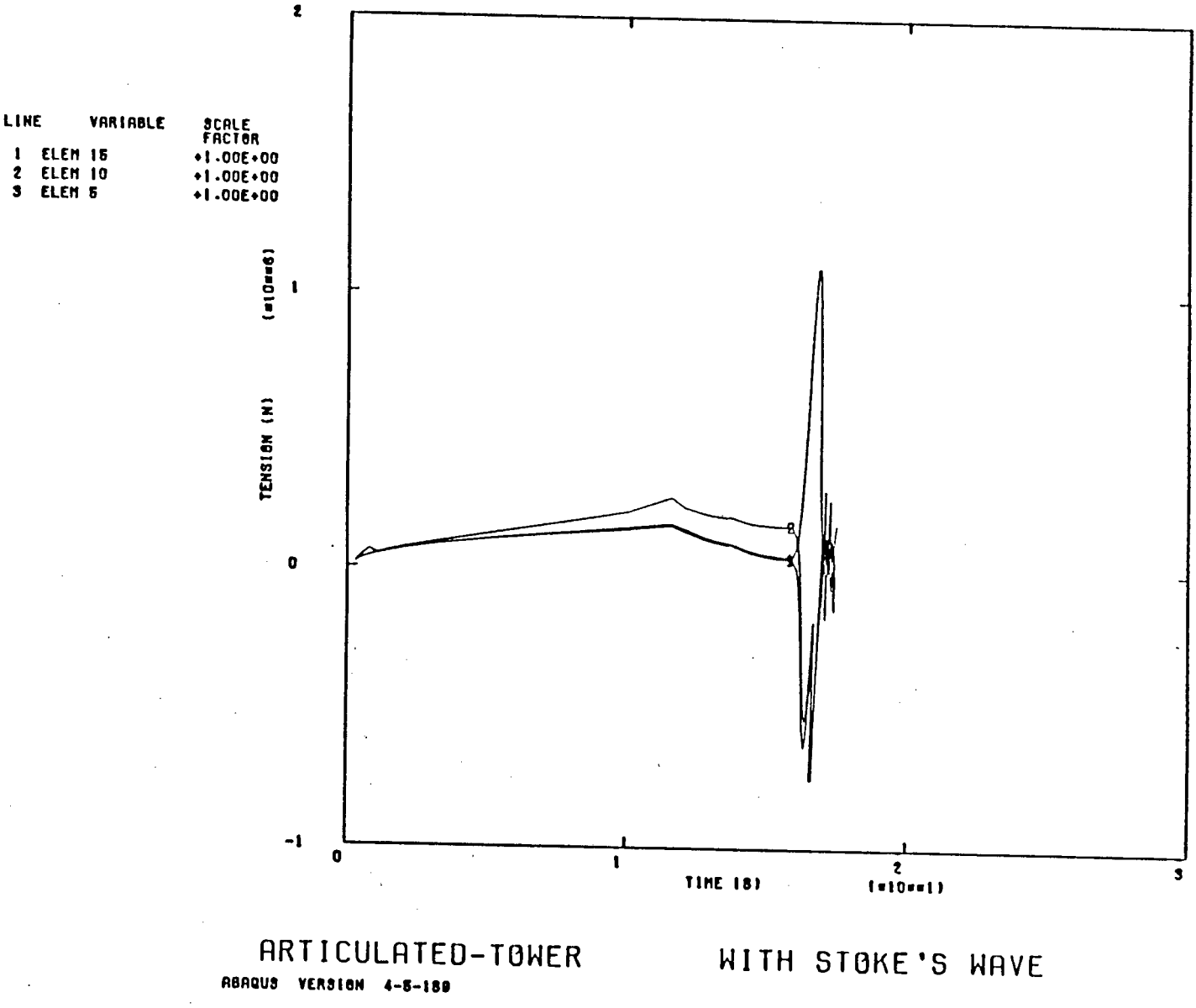

Fig 4.18 Wave Induced Cable Shock

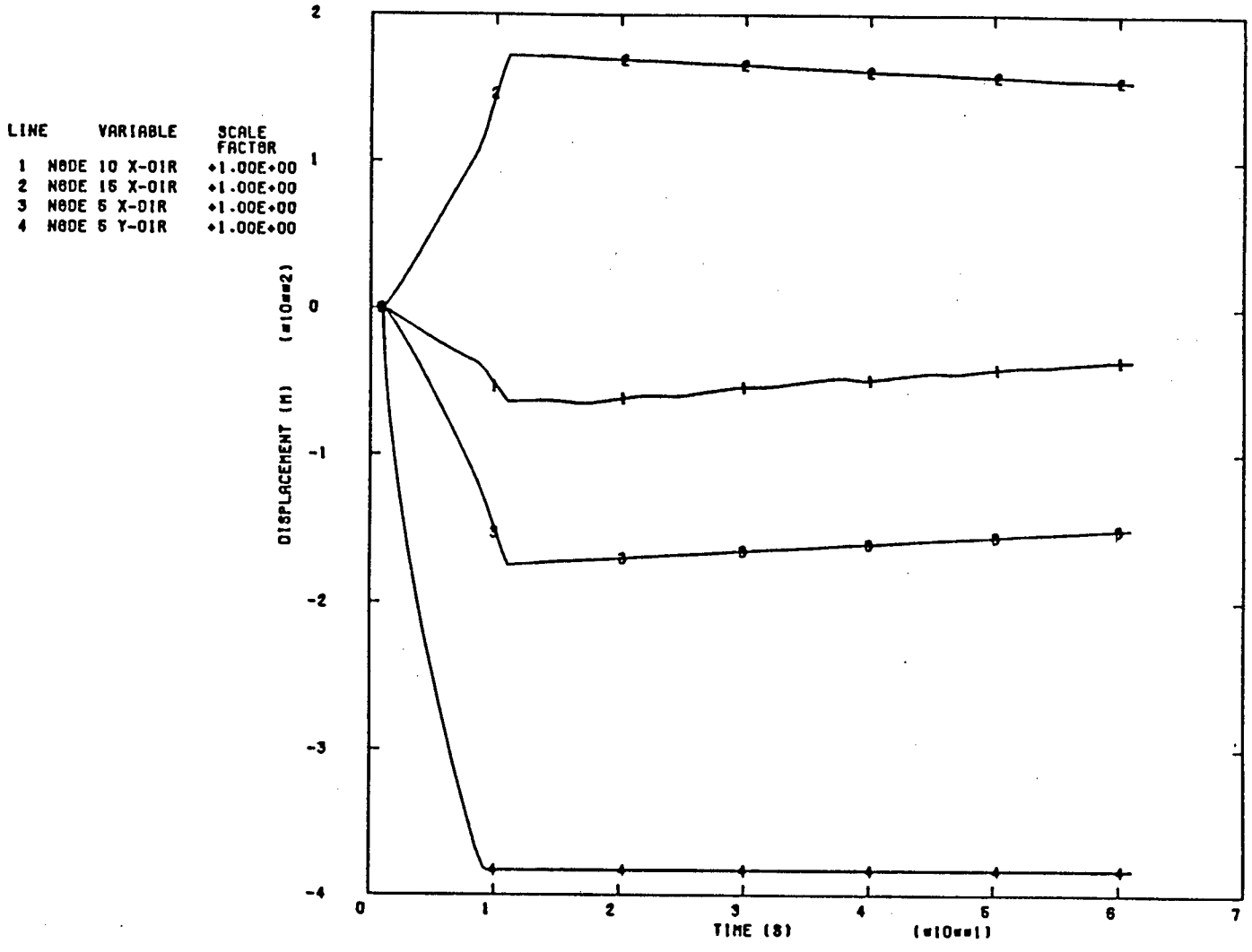

Fig 4.19 Response to Shock

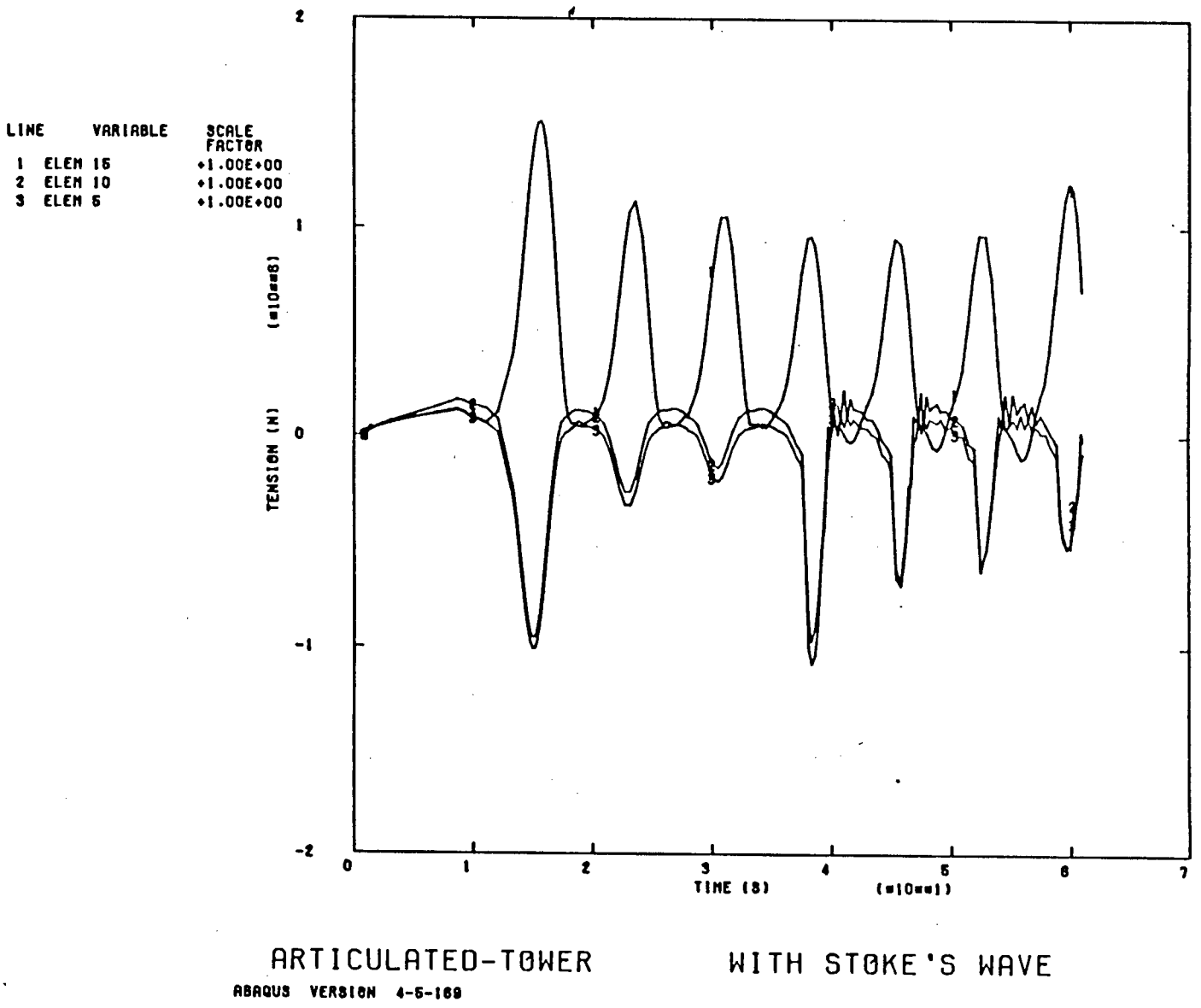

Fig 4.20 Cable Shock - Multiple Cycles

Notice in figure 4.18 how the cable tensions in the abandonment step peak at about 7.0 seconds. This occurs just prior to first ground contact and thereafter the tensions decrease as the rigid surface supports more of the cable weight.

In step 2 the initial residuals were of the order of 1.0E25 in a static analysis, but decreased as the time increment was automatically reduced. First convergence was achieved with a time increment of 8.0e-7 seconds in a step of 10.0 seconds, indicating start-up difficulties, thereafter time increments increased dramatically to about 1.0 seconds (see also 4.1 The Catenary). Once ground contact was made, time increments were decreased to between 0.5 and 3 seconds.

Having achieved the catenary, a Stokes' wave train of wave height 20m and period 7 seconds was passed over the model.

This resulted in very marked peaking of the tensions (the displacements were similar to those in figure 4.19) but more importantly, although the tensions on the wave side increased as expected, the tensions on the 'slack' or leeward side became negative ie. the cable came under a high compression of -5.0E5 N.

This had the appearance of the bending stiffness of the cable being too high, but on examination it was found to be slightly less (at 700 Nm per unit curvature) than that of a typical mooring cable.

As a further check, the bending stiffness was reduced to 20 Nm (below which ill-conditioning arises as mentioned earlier), the anchors were moved out 25m and the tower bending stiffness was increased to 2.3E9 Nm. The reason for this is that in the previous model, the tower appeared too flexible near the top whereas we want it to behave more as a pinned rigid body.

The maximum time increment was also decreased, but the total

time in the wave step was increased in order to see if the 'peaking' in figure 4.18 was simply a 'start of step ' convergence phenomenon.

In the next run, the tension versus time plot in figure 4.20 shows that the high stresses (tensile and compressive) at the start of the wave step were not spurious 'start-up' peaks. In fact the tensions oscillated with a period of 7 seconds - the same as that of the wave period - and were exactly in phase with each other. Therefore this high compression appears to be a 'shock wave' phenomenon, as a result of the leeward side cable not sagging sufficiently to stay in continual tension. The cable displacements, besides those of the fairlead position, hardly change from the catenary position as displayed in figure 4.19.

Perhaps the loading was imparted too quickly for the cable to respond and deform into a slack position. This would seemingly only be possible if the Morison's coefficient of the cable were too high ie. not allowing the cable to move very fast relative to the surrounding fluid. An impulse load then applied to the fairlead by the wave could then cause longitudinal wave propagation along the length of the cable.

However the coefficients for the cable are perfectly acceptable and have been successfully applied by other users. This run took 3 hours CPU time, necessitating care when trying parametric variations on this model.

A feature worth noting in figure 4.20, is that two large negative peaks occur at an interval of 23 seconds. This corresponds to the natural period of the cable/tower system combined with the third cycle of the wave. The system period was determined by moving the fairlead position by 20m to the right before releasing, and was found to be 22 seconds.

Also note the spurious oscillations at about 40 seconds, just after the second large negative peak. At this stage it is

still unclear as to whether these oscillations are caused by the infiltration of noise or by the large shock induced peak.

Three changes were made to the model; 1) reducing the cable length by half but still using 20 elements. This reduced the number of elements in contact with the ground and also increased the number of suspended elements, which would allow for greater flexibility; 2) reducing the drag coefficient of the tower to 2.0 from 15.0 for the purpose of reducing the fluid loading only; and 3) setting ocean currents to zero. This model is shown in figure 4.21.

Another model was run simultaneously using these changes, but instead of applying a load, the fairlead node was displaced 18m in a 10 second dynamic step.

Tension history results are displayed in figure 4.22 for the above 'wave' analysis and 4.17 for the 'prescribed boundary condition' analysis.

Firstly, and of prime importance we notice the disappearance of the shock wave phenomenon. This is because more elements allow for greater flexibility and or the reduced drag on the tower reduces the applied load on the cable. The largest displacement was 1m (smaller than expected) and occurred at the fairleader. At least no cable compression occurred even though the displacement seems unrealistic.

Tension oscillations can be observed in figure 4.22 which correspond to the 3rd harmonic of the wave period (7 seconds) with a period of 2.33 seconds. It seems possible that because the natural period of the cable/tower system is a multiple of the wave period, the accentuating of these harmonic oscillations occurs.

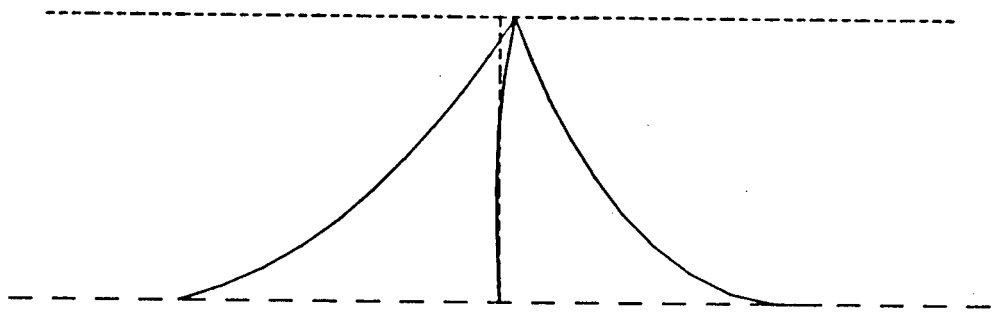

ARTICULATED TOWER PRESCRIBED B.C.

STEP 3 INCREMENT 24 ABAQUS VERSION 4-5-169

DISPL.
MAG. FACTOR = +1.0E+00
SOLID LINES - DISPLACED MESH
DASHED LINES - ORIGINAL MESH

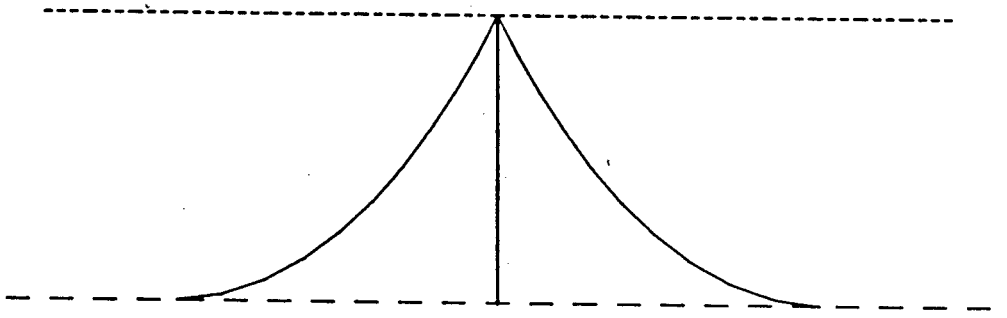

ARTICULATED TOWER PRESCRIBED B.C.

STEP 2 INCREMENT 55 ABAQUS VERSION 4-5-169

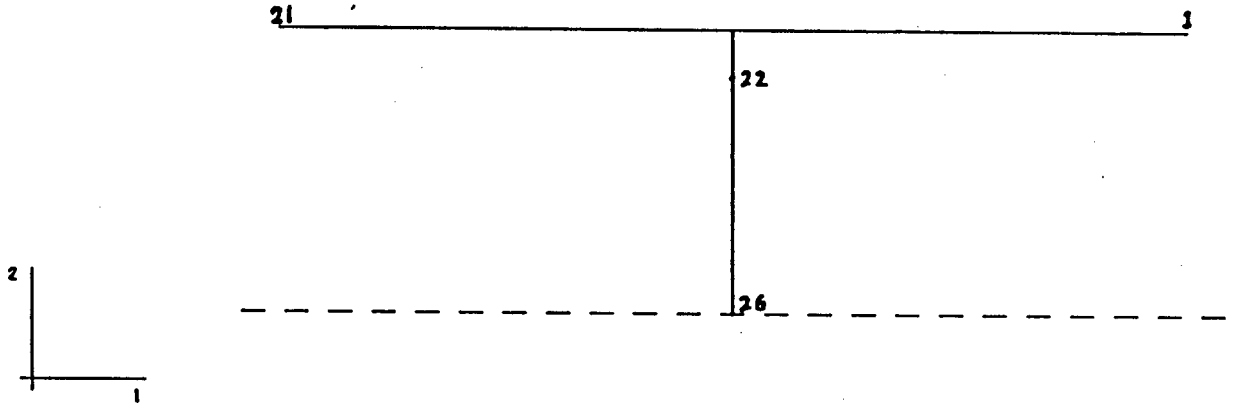

ARTICULATED TOWER PRESCRIBED B.C.

STEP 1 INCREMENT 1 ABAQUS VERSION 4-5-169

Fig 4.21 Reduced Tower Model

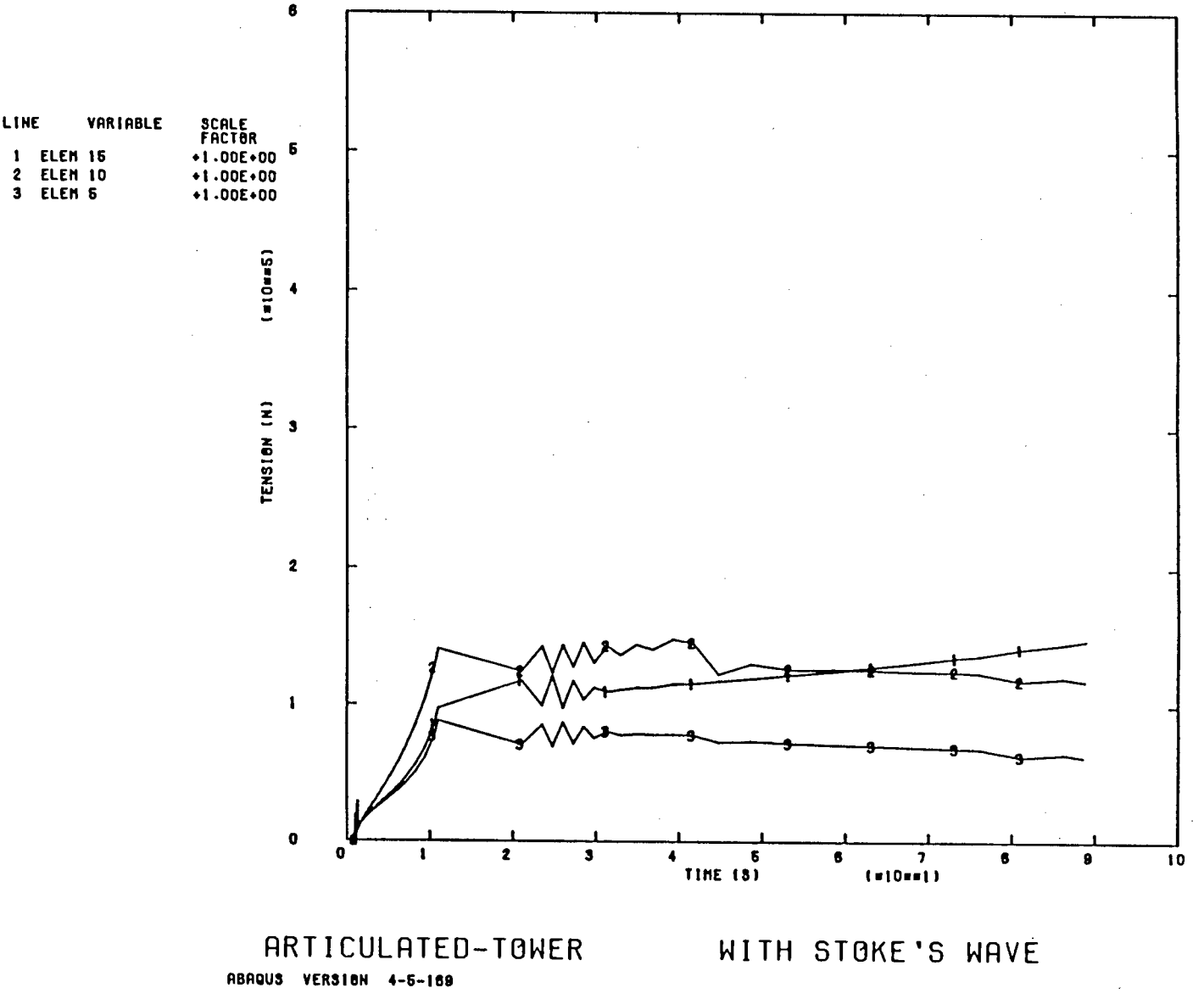

Fig 4.22 Reduced Wave Load

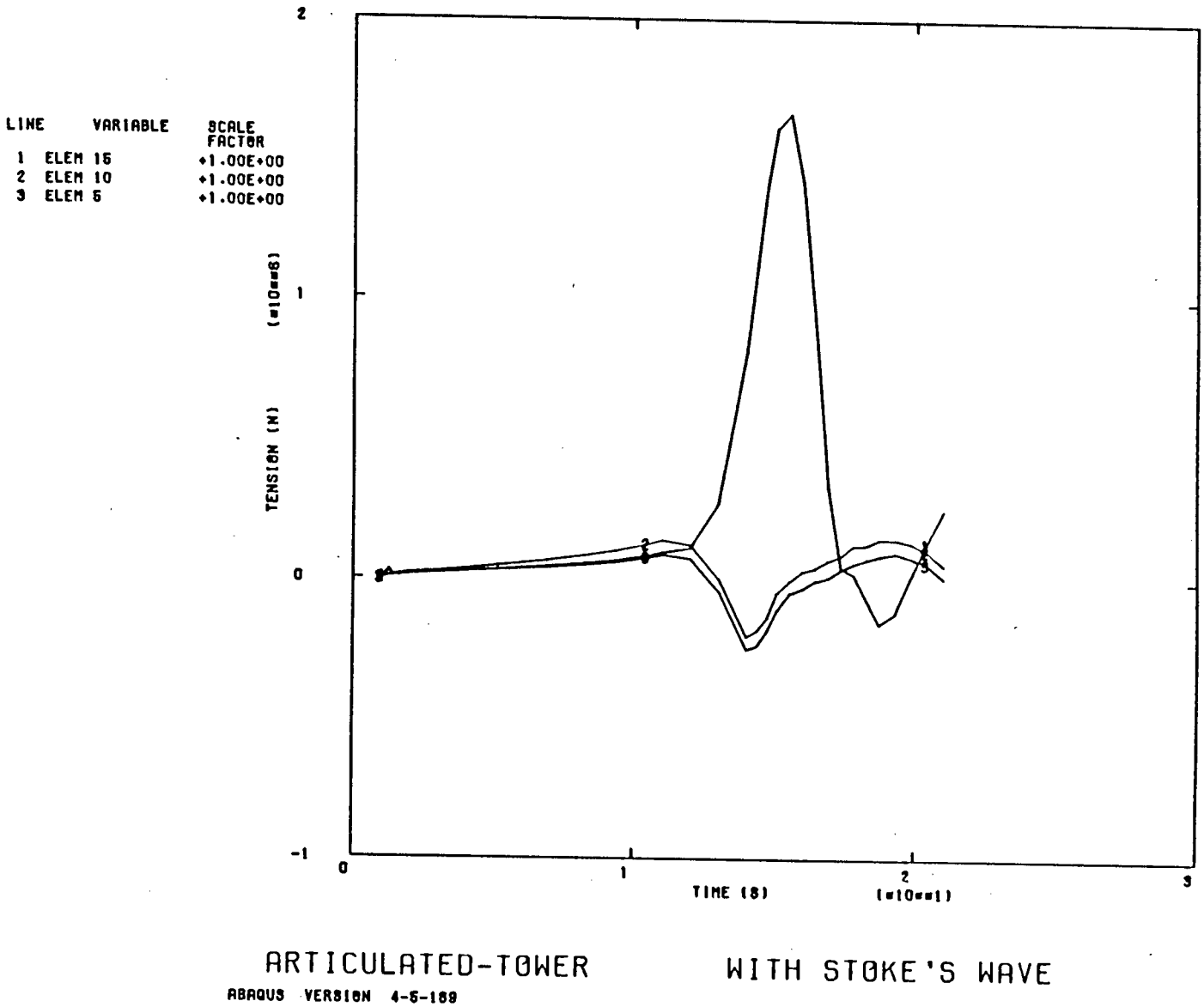

Fig 4.23 Small 'Shock' Wave

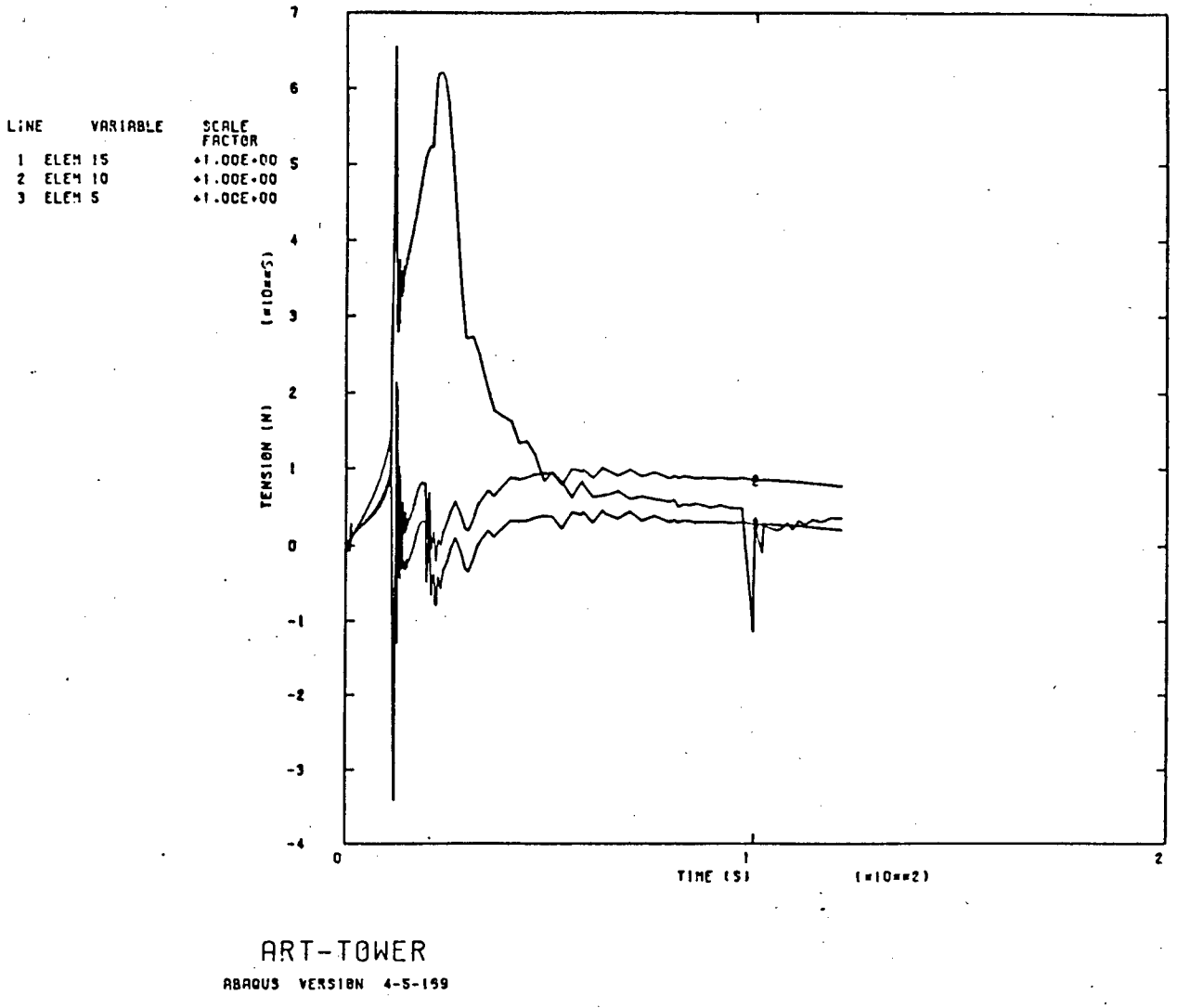

Fig 4.24 Prescribed Boundary Condition

Another interesting feature was that by halving the cable length but not the number of elements, ie. discarding that portion of the cable that forever rests on the sea bed, the CPU time was reduced by as much as half, again supporting the earlier statement that the monitoring of the surface contact conditions consumes much time.

Notice also the spurious peak in figure 4.22 at start-up. The catenary was obtained statically so it is not caused by dynamic oscillation. This peak is due to start-up difficulties and demonstrates the sensitivity of the cable problem. From past experience of noise, it is recommended that the numerical damping should be increased to HHT=-0.25

In a further run the effective tower diameter was increased, effectively increasing the applied load, and in this model the shock wave still occurred but not as radically (figure 4.23) as when fewer elements were used. This supports the view that more elements allow for a noticeable increase in flexibility and response time to the applied load.

Moving the fairlead at a velocity equal to that caused by the wave in the previous model produced the results shown in figure 4.24 where compression occurs at start-up in the same shape, but not as significantly as in the case of the applied wave. This indicates that the effect of a wave induced load acting on the cable is of importance with regard to the forces present in the cable, and a simple fairlead displacement input may not be sufficient. The displacement histories shown in figure 4.19 in these models were almost identical to those of the 'shock wave' model.

Again a start-up spike occurs at the first increment of the input displacement of the fairlead, as has been the case for most of the prescribed boundary condition models.

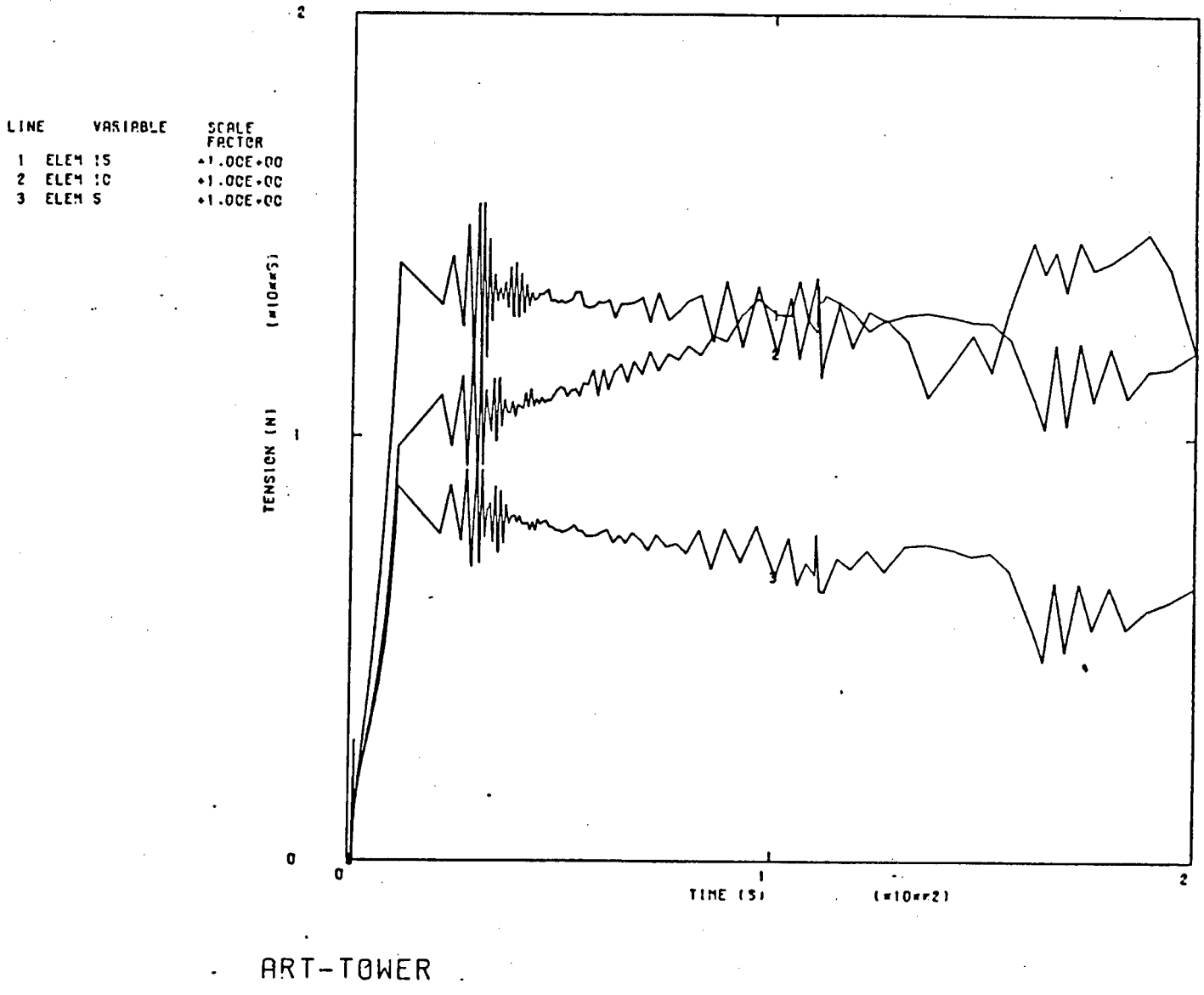

Fig 4.25 Slow Move of the Fairlead

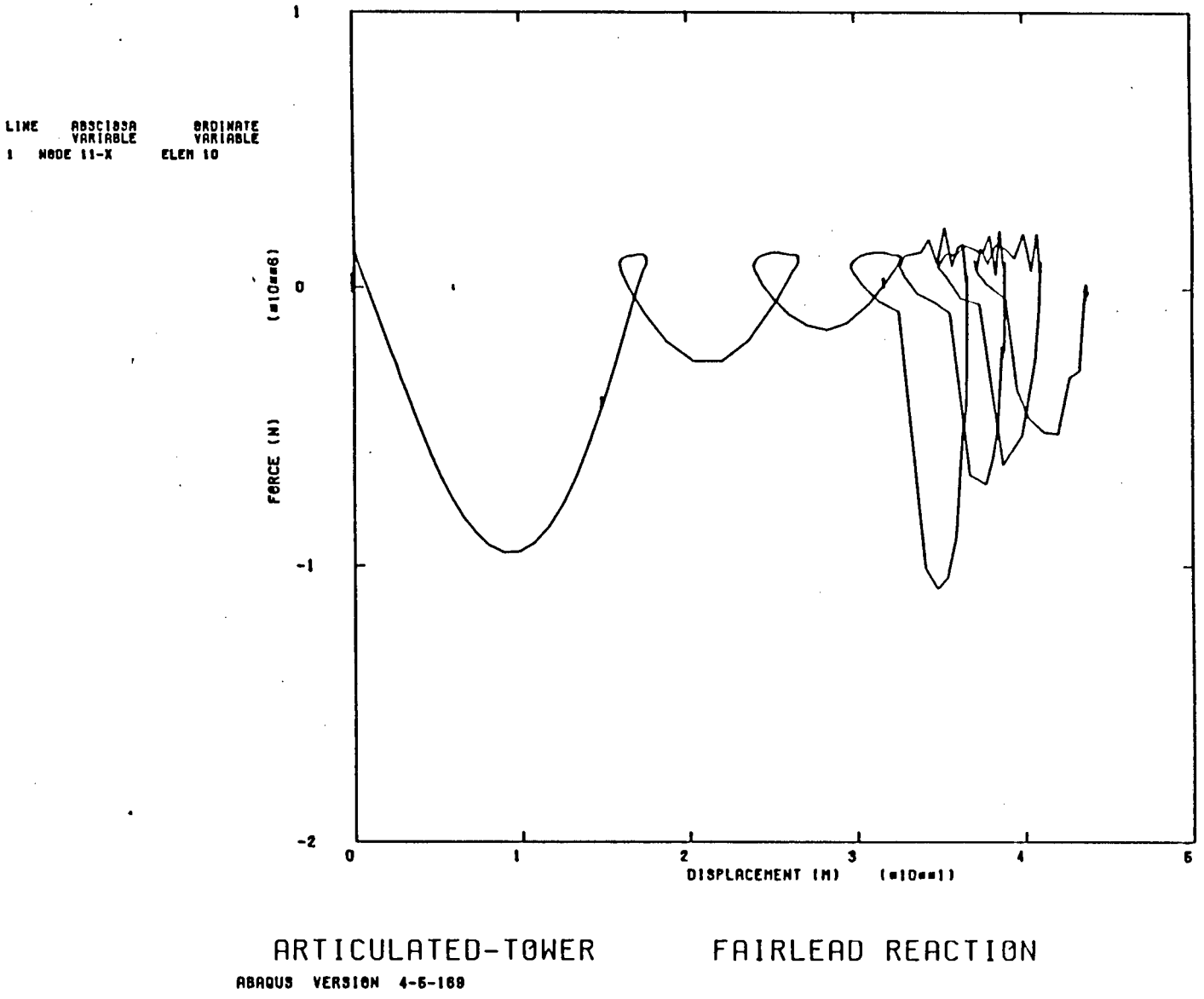

Fig 4.26 Tension at Tower

By moving the fairlead still slower, the plot in figure 4.25 was obtained, where it can be seen that no cable compression occurred, however there was still a spike at the start of the step albeit it substantially smaller. The amount of numerical damping was reduced in this model, which brings out the jaggedness in the plot, caused by the incrementing of the fairlead displacement.

In figure 4.26 we see the displacement results at the fairlead position, when the model was subjected to a Stokes' wave. The elliptical orbit of the fluid particles acting on the structure, is responsible for the 'doubling back'or 'looping' of the graph. The occurrence of cable compression is still evident.

From the above analyses it can be seen that the loading, or the manner of loading significantly affects cable stress response. Why the cable doesn't displace more under load instead of becoming negatively stressed, as has been found in these analyses, is cause for further study.

5. CONCLUSIONS AND RECOMMENDATIONS

In the previous chapter, a number of different models covering a range of problems was investigated. The conclusions of earlier models were required for later ones, and as a result, it was decided to insert the model data, results and conclusions together in chapter four. What follows, is a summary of conclusions and guidelines for the numerical analysis of flexible cables.

One of the differences between the analysis of cables versus eg. shells and rigid structures is that the starting or catenary position of a cable is unknown. The manufactured or unstressed form of the cable is a straight line and is the actual starting configuration for a numerical cable analysis.

The weight of a cable is simulated by a uniformly distributed load acting downwards and is applied while the cable is supported along it's length or at every node. This is necessary to avoid singularities occurring along the diagonals of the stiffness matrices in the solver routine, the root cause of which is the inherent flexibility of cables.

Dealing initially with truss elements, the next step is to move the centre node down typically 1% of the cable length, to both prestress the cable and displace it from it's straight line position. In the following step, either end of the cable can then be moved to form the catenary.

It is strongly advised that a midspan node be displaced downwards, as deviations from this could easily lead to non-convergence of the solution, due to the zero bending stiffness at the nodes. Applying tension is necessary to give an effective lateral stiffness to the cable. A phenomenon referred to as 'jamming' occurred when the cable was not displaced out of it's straight line configuration, possibly due to the very high axial versus the small transverse forces that are present, which in the examples discussed, restricted

the cable from displacing under it's own weight.

It is recommended that if truss elements are used for cable type problems, the analysis is performed dynamically. The resulting vast improvement in convergence criteria is because the cable inertia acts as a stabiliser and an effective lateral stiffener. Using a dynamic analysis may take marginally longer (CPU time), although it can often take less time, but of overiding importance is that it is much 'safer', meaning that there is a reduced likelihood of nonconvergence.

In general though, both linearly and quadratically interpolated truss elements are not suited to flexible structure type problems. On occasions they were found to behave erratically even in a dynamic analysis, especially if not under tension, due to their total lack of bending stiffness at the nodes.

Beam elements were found to be safer, and sometimes even more efficient for more involved problems, and also are permitted far more versatility and loading variety in ABAQUS, and as a result have been used exclusively.

For beam elements, it was found to be sufficient to simply ramp-off the supports in the 2nd step (after having applied weight) in both static and dynamic analyses, and thereafter move the cable end to form the desired catenary position.

As with truss elements, dynamic analyses are safer although static analyses take typically 50% less time to the end of step equilibrium, even though at start-up the time increments went as small as 1.0e-8 of a step compared to 1.0e-2 in the case of dynamics. As long as the minimum time increment in automatic time stepping is small, there are no anticipated problems.

Using a large tolerance at start-up with a subsequent reduction as recommended by Phaal [63] appears to have little

advantage over having a constant tolerance throughout the analysis, as after the first few iterations in an increment, the problem starts to stabilise and convergence to the tolerance becomes rapid (as indicated by the stress residuals). Thus the 'constant tolerance' approach is marginally less efficient, but is advantageous because of it's simplicity. Furthermore, convergence to a solution on the outer bounds of a large tolerance, could cause convergence difficulties in the next increment.

Methods of improving the efficiency in obtaining the catenary are; to keep the model under as high a tension for as long as possible in both static and dynamic analyses, and for the latter case, move the cable slowly in real time, with a high value of the Hilber-Hughes-Taylor operator (eg. -0.25).

Greater efficiency is achieved when a higher bending stiffness is used but this may obviously transgress the model constraints. This over stiffening in bending is worth noting because convergence difficulties can often be avoided, but reasonably accurate displacement results for the original model can still be obtained. In other words, if a user is having problems of an ill-posed nature, over stiffening with the resulting solution convergence, will give a feel for the direction that the problem is taking and possible hints to the improvement of the actual model.

The above paragraph also directs attention to a relevant point, which is that flexible structures are very sensitive to their degree of flexibility. For example, problems that have been experienced in cable analysis have not always been problems in flexible riser and pipe analysis which typically have larger bending stiffnesses, and thus greater attention is necessary to avoid singular matrices in cable analysis.

Hybrid beam elements, introduced to cater for highly flexible structures, were in general less efficient than isoparametric beam elements, although their rate of convergence was faster

(making them 'safer'), and thus it is suggested that the user initially perform analyses with both types of elements, and subsequently choose the 'best' option.

It is also recommended that initial catenary analyses are attempted with the safer dynamic analysis, but once confidence (or experience) has been gained, to use the more efficient and conceptually more elegant (it appears more logical to do a static analysis if only a static solution is required) static analysis.

It was found in the cable whip problem that the FEM can simulate a 'cracking of the whip' phenomenon. This occurred at the free end of the cable, but it seems that FEM could predict similar occurrences along the cable in for example a snap load situation.

From this whip model it was found to be 50% more efficient to number the nodes from a region of flexibility to a region of rigidity, but in neither case were convergence difficulties experienced.

Attention should be paid to the smoothness of the specified displacement input, in the analysis of the behaviour of a freely hanging cable in air, subjected to a prescribed boundary condition. Abrupt velocity changes which correspond to infinite accelerations could well cause wave propagation along the cable, as would be expected in reality, but at present, is beyond the scope of this mooring cable analysis. Thus care should be taken when investigating snap loadings on cables, which should be caused by at most rapid but not abrupt velocity changes. Special attention is necessary when dealing with unstable cable compression in this situation.

A slow prescribed displacement analysis results in fewer oscillations, and thus time increments (as fractions of a step) can be increased, leading to reduced computational time.

As before, a higher numerical damping (eg. -0.25) is desirable to avoid noise generated when solving for flexible structures.

It is generally recommended that a minimum bending to stiffness ratio for use in flexible structure analyses is 1 : 1.0e-9, below which ill-conditioning arises to an extent where convergence cannot be attained.

Choice of the tolerance was chosen typically as 0.1% of the maximum forces resulting in the analysis. For our purposes this provides greater accuracy than is required, but the added accuracy costs little more as the path of convergence is already steep. The point to note is firstly, if convergence is to be achieved, it is usually obvious within the first ten cycles, and secondly that even though small reaction forces are within the tolerance, they may be orders of magnitude incorrect. The reactions are sensitive to the cable displacement shape, and can vary significantly within the tolerance. This is of no concern however as we are interested in critical stress values and displacements.

A modal analysis for contact problems is meaningless for the catenary position, because no lift-off is catered for; the cable behaves as if it were pinned at the point of lift-off. Furthermore a modal analysis cannot be performed on immersed structures when Morison's nonlinear equation is used, as the nonlinear loading causes assymetrical matrices, for which there is no frequency domain solution in ABAQUS.

A word of warning about the *RESTART option is that, it was noticed in both static and dynamic analyses that even though all data from a previous run was both written and read properly, significant spurious peaks were encounted at the start of the restart analysis. Although the convergent solution at the end of the step was identical to that of a continuous run, the path of convergence was not always the same.

For situations where there is contact between a cable and a non-deformable boundary, interface elements are required to monitor either the contact pressure or the resulting gap.

Interface elements themselves use nominal storage, but the constant monitoring of the gap, the pressure and impact loads significantly increases CPU time. Thus the model should be organised in such a manner as to limit this ground contact by, for example, using 'abandonment' rather than 'recovery' procedures, and also by limiting superfluous cable lay.

Impact loadings between the cable and contact surface can be reduced in the 'abandonment' stage by using an artificially large drag coefficient, which can be subsequently reduced in the next step once contact has been made. This avoids the cable 'bouncing' on the ocean floor when contact is made.

When cables are used to constrain the motion of a large body, numerical ill-conditioning is further increased to a level where at present modelling the situation on ABAQUS may not be possible. In other words, cables when used in isolation are already ill-posed and require special procedures for safe convergence. By further adding highly stiff or heavy elements, to simulate for example clump weights or platforms, further increases the ill-conditioning of the problem.

This was evidenced during the modelling of a floating platform, where firstly there is an abrupt change in axial and bending stiffnesses between adjacent elements causing ill-conditioning in the stiffness matrix, and secondly an abrupt change in their inertias causing ill-conditioning in the mass matrix. This inherent ill-posing, coupled with large buouyancy forces that are needed to support the system, resulted in a total lack of convergence.

A further problem encountered as a result of ill-conditioning is that of convergence to a nonsense solution. For example, a particular reaction after 'equilibrium' was 1.0e36. In this

case it is obviously an unrealistic solution, but coincidental convergence to an erroneous approximate solution could lead to misleading interpretations.

Thus ill-conditioning can be caused from different souces,

- large mass discrepancies between adjacent elements,
- large axial stiffness discrepancies between adjacent elements,
- large axial to bending stiffnesses of adjacent or the same elements;

and can be noticed by either a lack of convergence, or convergence to an unrealistic solution, or worse, unnoticed because of convergence to an erroneous but realistic solution. This latter situation can be checked by trying a few runs of a similar nature.

Further ill-conditioning was initially experienced in the articulated tower model, but by reducing the tower mass and stiffness, this problem was by-passed.

As before node-numbering to the stiffer tower from the less stiff cable is more efficient, and again both alternatives converged. Greater efficiency is achieved by limiting ground contact by having just the anchor element still in ground contact at the maximum lift-off of the cable.

Cable compression can occur if the fluid loading is too abrupt (eg. a tidal wave, or very large tower drag in a rapidly accelerated fluid). This appears as a sort of 'shock wave' along the cable and can be reduced by flattening the loading curve and increasing the number of elements, which allows for greater flexibility.

It is suggested from experience that even for apparently trivial situations, models should be built up slowly ie. from simple to progressively more complex. This will help to eliminate strange phenomena and/or erroneous assumptions

besides building up confidence and heuristic knowledge about cable analysis.

Although numerical cable analyses are inherently ill-conditioned, and are sensitive to the choice of parameters (Young's Modulus, bending stiffness, HAFTOL, node numbering), intricate modelling of comprehensive cable systems is still possible if the guide lines mentioned above are followed.

Further work for cable analysis is to investigate:

i) Nonlinear material behaviour on the corrected version of ABAQUS

ii) Clumped weight and mud-suction effects on fairlead response,

iii) Transverse cable oscillations in a 3-D analysis

iv) Impact and snap loads

v) Further engineering applications of cables, and

vi) The use of specific algorithms for highly flexible structures, eg. P-Adic or Regularization techniques.

6. RFERENCES

1. Dean D.L. , STATIC AND DYNAMIC ANALYSIS OF GUY CABLES, J. Struct Div ASCE, January 1961, pp 1-21

2. Davenport A.G. and Steels G.N. , DYNAMIC BEHAVIOUR OF GUY CABLES, J. Struct Div ASCE, April 1965, pp 43-70 MASSIVE CABLES - PARABOLIC ASSUMPTION

3. Buchanan G.R. , TWO DIMENSIONAL CABLE ANALYSIS, J. Struct Div ASCE, vol 96, July 1970, pp 1581-1587

4. Soler A.I. , DYNAMIC RESPONSE OF SINGLE CABLES WITH INITIAL SAG, J. Franklin Institute, vol 290, pp 377-387, 1970

5. Chang P. Y. and Pilkey W. D. , THE ANALYSIS OF MOORING LINES, Offshore Technology Conference , Houston, April 1971, pp 845-854 INCREMENTAL LINEARIZATION.

6. Leonard J. W. and Recker W. W. , NONLINEAR DYNAMICS OF CABLES WITH LOW INITIAL TENSION, J. Eng Mech Div ASCE, April 1972, pp 293-307

7. Irvine H. M. and Caughey T. K. , THE LINEAR THEORY OF FREE VIBRATIONS OF A SUSPENDED CABLE, Proc. R. Soc. Lond. , vol 341. pp 299-315, 1974

8. Winget J. M. and Huston R. L. , CABLE DYNAMICS - A FINITE SEGMENT APPROACH, Computers and Structures, vol 6, pp 475-480, 1976

9. Henghold W. M. and Russel J. J. , EQUALIBRIUM AND NATURAL FREQUENCIES OF CABLE STRUCTURES (A NONLINEAR F.E.M. APPROACH), Computers and Structures, vol 6, pp 267-271, 1976

10. Nath J. H. STATE OF THE ART ON ANALYSIS OF CABLE DYNAMICS, Proceedings of Civil Engineering in the Oceans III, June 1975, p 623-631

11. Gambhir M. L. and Barrington dev. Batchelor , PARAMETRIC STUDY OF FREE VIBRATION OF SAGGED CABLES, Computers and Structures, vol 8, pp 641-648, 1978

12. Wilson J. W. and Wheen R. J. , INCLINED CABLES UNDER LOAD - DESIGN EXPRESSIONS, J. Struct Div ASCE, May 1977, pp 1061-1078

13. Ramberg S. E. and Owen M. G. , FREE VIBRATIONS OF TAUT AND SLACK MARINE CABLES, J. Struct Div ASCE, November 1977, pp 2079-2092

14. Monforton G. R. and El-Hakim N. M. , ANALYSIS OF TRUSS-CABLE STRUCTURES, Computers and Structures, vol 11, pp 327-335, 1980

15. Irvine H. M. , ENERGY RELATIONS FOR A SUSPENDED CABLE, Q. J. Mech and appl Math. , vol 33, Pt 2, pp 227-234, 1980

16. Griffin O. M., Pattison J. H., Skop R. A., Ramberg S. E. and Meggit D. J. , VORTEX-EXCITED VIBRATIONS OF MARINE CABLES, J. Waterway Port Coastal and Ocean Div, May 1980, pp 183-204

17. Meggit D. J. and Migliore H. J. , DYNAMIC RESPONSE OF CABLES SUBJECT TO OCEAN FORCES, Offshore Technolgy Conference 1980, pp 525-532

18. Huston R. L. and Kamman J. W. , A REPRESENTATION OF FLUID FORCES IN FINITE SEGMENT CABLE MODELS, Computers and Structures, vol 14, No. 3-4, pp 281-287, 1981

19. Fried I. , LARGE DEFORMATION STATIC AND DYNAMIC ANALYSIS OF EXTENSIBLE CABLES, Computers and Structures, vol 15, No. 3, ppc 315-319, 1982

20. Pugsley A. , THE NONLINEAR BEHAVIOUR OF A SUSPENDED CABLE, Q. J. Mech and appl Math, vol 36, Pt 2, pp 157-162, 1983

21. Huston R. L. and Kamman J. W. , VALIDATION OF IN FINITE SEGMENT CABLE MODELS, Computers and Structures, vol 15, No. 6, pp 653-660, 1982

22. Bastero C. , Tarrago J.A. , Serna M. A. and Jaen J. A. , CABLE DYNAMICS: APPLICATION OF THE GENERALISED HAMILTON PRINCIPLE, Int. J. Mech Eng Education, vol 11, no 3, 1982

23. Lo A. and Leonard J. W. , DYNAMIC ANALYSIS OF UNDERWATER CABLES, J. Eng Mech Div ASCE, vol 108, No. EM4, August 1982

24. Brinkmann C. R. , DYNAMIC INTERACTION OF A GUYED TOWER WITH ITS GUYING SYSTEM, J. Energy Resourses Technolgy ASME, vol 105, September 1983, pp 290-295

25. Triantafyllou M. S. , THE DYNAMICS OF TAUT INCLINED CABLES, May 1983, pp 421-440.

26. Triantafyllou M. S. and Bliek A. , THE DYNAMICS OF TAUT AND SLACK MARINE CABLES, Offshore Technology Conference , Houston, May 1983, pp 469-476

27. Ormberg H. , Fylling I.J. and Morch M. , DYNAMIC RESPONSE IN ANCHOR LINES: NUMERICAL SIMULATIONS COMPARED WITH FIELD MEASUREMENTS, Offshore Technology Conference , Houston, May 1983, pp 459-467

28. Palo P. A. , Meggitt D. J. and Nordell W. J. , DYNAMIC CABLE ANALYSIS MODELS, Offshore Technology Conference , Houston, May 1983, pp 487-494

29. Veletsos A. S. and Darbre G. R. , FREE VIBRATION OF PARABOLIC CABLES, J. Struct Eng ASCE, vol 109, No 2, pp 503-516, Feb 1983

30. Morrison D. G. , GUYED TOWER WITH DYNAMIC MOORING PROPERTIES, J. Struct Eng , vol 109, No 11, pp 2578-2590, Nov 1983

31. Morrison D. G. and Will S. A. , SIMPLE MODELS TO EVALUATE DYNAMIC GUYED TOWER RESPONSE, J. Eng Res Tech ASME, vol 105, pp 296-299, Sept 1983

32. Morrison D. G. , STIFFNESS AND ENERGY DISSIPATION CHARACTERISTICS OF GUYED TOWER WITH DYNAMIC MOORING PROPERTIES, J. Eng Res Tech ASME, vol 106, No 11, pp 18-23, March 1984

33. Bergen P. G. , Mollestad E. and Sandsmark N. , NONLINEAR STATIC AND DYNAMIC ANALYSIS FOR FLOATING OFFSHORE STRUCTURES, Eng Comput, vol 2, pp 13-20, March 1985

34. Pastorel H. and Beaulieu G. , NONLINEAR VIBRATIONS OF GUY CABLE SYSTEMS, Computer and Structures, vol 21, No 1/2, pp 33-50, 1985

35. Ali S. A. , DYNAMIC RESPONSE OF SAGGED CABLES, Computers and Structures, vol 23, No 1, pp 51-57, 1986

36. Khan N. U. and Ansari K. A. , ON THE DYNAMICS OF A MULTICOMPONENT MOORING LINE, Computers and Structures, vol 22, No 3, pp 311-334, 1986

37. Ansari K. A. and Khan N. U. , THE EFFECT OF CABLE DYNAMICS ON THE STATION-KEEPING RESPONSE OF A MOORED OFFSHORE VESSEL, J. Eng Res Tech ASME, vol 108, pp 52-58, March 1986

38. Patrikalakis N. M. and Chryssostomidis C. , VORTEX-INDUCED RESPONSE OF A FLEXIBLE CYLINDER IN A SHEARED CURRENT, J. Eng Res Tech ASME, vol 108, pp 59-64, March 1986

39. Kim Y. H. , Vandiver J. K. and Holler R. , VORTEX-INDUCED VIBRATION AND DRAG COEFFICIENTS OF LONG CABLES SUBJECTED TO SHEARED FLOWS, J. Eng Res Tech ASME, vol 108, pp 77-83, March 1986

40. Leonard J. W. and Tuah H. , NONLINEAR DETERMINISTIC AND STOCHASTIC RESPONSE OF CABLE SYSTEMS WITH LARGE BODIES UNDER HYDRODYNAMIC LOADS , Engineering Structures, vol 8, pp 93-106, April 1986

41. Jayaraman H. B. and Knudson W.C. ,A CURVED ELEMENT FOR THE ANALYSIS OF CABLE STRUCTURES, Computers and Structures, vol 14 no. 3-4, pp 325-333, 1981

42. Karakostas C. Z. , Baniotopoulos C.C. and Panagiotopoulos, SEA BED STRUCTURE INTERACTION FOR SUBMARINE CABLES, Computers and Structures , vol 22 p 213, 1986

43. Peyrot A. H. , MARINE CABLE STRUCTURES, J. Struct. Div. , pp 2391-2404, ST12 Dec 1986

44. Nordell W. J. and Meggit D. J. , UNDERSEA SUSPENDED CABLE STRUCTURES, J. Struct. Div. , PP 1025-1040 ST6 June 1981

45. Leonard J. W. , Garrison C. J. and Hudspeth R. T. , DETERMINISTIC FLUID FORCES ON STRUCTURES: A REVIEW, J. Struct. Div. , PP 1040-1057 ST6 June 1981

46. Babuska I. and Noor A. K. , QUALITY ASSESSMENT AND CONTROL OF FINITE ELEMENT SOLUTIONS, F. E. in Analysis and Design, 3 pp 1-26 , 1987

47. Paliou C. , Shinozuka M. and Chen Y. N. , RELIABILITY AND DURABILITY OF MARINE STRUCTURES, J. Struct Eng , v 113 no. 6 , June 1987

48. Mo M. and Moan T. , ENVIRONMENTAL LOAD EFFECT ANALYSIS OF GUYED TOWERS, Trans ASME , 24 v 107 , March 1985

49. Zimmerman M. et al , DYNAMIC BEHAVIOR OF DEEP OCEAN PIPELINE, J. Waterway Port Coastal and Ocean Eng. v 112 No. 2, March 1986

50. Chih-Young Liaw , SUBHARMONIC RESPONSE OF OFFSHORE STRUCTURES, J. Eng Mech, v 113, No. 3, March 1987

51. Dawson T. H. , IN-LINE FORCES ON VERTICAL CYLINDERS IN DEEPWATER WAVES, Trans ASME, 18 vol 107, March 1985

52. Overik T. and Moe G. , ADDED MASS AND IN-LINE STEADY DRAG COEFFICIENT OF MULTIPLE RISERS, Trans ASME 2 vol 107, March 1985

53. Kato M., Abe T., Tamiya M. and Kumakiri T. , DRAG FORCES ON OSCILLATING CYLINDERS IN A UNIFORM FLOW, Trans ASME 12 vol 107, March 1985

54. Bokaian A. and Geoola F. , FLOW INDUCED VIBRATIONS OF MARINE RISERS, J. Waterway Port Coastal and Ocean Eng. , vol 113 No. 1, Jan 1987